63-3-1

FTD-TT- 62-1521

TRANSLATION

AUTOMATION

FOREIGN TECHNOLOGY DIVISION

AIR FORCE SYSTEMS COMMAND

WRIGHT-PATTERSON AIR FORCE BASE

OHIO

UNEDITED ROUGH DRAFT TRANSLATION

AUTOMATION

English Pages: 112

S/102-62-0-2

THIS TRANSLATION IS A RENDITION OF THE ORIGINAL FOREIGN TEXT WITHOUT ANY ANALYTICAL OR EDITORIAL COMMENT. STATEMENTS OR THEORIES ADVOCATED OR IMPLIED ARE THOSE OF THE SOURCE AND DO NOT NECESSARILY REFLECT THE POSITION OR OPINION OF THE FOREIGN TECHNOLOGY DIVISION.	PREPARED BY: TRANSLATION SERVICES BRANCH FOREIGN TECHNOLOGY DIVISION WP-AFB, OHIO.

AKADEMIYA NAUK UKRAINS'KOY RSR
Institut Elektrotekhniki

AVTOMATIKA

Nr. 2

Vidavnitstvo Akademii Nauk Ukrains'koy RSR
Kiev - 1962

Pages: 1-89

FTD-TT-62-1521/1+2

TABLE OF CONTENTS

ON THE INVARIANCE OF PULSED AUTOMATIC CONTROL SYSTEMS*

By

L. Z. Grishchenko and D. F. Boldireva

Recently in various fields of technology (automatics, telemechanics, computers) pulsed systems are finding broad application. Problems of the theory of control, investigation and construction of optimum pulsed systems are acquiring first rate importance.

As is known, one of the actual improvements in control quality is the construction of invariant systems. But until now the invariance theory was basically developed on the basis of continuous systems [1 - 11]. We could mention here only several studies devoted to this problem for pulsed systems.

Prof. Ya. Z. Tsipkin introduced a number of quality criteria of transient processes and conditions of obtaining astatism of r-order [12 - 13].

For the following systems were found conditions, within which the error of reproducing equals zero in discrete moments of time [14 - 15].

In the report by Yu. V. Krementulo are discussed conditions of absolute invariance in open pulsed systems [16].

This report is devoted to the study of conditions of invariance in a closed pulsed system of control with respect to outer disturbances.

Introduction of Differential Equations for a Closed Pulsed System

We will discuss a system of discrete control, which works on the principle of deviation of the controlled system. We will assume that the pulsed element transforms the input value which changes continuously in a sequence of equally spaced from each other pulses, proportional to the input value at the moment of time nT. Here T - control time constant, n - integral nonseparable number. Duration of the pulse equals γT, where γ - coefficient, which does not exceed unity.

---

*Printing of report was authorized by Kiev City Seminar on Automatic Control.

The discussed system of discontinuous control (see drawing) is described by equations

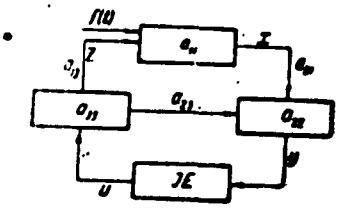

$$a_{11}(\bar{p})\,x(\bar{t})+a_{12}(\bar{p})\,y(\bar{t})+a_{13}(\bar{p})\,z(\bar{t})=f(\bar{t}), \tag{1}$$

$$a_{21}(\bar{p})\,x(\bar{t})+a_{22}(\bar{p})\,y(\bar{t})+a_{23}(\bar{p})\,z(\bar{t})=0, \tag{2}$$

$$\left.\begin{aligned} u(\bar{t})&=0 \quad \text{при} \quad n+\gamma \le \bar{t} \le n+1 \\ u(\bar{t})&=ky[n] \quad \text{при} \quad n \le \bar{t} \le n+\gamma \end{aligned}\right\}, \tag{3}$$

$$u(\bar{t})+a_{33}(\bar{p})\,z(\bar{t})=0. \tag{4}$$

Here is introduced a dimensionless time $\bar{t} = \frac{t}{T}$ and defined $Tp = \bar{p}$, where $p = \frac{d}{dt}$. But further on for the sake of simplicity we will write t an p leaving out the dash.

Let us discuss more thoroughly the equations (1-4).

Equations of the control object (1), x-controlled parameter, $a_{11}(p) = m_{11}p^2 + l_{11}p + k_{11}$ - polynomial, which characterizes the dynamics of the object of control, $a_{13}(p) = m_{13}p^2 + m_{13}p^2 + l_{13}p + k_{13}$ - reflects the effect of the executing mechanism on the control object.

Equations of measuring device (2), equations $a_{21}(p) = m_{21}p^2 + l_{21}p + k_{21}$ characterize the effect of the controlled parameter on the measuring device, $a_{22}(p) = m_{22}p^2 + l_{22}p + k_{22}$ - describes the dynamics of the measuring system, $a_{23}(p) = m_{23}p^2 + l_{23}p + k_{23}$ - reverse effect of the operational mechanism on the measuring device.

Equations of the pulse element of the first type are described (3)

Equations of operational mechanism have the form of (4).

The pulsed control system cannot be described by a single system of linear differential equations because of the compelled periodic opening of the control ring. The apparatus of differential equations allows to investigate control at the discrete moment of time, because to describe the dynamics of the process of the mentioned system it is necessary to solve differential equations.

Let us examine equations (4) together with (3)

$$m_{33}\frac{d^2z}{dt^2}+l_{33}\frac{dz}{dt}+k_{33}z+ky[n]=0,\quad n\leqslant t\leqslant n+\gamma;$$
$$m_{33}\frac{d^2z}{dt^2}+l_{33}\frac{dz}{dt}+k_{33}z=0,\quad n+\gamma\leqslant t\leqslant n+1. \tag{5}$$

By integrating equations (5), we will obtain

$$z(t)=A_1e^{\lambda_1(t-n)}+A_2e^{\lambda_2(t-n)}-\frac{ky[n]}{k_{33}}\quad \text{при } n\leqslant t\leqslant n+\gamma,$$
$$z(t)=B_1e^{\lambda_1(t-n-\gamma)}+B_2e^{\lambda_2(t-n-\gamma)}\quad \text{при } n+\gamma\leqslant t\leqslant n+1, \tag{6}$$

where λ_1 and λ_2 - roots of characteristic equation $m_{33}p^2+l_{33}p+k_{33}=0$. The constants A_1, A_2, B_1, B_2 are designated from conditions of joinint together the solutions at the moment of time n + γ and initial conditions at the moment of time t = n.

$$A_1=-\frac{\lambda_2z[n]-\dot z[n]}{\lambda_1-\lambda_2}-\frac{ky[n]}{\lambda_1(\lambda_1-\lambda_2)m_{33}},$$
$$A_2=\frac{\lambda_1z[n]-\dot z[n]}{\lambda_1-\lambda_2}+\frac{ky[n]}{\lambda_2(\lambda_1-\lambda_2)m_{33}},$$
$$B_1=A_1e^{\lambda_1\gamma}+\frac{ky[n]}{\lambda_1(\lambda_1-\lambda_2)m_{33}}, \tag{7}$$
$$B_2=A_2e^{\lambda_2\gamma}+\frac{ky[n]}{\lambda_2(\lambda_1-\lambda_2)m_{33}}.$$

Substituting the obtained values of constants, we find values z(t) and $\dot z$(t) at the moment of time (n + 1)

$$z[n+1]=\frac{\lambda_1e^{\lambda_2}-\lambda_2e^{\lambda_1}}{\lambda_1-\lambda_2}z[n]+\frac{e^{\lambda_1}-e^{\lambda_2}}{\lambda_1-\lambda_2}\dot z[n]-\frac{k\gamma(e^{\lambda_1}-e^{\lambda_2})}{(\lambda_1-\lambda_2)m_{33}}y[n], \tag{8}$$
$$\dot z[n+1]=-\frac{\lambda_1\lambda_2(e^{\lambda_1}-e^{\lambda_2})}{\lambda_1-\lambda_2}z[n]+\frac{\lambda_1e^{\lambda_1}-\lambda_2e^{\lambda_2}}{\lambda_1-\lambda_2}\dot z[n]-$$
$$-\frac{k\gamma(\lambda_1e^{\lambda_1}-\lambda_2e^{\lambda_2})}{(\lambda_1-\lambda_2)m_{33}}y[n]. \tag{9}$$

We like to point out, that because of the smallness of γ ($\gamma\ll1$), the items of the type $e^{\alpha}\gamma$ change by $1+\alpha\gamma$, where alpha is a constant value. We will rewrite equation (8) for (n + 1)-interval of time.

$$z[n+2]=\frac{\lambda_1e^{\lambda_2}-\lambda_2e^{\lambda_1}}{\lambda_1-\lambda_2}z[n+1]+\frac{e^{\lambda_1}-e^{\lambda_2}}{\lambda_1-\lambda_2}\dot z[n+1]-$$
$$-\frac{k\gamma(e^{\lambda_1}-e^{\lambda_2})}{m_{33}(\lambda_1-\lambda_2)}y[n+1]. \tag{10}$$

Having exluded from equations (8), (9) and (10) the values z[n] and z[n+1] we will obtain a differential equation, which describes the dynamic properties of the operational mechanism of the regulator in discrete moment of time

$$z[n+2]=(e^{\lambda_1}+e^{\lambda_2})z[n+1]-e^{\lambda_1+\lambda_2}z[n]-\frac{k\gamma(e^{\lambda_1}-e^{\lambda_2})}{(\lambda_1-\lambda_2)m_{33}}y[n+1]. \tag{11}$$

In an analogous way are solved differential equations, which describe the dynamic properties of the object (12) and measuring element (13)

$$x[n+2]=(e^{\alpha_1}+e^{\alpha_2})x[n+1]-e^{\alpha_1+\alpha_2}x[n]-\frac{A-B}{m_{11}}z[n+1]+$$
$$+\frac{Ae^{\lambda_2}-Be^{\lambda_1}}{m_{11}}z[n]-\frac{k_1^{\gamma}}{m_{11}m_{33}}Cy[n+1]-\frac{e^{\alpha_1+\alpha_2}}{m_{11}(\alpha_2-\alpha_1)}\times$$
$$\times\int_n^{n+1}f(t)e^{-\alpha_1(t-n)}dt+\frac{e^{\alpha_1+\alpha_2}}{m_{11}(\alpha_1-\alpha_2)}\int_n^{n+1}f(t)e^{-\alpha_2(t-n)}dt+$$
$$+\frac{e^{2\alpha_1}}{m_{11}(\alpha_1-\alpha_2)}\int_{n+1}^{n+2}f(t)e^{-\alpha_1(t-n)}dt-\frac{e^{2\alpha_2}}{m_{11}(\alpha_1-\alpha_2)}\int_{n+1}^{n+2}f(t)e^{-\alpha_2(t-n)}dt, \quad (12)$$

where

$$A=\frac{a_{13}(\lambda_1)(e^{\lambda_1}-e^{\alpha_1})(e^{\lambda_1}-e^{\alpha_2})}{(e^{\lambda_1}-e^{\lambda_2})(\lambda_1-\alpha_1)(\lambda_1-\alpha_2)},\quad B=\frac{a_{13}(\lambda_2)(e^{\lambda_2}-e^{\alpha_1})(e^{\lambda_2}-e^{\alpha_2})}{(e^{\lambda_1}-e^{\lambda_2})(\lambda_2-\alpha_1)(\lambda_2-\alpha_2)},$$
$$C=\frac{a_{13}(\lambda_1)e^{\lambda_1}}{(\lambda_1-\alpha_1)(\lambda_1-\alpha_2)(\lambda_1-\lambda_2)}-\frac{a_{13}(\lambda_2)e^{\lambda_2}}{(\lambda_2-\alpha_1)(\lambda_2-\alpha_2)(\lambda_1-\lambda_2)}+$$
$$+\frac{a_{13}(\alpha_1)e^{\alpha_1}}{(\alpha_1-\lambda_1)(\alpha_1-\lambda_2)(\alpha_1-\alpha_2)}-\frac{a_{13}(\alpha_2)e^{\alpha_2}}{(\alpha_2-\lambda_1)(\alpha_2-\lambda_2)(\alpha_1-\alpha_2)},$$

α_1, α_2 — корені характеристичного рівняння $m_{11}p^2+l_{11}p+k_{11}=0$, $a_{13}(\alpha_i)$, $a_{13}(\lambda_i)$ — поліноми типу $a_{13}(\alpha_i)=m_{13}\alpha_i^2+l_{13}\alpha_i+k_{13}$ $(i=1, 2)$;

$$y[n+2]=(e^{\beta_1}+e^{\beta_2})y[n+1]-e^{\beta_1+\beta_2}y[n]-$$
$$-\frac{k_1^{\gamma}}{m_{22}m_{33}}Zy[n+1]-\frac{R-P}{m_{22}}z[n+1]+\frac{Re^{\lambda_2}-Pe^{\lambda_1}}{m_{22}}z[n]-$$

alpha$_1$ and alpha$_2$ - roots of characteristic equation $m_{11}p^2 + l_{11}p + k_{11} = 0$, $a_{13}(\alpha_1)$, $a_{13}(\lambda_1)$ - polynomials of the type $a_{13}(\alpha_1) = m_{13}\alpha_1^2 + l_{13}\alpha_1 + k_{13}$ ($i = 1, 2$);

$$-\frac{M-N}{m_{22}}x[n+1]+\frac{Me^{\alpha_1}-Ne^{\alpha_2}}{m_{22}}x[n]+b_1\int_n^{n+1}f(t)e^{-\alpha_1(t-n)}dt+$$
$$+b_2\int_{n+1}^{n+2}f(t)e^{-\alpha_1(t-n)}dt+b_3\int_n^{n+1}f(t)e^{-\alpha_2(t-n)}dt+$$
$$+b_4\int_{n+1}^{n+2}f(t)e^{-\alpha_2(t-n)}dt+b_5\int_n^{n+1}f(t)e^{-\alpha_1(t-n)}dt+ \quad (13)$$
$$+b_6\int_{n+1}^{n+2}f(t)e^{\alpha_1(t-n)}dt+b_7\int_n^{n+1}f(t)e^{-\alpha_2(t-n)}dt+b_8\int_{n+1}^{n+2}f(t)e^{-\alpha_2(t-n)}dt.$$

Values Z, M, N, R, P, b_i ($i = 1, 2, \ldots 8$) - certain constant coefficients depending upon the parameters of the system

$$Z=\frac{1}{m_{11}}\left\{\frac{e^{\beta_1}a_{11}(\beta_1)\,a_{13}(\beta_1)}{(\beta_1-\beta_2)(\beta_1-\alpha_1)(\beta_1-\alpha_2)(\beta_1-\lambda_1)(\beta_1-\lambda_2)}-\right.$$
$$-\frac{e^{\beta_2}a_{21}(\beta_2)\,a_{13}(\beta_2)}{(\beta_1-\beta_2)(\beta_2-\alpha_1)(\beta_2-\alpha_2)(\beta_2-\lambda_1)(\beta_2-\lambda_2)}+$$
$$+\frac{e^{\alpha_1}a_{21}(\alpha_1)\,a_{13}(\alpha_1)}{(\alpha_1-\alpha_2)(\alpha_1-\beta_1)(\alpha_1-\beta_2)(\alpha_1-\lambda_1)(\alpha_1-\lambda_2)}-$$
$$-\frac{e^{\alpha_2}a_{21}(\alpha_2)\,a_{13}(\alpha_2)}{(\alpha_1-\alpha_2)(\alpha_2-\beta_1)(\alpha_2-\beta_2)(\alpha_2-\lambda_1)(\alpha_2-\lambda_2)}+$$
$$+\frac{e^{\lambda_1}a_{21}(\lambda_1)\,a_{13}(\lambda_1)}{(\lambda_1-\lambda_2)(\lambda_1-\alpha_1)(\lambda_1-\alpha_2)(\lambda_1-\beta_1)(\lambda_1-\beta_2)}-$$
$$-\frac{e^{\lambda_2}a_{21}(\lambda_2)\,a_{13}(\lambda_2)}{(\lambda_1-\lambda_2)(\lambda_2-\alpha_1)(\lambda_2-\alpha_2)(\lambda_2-\beta_1)(\lambda_2-\beta_2)}-$$
$$-\frac{e^{\beta_1}a_{23}(\beta_1)\,m_{11}}{(\beta_1-\beta_2)(\beta_1-\lambda_1)(\beta_1-\lambda_2)}+\frac{e^{\beta_2}a_{23}(\beta_2)\,m_{11}}{(\beta_1-\beta_2)(\beta_2-\lambda_1)(\beta_2-\lambda_2)}-$$
$$\left.-\frac{e^{\lambda_1}a_{23}(\lambda_1)\,m_{11}}{(\lambda_1-\lambda_2)(\lambda_1-\beta_1)(\lambda_1-\beta_2)}+\frac{e^{\lambda_2}a_{23}(\lambda_2)\,m_{11}}{(\lambda_1-\lambda_2)(\lambda_2-\beta_1)(\lambda_2-\beta_2)}\right|; \quad (32)$$

$$M=\frac{(e^{\alpha_1}-e^{\beta_1})(e^{\alpha_1}-e^{\beta_2})\,a_{21}(\alpha_1)}{(\alpha_1-\beta_1)(\alpha_1-\beta_2)(e^{\alpha_1}-e^{\alpha_2})};\quad N=\frac{(e^{\alpha_2}-e^{\beta_1})(e^{\alpha_2}-e^{\beta_2})\,a_{21}(\alpha_2)}{(\alpha_2-\beta_1)(\alpha_2-\beta_2)(e^{\alpha_1}-e^{\alpha_2})};$$

$$R=\frac{1}{m_{11}}\left\{\frac{(e^{\alpha_1}-e^{\beta_1})(e^{\alpha_1}-e^{\beta_2})(e^{\lambda_1}-e^{\alpha_1})\,a_{21}(\alpha_1)\,a_{13}(\lambda_1)}{(e^{\lambda_1}-e^{\lambda_2})(e^{\alpha_1}-e^{\alpha_2})(\alpha_1-\beta_1)(\alpha_1-\beta_2)(\lambda_1-\alpha_1)(\lambda_1-\alpha_2)}-\right.$$
$$-\frac{(e^{\alpha_2}-e^{\beta_1})(e^{\alpha_2}-e^{\beta_2})(e^{\lambda_1}-e^{\alpha_2})\,a_{21}(\alpha_2)\,a_{13}(\lambda_1)}{(e^{\alpha_1}-e^{\alpha_2})(e^{\lambda_1}-e^{\lambda_2})(\alpha_2-\beta_1)(\alpha_2-\beta_2)(\lambda_1-\alpha_1)(\lambda_1-\alpha_2)}-$$
$$\left.-\frac{(e^{\lambda_1}-e^{\beta_1})(e^{\lambda_1}-e^{\beta_2})[a_{13}(\lambda_1)\,a_{21}(\lambda_1)-m_{11}a_{23}(\lambda_1)(\lambda_1-\alpha_1)(\lambda_1-\alpha_2)]}{(\lambda_1-\alpha_1)(\lambda_1-\alpha_2)(\lambda_1-\beta_1)(\lambda_1-\beta_2)(e^{\lambda_1}-e^{\lambda_2})}\right\};$$

$$P=\frac{1}{m_{11}}\left\{\frac{(e^{\alpha_1}-e^{\beta_1})(e^{\alpha_1}-e^{\beta_2})(e^{\lambda_2}-e^{\alpha_1})\,a_{21}(\alpha_1)\,a_{13}(\lambda_2)}{(e^{\alpha_1}-e^{\alpha_2})(e^{\lambda_1}-e^{\lambda_2})(\alpha_1-\beta_1)(\alpha_1-\beta_2)(\lambda_2-\alpha_1)(\lambda_2-\alpha_2)}-\right.$$

See Page 5a for continuation of Equation 13a

Equation 13a (Continued)

$$
\left.
\begin{aligned}
&- \frac{(e^{\alpha_1}-e^{\beta_1})(e^{\beta_2}-e^{\alpha_2})(e^{\lambda_1}-e^{\alpha_1})\,a_{21}(\alpha_2)\,a_{13}(\lambda_2)}{(e^{\alpha_1}-e^{\alpha_2})(e^{\lambda_1}-e^{\lambda_2})(\alpha_2-\beta_1)(\alpha_2-\beta_2)(\lambda_2-\alpha_1)(\lambda_2-\alpha_2)} \\
&- \frac{(e^{\alpha_1}-e^{\beta_1})(e^{\beta_2}-e^{\alpha_2})\left[a_{13}(\lambda_2)\,a_{21}(\lambda_2)-m_{11}(\alpha_{23}(\lambda_2)(\lambda_2-\alpha_1)(\lambda_2-\alpha_2)\right]}{(e^{\alpha_1}-e^{\lambda_2})(\lambda_2-\alpha_1)(\lambda_2-\alpha_2)(\lambda_2-\beta_1)(\lambda_2-\beta_2)}
\end{aligned}
\right\};
$$

$$
b_1=\frac{a_{21}(\beta_1)\,e^{\beta_1}e^{\beta_2}}{m_{11}(\beta_1-\alpha_1)(\beta_1-\alpha_2)(\beta_1-\beta_2)}, \qquad b_2=-\frac{a_{21}(\beta_1)\,e^{\beta_1}e^{\beta_2}}{m_{11}(\beta_2-\beta_2)(\beta_2-\alpha_1)(\beta_2-\alpha_2)};
$$

$$
b_3=-\frac{a_{21}(\beta_2)\,e^{\beta_1}e^{\beta_2}}{m_{11}(\beta_1-\beta_2)(\beta_2-\alpha_1)(\beta_2-\alpha_2)}, \qquad b_4=\frac{a_{21}(\beta_2)\,e^{\beta_1}e^{\beta_2}}{m_{11}(\beta_1-\beta_2)(\beta_2-\alpha_1)(\beta_2-\alpha_2)};
$$

$$
b_5=\left[\frac{a_{21}(\alpha_1)(e^{\alpha_1+\alpha_2}-e^{\beta_1+\alpha_2}-e^{\beta_2+\alpha_2}+e^{\beta_1+\beta_2})}{(\alpha_1-\alpha_2)(\alpha_1-\beta_1)(\alpha_1-\beta_2)(e^{\alpha_1}-e^{\alpha_2})}-\right.
$$

$$
\left.-\frac{a_{21}(\alpha_2)(e^{2\alpha_2}-e^{\beta_1+\alpha_2}-e^{\beta_2+\alpha_2}+e^{\beta_1+\beta_2})}{(\alpha_2-\alpha_2)(\alpha_2-\beta_1)(\alpha_2-\beta_2)(e^{\alpha_1}-e^{\alpha_2})}\right]e^{\alpha_2};
$$

13a

$$
b_6=-\frac{a_{21}(\alpha_1)\,e^{2\alpha_1}}{(\alpha_1-\alpha_2)(\alpha_1-\beta_1)(\alpha_1-\beta_2)};
$$

$$
b_7=-\left[\frac{a_{21}(\alpha_1)(e^{2\alpha_1}-e^{\beta_1+\alpha_1}-e^{\beta_2+\alpha_1}+e^{\beta_1+\beta_2})}{(\alpha_1-\alpha_2)(\alpha_1-\beta_1)(\alpha_1-\beta_2)(e^{\alpha_1}-e^{\alpha_2})}-\right.
$$

$$
\left.-\frac{a_{21}(\alpha_2)(e^{\alpha_1+\alpha_2}-e^{\beta_1+\alpha_2}-e^{\beta_2+\alpha_2}+e^{\beta_1+\beta_2})}{(\alpha_2-\alpha_2)(\alpha_2-\beta_1)(\alpha_2-\beta_2)(e^{\alpha_1}-e^{\alpha_2})}\right]e^{2\alpha_2};
$$

$$
b_8=\frac{a_{21}(\alpha_2)\,e^{2\alpha_2}}{(\alpha_1-\alpha_2)(\alpha_2-\beta_1)(\alpha_2-\beta_2)}.
$$

Coefficients of differential equations come out here bulky because of the fact that a pulsed system of quite general type is discussed. Its continuous part, which consists of the objects, measuring and operational elements described by equations of sixth magnitude, because each element is charged with a mass (m_{ij}), dissipative (l_{ij}) and elastic (k_{ij}) properties.

Invariance conditions of discontinuous control systems for deviations

To operate the obtained differential equations as algebraic, we will subject same to the discrete Laplace transformation and we will utilize the lag theorem (13).

(17)
$$D\{f[n+k]\}=e^{qk}\left[F^*(q)-\sum_{n=0}^{k-1}e^{-qn}f[n]\right]. \qquad 13b$$

where $F^*(q)=D\left\{f\left[n\right]\right\}$ - images of gradual function $f\left[n\right]$. Before applying discrete Laplace transforms to integral items of equations (12) and (13) we will change in the integrals the variables : $t = n + \xi$ - for integrals with boundaries from n to n + 1 and $t = n + 1 + \xi$ - for integrals with boundaries from n + 1 to n +2.

Having applied D-transforms, we will obtain appropriate integrals of the type

$$\int_0^1 F^*(q,\varepsilon)e^{-q\varepsilon}d\varepsilon \text{ та } e^{-q}\int_0^1[F^*(q,\varepsilon)-f(0,\varepsilon)]e^{-q\varepsilon}d\varepsilon. \qquad 13c$$

To obtain $F^*(q,\xi)$, which is not included in the sign if the integral, we must take averageadvantage of the theorem. Then, for example, we have

$$\int_0^1 F^*(q,\varepsilon)e^{-q\varepsilon}d\varepsilon=F^*(q,\varepsilon_1)\int_0^1 e^{-q\varepsilon}d\varepsilon=F^*(q,\varepsilon)\frac{e^{-q}-1}{-q}, \qquad 13d$$

$$\int_0^1[F^*(q,\varepsilon)-f(0,\varepsilon)]e^{-q\varepsilon}d\varepsilon=[F^*(q,\varepsilon_1)-f(0,\varepsilon_2)]\frac{e^{-q}-1}{-q},$$

where ξ_1 and ξ_2 - certain points on the interval (0.1).

Having made such transformations with differential equations (11), (12) and (13) and having selected the period of control T so that the distortions f(t) would be little changed, we will obtain a system of equations

See Page 6a for Equation 14

Equation 14

$$
\begin{aligned}
&\text{I.}\quad m_{11}\left[e^{2q}-(e^{\alpha_1}+e^{\alpha_2})\,e^{q}+e^{\alpha_1+\alpha_2}\right]x^{*}(q)-\frac{k_1^{\sim}}{m_{33}}\,Ce^{q}y^{*}(q)+\\
&\quad+\left[A\,(e^{q}-e^{\lambda_2})-B\,(e^{q}-e^{\lambda_1})\right]z^{*}(q)=Q_1F^{*}(q,\ \varepsilon_1)+\\
&\quad+Q_2e^{q}\left[F^{*}(q,\ \varepsilon_1)-f\,(0,\ \varepsilon_2)\right]+R_1(0);\\
&\text{II.}\quad\left[M\,(e^{q}-e^{\alpha_2})-N(e^{q}-e^{\alpha_1})\right]x^{*}(q)+\\
&\quad+m_{22}\left[e^{2q}-(e^{\beta_1}+e^{\beta_2})\,e^{q}+e^{\beta_1+\beta_2}+\frac{k_1^{\sim}}{m_{22}}\,Ze^{q}\right]y^{*}(q)+\\
&+\left[R\,(e^{q}-e^{\lambda_2})-P\,(e^{q}-e^{\lambda_1})\right]z^{*}(q)=Q_1F^{*}(q,\ \varepsilon_1)+Q_1e^{q}\left[F^{*}(q,\ \varepsilon_1)-f\,(0,\ \varepsilon_2)\right]+R_2(0);\\
&\text{III.}\quad k_1^{\sim}\frac{e^{\lambda_1}-e^{\lambda_2}}{\lambda_1-\lambda_2}\,e^{q}y^{*}(q)+m_{33}\left[e^{2q}-(e^{\lambda_1}+e^{\lambda_2})\,e^{q}+e^{\lambda_1+\lambda_2}\right]z^{*}(q)=R_3(0).
\end{aligned}
\tag{14}
$$

where R_1, R_2, R_3 - items which depend upon the initial conditions of variables x, y, z, that is upon x[0], y[0], z[0] x[1], y[1], z[1]

$$Q_1=\frac{e^{\alpha_1}(1-e^{\alpha_1})}{\alpha_1(\alpha_1-\alpha_2)}-\frac{e^{\alpha_2}(1-e^{\alpha_2})}{\alpha_2(\alpha_1-\alpha_2)},\quad Q_2=\frac{1-e^{\alpha_1}}{\alpha_2(\alpha_1-\alpha_2)}-\frac{1-e^{\alpha_2}}{\alpha_1(\alpha_1-\alpha_2)};$$

$$Q_3=-\frac{a_{21}(\beta_1)e^{\beta_1}(1-e^{\beta_1})}{(\beta_1-\alpha_1)(\beta_1-\alpha_2)(\beta_1-\beta_2)\beta_1 m_{11}}+\frac{a_{21}(\beta_2)e^{\beta_2}(1-e^{\beta_2})}{(\beta_2-\alpha_1)(\beta_2-\alpha_2)(\beta_1-\beta_2)\beta_2 m_{11}}-$$
$$-\left\{\frac{a_{21}(\alpha_1)(e^{\alpha_1+\alpha_2}-e^{\beta_1+\alpha_2}-e^{\beta_2+\alpha_1}+e^{\beta_1+\beta_2})}{(\alpha_1-\alpha_2)(\alpha_1-\beta_1)(\alpha_1-\beta_2)(e^{\alpha_1}-e^{\alpha_2})}-\right.$$
$$\left.-\frac{a_{21}(\alpha_2)(e^{2\alpha_2}-e^{\beta_2+\alpha_2}-e^{\beta_1+\alpha_2}+e^{\beta_1+\beta_2})}{(\alpha_1-\alpha_2)(\alpha_2-\beta_1)(\alpha_2-\beta_2)(e^{\alpha_1}-e^{\alpha_2})}\right\}\frac{1-e^{\alpha_1}}{\alpha_1 m_{11}}+$$
$$+\left\{\frac{a_{21}(\alpha_1)(e^{2\alpha_1}-e^{\alpha_1+\beta_1}-e^{\alpha_1+\beta_2}-e^{\beta_1+\beta_2})}{(\alpha_1-\alpha_2)(\alpha_1-\beta_1)(\alpha_1-\beta_2)(e^{\alpha_1}-e^{\alpha_2})}\right. \qquad 14a$$
$$\left.-\frac{a_{21}(\alpha_2)(e^{\alpha_1+\alpha_2}-e^{\alpha_1+\beta_1}-e^{\alpha_1+\beta_2}+e^{\beta_1+\beta_2})}{(\alpha_1-\alpha_2)(\alpha_2-\beta_1)(\alpha_2-\beta_2)(e^{\alpha_1}-e^{\alpha_2})}\right\}\frac{1-e^{\alpha_2}}{\alpha_2 m_{11}},$$

$$Q_4=\left[\frac{a_{21}(\beta_1)(1-e^{\beta_1})}{(\beta_1-\alpha_1)(\beta_1-\alpha_2)(\beta_1-\beta_2)\beta_1}-\frac{a_{21}(\beta_2)(1-e^{\beta_2})}{(\beta_2-\alpha_1)(\beta_2-\alpha_2)(\beta_1-\beta_2)\beta_2}+\right.$$
$$\left.+\frac{a_{21}(\alpha_1)(1-e^{\alpha_1})}{(\alpha_1-\beta_1)(\alpha_1-\beta_2)(\alpha_1-\alpha_2)\alpha_1}-\frac{a_{21}(\alpha_2)(1-e^{\alpha_2})}{(\alpha_2-\beta_1)(\alpha_2-\beta_2)(\alpha_1-\alpha_2)\alpha_2}\right]\frac{1}{m_{11}}.$$

For the convenience of recording we will rewrite the system of equations (14) into more compact form, introducing new designations of the proper coefficients at independent variables.

$$b_{11}x^*(q)+b_{12}y^*(q)+b_{13}z^*(q)=Q_1F^*(q,\varepsilon_1)+$$
$$+Q_2e^q[F^*(q,\varepsilon_1)-f(0,\varepsilon_1)]+R_1(0);$$
$$b_{21}x^*(q)+b_{22}y^*(q)+b_{23}z^*(q)=Q_3F^*(q,\varepsilon_1)+Q_4e^q[F^*(q,\varepsilon_1)-f(0,\varepsilon_1)]+R_2(0);$$
$$b_{32}y^*(q)+b_{33}z^*(q)=R_3(0). \qquad (15)$$

Solution for $x^*(q)$ is found from equation

Розв'язок $x^*(q)$ знаходиться з рівняння

$$Dx^*(q)=A_{11}\{Q_1F^*(q,\varepsilon_1)+Q_2e^q[F^*(q,\varepsilon_1)-f(0,\varepsilon_2)]+R_1\}-$$
$$-A_{21}\{Q_3F^*(q,\varepsilon_1)+Q_4e^q[F^*(q,\varepsilon_1)-f(0,\varepsilon_2)]+R_2\}+A_{31}R_3, \qquad (16)$$

where the determinant of the system has the form of

$$D=\begin{vmatrix}b_{11}&b_{12}&b_{13}\\b_{21}&b_{22}&b_{23}\\0&b_{32}&b_{33}\end{vmatrix}, \qquad 16a$$

$$A_{11}=b_{22}b_{33}-b_{23}b_{32},\quad A_{21}=b_{12}b_{33}-b_{32}b_{13},\quad A_{31}=b_{12}b_{23}-b_{13}b_{22}, \qquad (17)$$

причому $A_{11}\neq 0$, $A_{21}\neq 0$.

at which $A_{11} \neq 0$, $A_{21} \neq 0$.

It is evident from equation (16), that for the independence of $x^*(q)$ from the image of disturbances it is necessary to perform equations

$$\frac{Q_1}{Q_3} = \frac{Q_2}{Q_4} = \frac{A_{21}}{A_{11}}. \tag{18}$$

The values A_{21} and A_{11} found from (14), (15) and (17) will be substituted in (18); hence we will obtain conditions of invariance in unfolded form

$$\frac{Q_1}{Q_3} = \frac{Q_2}{Q_4} = \frac{A}{R} = \frac{B}{P} = -\frac{C}{L}, \tag{19}$$

$$m_{22}m_{33} = 0 \tag{20}$$

The condition $m_{22}m_{33} = 0$ is not accurately realized because of the presence of inertia in the measuring and operational organs ($m_{22} \neq 0$, $m_{33} \neq 0$)/. In the system of discontinuous regulation of one parameter of deviation we can speak only about approximate fulfillment of condition (20), that is for ξ - invariance.

We will assume, that the investigated system of pulsed control, which consists of object, measuring and operational elements is a fixed one, i.e. the properties of the operator $a_{11}(p)$, $a_{22}(p)$, $a_{33}(p)$ are known. Condition (19) does then allow to select the parameters of correcting junctions $a_{21}(p)$, $a_{13}(p)$, $a_{23}(p)$ in such a way, that this system will become invariant.

And so, the realization of condition $\frac{Q_1}{Q_3} = \frac{Q_2}{Q_4}$ leads in open form to equation

$$\frac{a_{21}(\beta_1)(1-e^{\beta_1})(1-e^{\alpha_1})(e^{\alpha_2}-e^{\beta_2})}{\alpha_1\beta_1(\beta_1-\beta_2)(\beta_1-\alpha_1)(\beta_1-\alpha_2)} - \frac{a_{21}(\beta_1)(1-e^{\beta_1})(1-e^{\alpha_2})(e^{\alpha_1}-e^{\beta_2})}{\alpha_2\beta_1(\beta_1-\beta_2)(\beta_1-\alpha_1)(\beta_1-\alpha_2)} -$$

$$- \frac{a_{21}(\beta_2)(1-e^{\beta_2})(1-e^{\alpha_1})(e^{\alpha_2}-e^{\beta_1})}{\alpha_1\beta_2(\beta_1-\beta_2)(\beta_2-\alpha_1)(\beta_2-\alpha_2)} +$$

$$+ \frac{a_{21}(\beta_2)(1-e^{\beta_2})(1-e^{\alpha_2})(e^{\alpha_1}-e^{\beta_1})}{\alpha_2\beta_2(\beta_1-\beta_2)(\beta_2-\alpha_1)(\beta_2-\alpha_2)} - \left\{ \frac{(1-e^{\alpha_1})^2(e^{\alpha_2}-e^{\beta_1})(e^{\alpha_2}-e^{\beta_2})}{\alpha_1^2} - \right. \tag{21}$$

$$- \frac{(1-e^{\alpha_1})(1-e^{\alpha_2})[(e^{\alpha_1}-e^{\beta_1})(e^{\alpha_2}-e^{\beta_2})+(e^{\alpha_1}-e^{\beta_2})(e^{\alpha_2}-e^{\beta_1})]}{\alpha_1\alpha_2} +$$

$$\left. + \frac{(1-e^{\alpha_2})^2(e^{\alpha_1}-e^{\beta_1})(e^{\alpha_1}-e^{\beta_2})}{\alpha_2^2} \right\} \left[\frac{a_{21}(\alpha_1)}{(\alpha_1-\beta_1)(\alpha_1-\beta_2)} - \frac{a_{21}(\alpha_2)}{(\alpha_2-\beta_1)(\alpha_2-\beta_2)} \right] \times$$

$$\times \frac{1}{(\alpha_1-\alpha_2)(e^{\alpha_1}-e^{\alpha_2})} = 0.$$

from which it is possible to designate one the parameters of transmission function corrected by increase in $a_{21}(p) = m_{21}p^2 + l_{21}p + k_{21}$, for example $k_{21} = -\frac{H1}{H2}$ where

$$H_1 = \frac{(m_{21}\beta_1 + l_{21})(1-e^{\beta_1})}{(\beta_1-\beta_2)(\beta_1-\alpha_1)(\beta_1-\alpha_2)}\left[\frac{(1-e^{\alpha_1})(e^{\alpha_2}-e^{\beta_2})}{\alpha_1} - \frac{(1-e^{\alpha_2})(e^{\alpha_1}-e^{\beta_2})}{\alpha_2}\right] -$$

$$- \frac{(m_{21}\beta_2 + l_{21})(1-e^{\beta_2})}{(\beta_1-\beta_2)(\beta_2-\alpha_1)(\beta_2-\alpha_2)}\left[\frac{(1-e^{\alpha_1})(e^{\alpha_2}-e^{\beta_1})}{\alpha_1} - \frac{(1-e^{\alpha_2})(e^{\alpha_1}-e^{\beta_1})}{\alpha_2}\right] -$$

$$- \left[\frac{(1-e^{\alpha_1})(e^{\alpha_2}-e^{\beta_1})(e^{\alpha_2}-e^{\beta_2})}{\alpha_1^2} -\right.$$

$$\left. - \frac{(1-e^{\alpha_1})(1-e^{\alpha_2})[(e^{\alpha_1}-e^{\beta_1})(e^{\alpha_2}-e^{\beta_2}) + (e^{\alpha_1}-e^{\beta_2})(e^{\alpha_2}-e^{\beta_1})]}{\alpha_1\alpha_2} + \right.$$

$$\left. + \frac{(1-e^{\alpha_2})^2(e^{\alpha_1}-e^{\beta_1})(e^{\alpha_1}-e^{\beta_2})}{\alpha_2^2}\right]\cdot\left[\frac{m_{21}\alpha_1^2 + l_{21}\alpha_1}{(\alpha_1-\beta_1)(\alpha_1-\beta_2)} - \right.$$

$$\left. - \frac{m_{21}\alpha_2^2 + l_{21}\alpha_2}{(\alpha_2-\beta_1)(\alpha_2-\beta_2)}\right]\frac{1}{(\alpha_1-\alpha_2)(e^{\alpha_1}-e^{\alpha_2})}, \qquad 22$$

$$H_2 = \frac{1-e^{\beta_1}}{\beta_1(\beta_1-\beta_2)(\beta_1-\alpha_1)(\beta_1-\alpha_2)}\left[\frac{(1-e^{\alpha_1})(e^{\alpha_2}-e^{\beta_2})}{\alpha_1} - \right.$$

$$\left. - \frac{(1-e^{\alpha_2})(e^{\alpha_1}-e^{\beta_2})}{\alpha_2}\right] - \frac{1-e^{\beta_2}}{\beta_2(\beta_1-\beta_2)(\beta_2-\alpha_1)(\beta_2-\alpha_2)}\left[\frac{(1-e^{\alpha_1})(e^{\alpha_2}-e^{\beta_1})}{\alpha_1} - \right.$$

$$\left. - \frac{(1-e^{\alpha_2})(e^{\alpha_1}-e^{\beta_1})}{\alpha_2}\right] - \left[\frac{(1-e^{\alpha_1})^2(e^{\alpha_2}-e^{\beta_1})(e^{\alpha_2}-e^{\beta_2})}{\alpha_1^2} - \right.$$

$$\left. - \frac{(1-e^{\alpha_1})(1-e^{\alpha_2})[(e^{\alpha_1}-e^{\beta_1})(e^{\alpha_2}-e^{\beta_2}) + (e^{\alpha_1}-e^{\beta_2})(e^{\alpha_2}-e^{\beta_1})]}{\alpha_1\alpha_2} + \right.$$

$$\left. + \frac{(1-e^{\alpha_2})^2(e^{\alpha_1}-e^{\beta_1})(e^{\alpha_1}-e^{\beta_2})}{\alpha_2^2}\right]\left[\frac{1}{(\alpha_1-\beta_1)(\alpha_1-\beta_2)} - \right.$$

$$\left. - \frac{1}{(\alpha_2-\beta_1)(\alpha_2-\beta_2)}\right]\frac{1}{(\alpha_1-\alpha_2)(e^{\alpha_1}-e^{\alpha_2})}.$$

From other three invariance conditions (19) can be found certain three parameters of correcting elements $a_{21}(p)$, $a_{23}(p)$, $a_{13}(p)$.

The obtained results can be easily expanded for more simple single circuit pulsed control systems with the aid of a boundary transition in formulae (19).

Literature

1. G. V. Shchipanov, Theory, Calculation and Methods of Planning Automatic Regulators "Avtomatika i Telemekhanika" No. 1. 1939.
2. V. S. Kulebakin. On the Application of the Absolute Invariance Principal In Physi-

cally Real Systems, Doklady Akademii Nauk SSSR, vol.60, No.2.1948
3. V.S.Kulebakin; On Basic Problems and Methods of Increasing the Quality of Automatic control systems. Transaction of II All Union Conference on the Theory of Automatic Control, vol.II,Izdatel'stvo Akademii Nauk SSSR, 1955.
4. N.N.Luzin, Studying the Matrix Theory of Differential Equations "Avtomatika i Telemekhanika" No.5, 1940
5. N.N.Luzin;P.I.Kuznetsov; On absolute Invariance and Invariance to ξ in the Theory of Differential Equations,Doklady Akademii Nauk SSSR, vol.51,No.4 and 5, 1946,vol. 80, No.30, 1951
6. A.G.Ivakhnenko, Elektroavtomatika, No.1,and 2, 1954
7. O.G.Ivakhnenko; Relation of Condition of Inabsolute Invariance with Works on the Synthesis of Structures of High Accuracy Systems "Avtomatika" No.1, 1960
8. Theory of Invariance and Its Application in Automatic Devices, Transactions of the Kiev Conference on the Theory of Invariance , Moscow 1960
9. G.M.Ulanov; Perturbation Control, Gosenergoizdat, 1960
10. O.G.Ivakhnenko; Relation between the Theory of Invariance and the Theory of Differential Regulators Avtomatika No.1,1961
11. M.M.Chumakov. On the Question of Creating Automatic Systems, Invariant to Disturbances Avtomatika No.1,1961.
12. Ya.Z.Tsypkin; Correction of Pulsed Systems Avtomatika i Telemekhanika No.2,1957
13. Ya.Z.Tsypkin; Theory of Pulsed Systems, Fizmatgiz, 1958
14. Julius Tou, Digital Compensation for Control Simulation, Proc.IRE,vol.45,No.9 September 1957.
15. Nakamura ; Investigating High Speed Pulsed Control Systems. Notes from the First International Congress IFAK on Automatic Control, vol.1., No.6, Moscow,1960
16. Yu.V.Krementulo. On the Subject of Absolute Invariance of Open Pulsed Systems Avtomatika No.2,1960, and No. 1, 1962.
17. Ya.Z.Tsypkin; Theory of Discontinuous Control Avtomatika i Telemekhanika vol.10 No.3 and 5, 1949; vol.11, No.5, 1950.

Submitted February 17, 1961

Russian and English Summaries follow

STABLE AND DYNAMIC CONDITIONS OF OPERATION OF AN EXTREMAL SYSTEM FOR CONTROLLING A HYDROMONITOR

Part II*

By

B. Yu. Mandrovskiy-Sokolov

In this report is discussed a step-by-step extremal system with two controlling effects. The object of control of such a system is described in [8]. The task of the extremal system of controlling the hydromonitor is to properly select program elements (arm of repulsing, rate of movement of stream of water after stopping) in order to obtain maximum operational productiveness of the hydromonitor. The magnitude of the repulsing arm changes within certain intervals of time, which are designated by the program and the rate of flow of the stream of water after stopping can change continuously because the program imposes limitations on the moment of change in control influences. In this report is discussed an extremal step-by-step system with two regulating effects at just such limitations.

Method of Searching for the Extremum

The known methods of searching for the extremum [3 - 5] consider the object of control as inertialess and the regulating effects as independent variable values, which change at will, unlimited or limited in value. The time limitations imposed by the program on the moment of change in regulating effects, see [8] stipulates the difficulties in the application of such effective method of searching for the extremum as maximum descent gradient methods, because in this case are necessary simultaneous continuous or periodic changes of all regulating effects [4, 5]. In this case it is advisable to utilize the Gauss-Seidel searching method by searching for the extremum by the "through method" for each regulating effect. It is apparent, that limitations in the movements of change of one of the controlling effects will only increase the time of searching for the extremum. In this case is possible to apply also the "OPKON" type searching method [5].

*The first part of this report was published in No.5 of our Journal for 1961

The natural development of the Gauss-Seidel method will be the method, which is called the multiple interval method. We will assume, that the control interval for another controlling effect ν (another channel) is given by the program and it equals T_2. The control interval for the first control effect μ (first channel) can be selected independently of the program and b K times smaller than the control intervals T_2. that is multiplicity coefficient of periods $K = \frac{T_2}{T_1}$ can be an integral numbered and an irregular fraction as well. Here was investigated only the first case.

The method of multiple intervals consists of such stages:

1. Storing of extremum indicator values φ_0 at values μ_0 and ν_0.

2. Simultaneous imparting to μ_0 and ν_0 values of $\Delta\mu$ and $\Delta\nu$ increments; the sign of increments for the first stage can be arbitrary.

3. Next, along the extend of K-1 control intervals the values μ are given with $\Delta\mu$ increments. The increment signs should be such, that the value φ_1 would approach extremum.

4. In the K-control interval, knowing the increment sign $\Delta\nu$, is designated the value φ_k and the signs of its increments $\varphi_k - \varphi_0$ and $\varphi_k - \varphi_{k-1}$.

Equations which designate the direction of motion of the system in the following control interval (law of control) have the form of

$$\left.\begin{array}{lll} \Sigma_n = -\operatorname{sign}(\varphi_n - \varphi_{n-1})\Sigma_{n-1} & \text{при} & \varphi_n - \varphi_{n-1} > \Delta_1 \\ \text{або} & & \\ \Sigma_n = \Sigma_{n-1} & \text{при} & \varphi_n - \varphi_{n-1} < \Delta_1 \\ \text{та} & & \\ \xi_i = -\operatorname{sign}(\varphi_i - \varphi_{i-1})\xi_{i-1} & \text{при} & \varphi_i - \varphi_{i-1} > \Delta_2 \\ \text{або} & & \\ \xi_i = \xi_{i-1} & \text{при} & \varphi_i - \varphi_{i-1} < \Delta_2 \end{array}\right\} \quad (1)$$

where n = 1, 2,...,K,K + 1,...,2K,2K + 1,... and so on; i = 1, 1,...,2,...,3,3,... and so on; Δ_1 and Δ_2 - sensitivity of the regulator.

The search for the extremum with two controlling effects is realized simultaneously and not by the "through method" like with the Gauss-Seidel method.

The sign of increment in regulation effect may be distinguished not by the difference of extremum indications in two adjacent time intervals, but by the difference of two intervals in the extremum indication within adjacent control intervals. In this case the law of control can be written as

See Page 13a for Equation 2

The block diagram of the extremal step-by-step system with two controlling effects with constant values of the control steps is shown in fig.1. The system performs a search by the multiple interval method.

If we should write for the sake of simplicity, that the linear transmission function for the first control effect μ will be an aperiodic link of the first order, then the linear inertial part of the object (link 1) is described by linear differen

$$\Sigma_n = -\operatorname{sign}\left[\int_{n-1}^{n}\varphi_n dt - \int_{n-2}^{n-1}\varphi_{n-1}dt\right]\Sigma_{n-1}$$

при

$$\left[\int_{n-1}^{n}\varphi_n dt - \int_{n-2}^{n-1}\varphi_{n-1}dt\right] > \Delta_1,$$

або

$$\Sigma_n = \Sigma_{n-1}$$

при

$$\left[\int_{n-1}^{n}\varphi_n dt - \int_{n-2}^{n-1}\varphi_{n-1}dt\right] < \Delta_1 \qquad (2)$$

та

$$\xi_i = -\operatorname{sign}\left[\int_{i-1}^{i}\varphi_i dt - \int_{i-2}^{i-1}\varphi_{i-1}dt\right]\xi_{i-1}$$

при

$$\left[\int_{i-1}^{i}\varphi_i dt - \int_{i-2}^{i-1}\varphi_{i-1}dt\right] > \Delta_2,$$

або

$$\xi_i = \xi_{i-1}$$

при

$$\left[\int_{i-1}^{i}\varphi_i dt - \int_{i-2}^{i-1}\varphi_{i-1}dt\right] < \Delta_2.$$

tial equations

$$X_n = D_1 X_{n-1} + a_1(1 - D_1)\mu_n. \qquad (3)$$

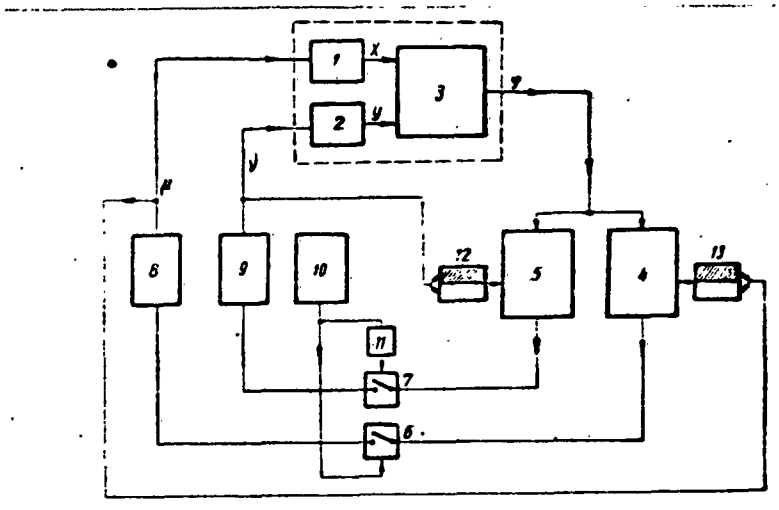

Fig.1. Block diagram of extremal step-by-step system with two control effects with constant control step.
1-2 - linear inertia links of the control object; 3-nonlinear inertialess link of the control object; 4-5 - elements of logical action; 6-7 -pulse elements; 8-9 - operational motors; 10-pulse generator; 11-pulse distrubutor; 12-13 - sign triggers.

For the second control effect ν we obtain analogously

$$Y_i = D_2 Y_{i-1} + a_2(1 - D_2)\nu_i. \qquad (4)$$

The nonlinear inertialess part of the object during approximation of extremal dependence by a paraboloid are equallized

$$\varphi_n = a_1(X_n + \lambda_x)^2 + 2a_{12}(X_n + \lambda_x)(Y_n + \lambda_y) + a_2(Y_n + \lambda_y)^2 + \lambda. \qquad (5)$$

The operational inertialess devices with stable control step have the form of

$$\mu_n = \mu_{n-1} + Q_1 \Sigma_n \quad \text{та} \quad \nu_i = \nu_{i-1} + Q_2 \xi_i. \qquad (6)$$

where a_1, a_2, a_1, a_2, a_{12} - transmission coefficients; $D_1 = e^{-T_1/\tau_i}$, $D_2 = e^{-T_2/\tau_2}$ - parameters, which characterize the inertia properties of the control object; λ_x, λ_y, λ - outer disturbances; Q_1 and Q_2 - control steps for first and second channels respectively.

In equation (3), (4) the values D_1 and D_2 depend upon the time constants of

inertia links and upon the control intervals as well. If the values of the time constants τ_1 and τ_2 are different and $tau_1 \ll tau_2$, then the application of the multiple interval method does not increase the time of searching in comperison with other search methods. In fig.2 is shown the search for the extremum by different methods: by the gradient, fastest descent, Gauss-Seidel and multiple intervals.

See Page 15a for Figure 2

Fig.2. Trajections of motions when searching for the extremum in plane of control effects
I-tau_1 and tau_2; II - $tau_1 \ll tau_2$; a- gradient method; b- fastes descent method; c- Gauss-Seidel method; d-multiple intervals method.

It is assumed, that the control interval and time of determining gradient values are limited. As is evident from fig.2,a, the number of control intervals and trajectories of motion of the working point of the system, as well as time of searching do increase. For Gauss-Seider methods and for methods of multiple intervals the condition $tau_1 \ll tau_2$ has no effect on the increase in searching time, if we take into consideration the reduction in sensitivity.

For the case of the multiple intervals method are revealed additional possibilities of removing the negative effect of the condition $tau_1 \ll tau_2$ for the time of searching by a proper selection of coefficients of period multiplicity K.

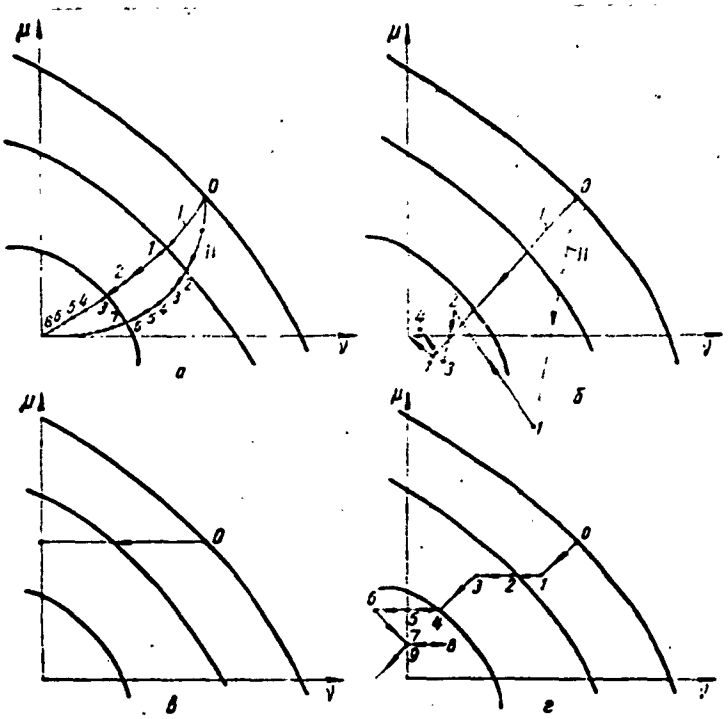

Фиг. 2.

Next we will investigate only the inertialess objects, writing $D_1 = D_2 = 0$.

The disatvantage of such methods fo searching for the extremum, such as the gradient method, fastest descent method, Gauss and Seidel method, is that they assure only the necessary conditions of attaining extremum-partial derivatives for all control effects equalling zero. Consequently, if the extremal function has peculiar lines of the #crest" "saddle" type [5, 6], then the system will not attain actual extremum, but will around a certain point of the "crest" or "saddle". Search by the multiple intervals method at a certain selection of the parameters of the system can be deprived of this disadvahtage.

Fig.3 gives a graphic representation of the movements of the system when the Gauss-Seidel and the multiple intervals methods are in searching for the extremum under identical initial conditions. If the system was in position "0", then , as shown by calculations, it will move along the trajectory 0-1-2-3-4-5-0 at the Gauss-Seidel search method, and by trajectory 0-1'-2'-3'-4'-5'-6'-7'-8' and so on when searching by the multiple intervals method. In this case $\int \varphi_n dt - \int \varphi_{n-1} dt \geq \Delta_1$ (for maximum) or $\int \varphi_n dt - \int \varphi_{n-1} dt \leq \Delta_1$ (for minimum) and the next step will be made in the very same direction, i.e. the system is moving in direction of the general extremum.

The system with multiple intervals of changing the control effects during the application of the control law (2) has even greater possibilities in this respect. As is evident from the given example, at multiple intervals method it is possible to assure adequately the conditions of attaining extremum.

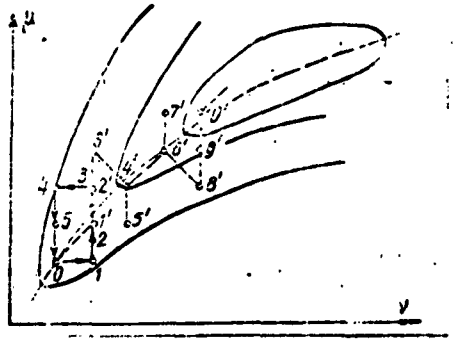

Fig.3. Trajectories of motion in the system when searching for the extremum in the plane of controlling effects $\mu - \nu$ in presence of a crest: by the Gauss-Seidel method (0-1-2-3-4-5-0) and by the multiple intervals method (0-1'-2'-3'-4'-5'-4'-6'-7'-6'-8' etc.).

Established Working Condition of the Extremal Step-By-Step System with Two Controlling Effects.

We will investigate the established movements of the system around the extremum. The operational quality of the control system is estimated by the values of losses due to looking around [1, 2]

$$\bar{H}_p = \frac{\Sigma \varepsilon_i}{1 - j}. \qquad (7)$$

The system have been investigated theoretically and experimentally. Theoretical investigations were carried out by the numerical method, the experimental - by an active model of a step-by-step extremal system with two control effects at the law of control (1).

Just as in the case of an extremal step system with one control effect, auto-oscillations in the system with two control effects depend not only upon the parameters of the system, but also upon the initial conditions. In all investigations were accepted zero initial conditions. For the system with two control effects the magnitude $\bar{H}_p$ depends also upon the coefficient of period multiplicity K. In fig.4 is plotted an oscillogram of motion in the system around the extremum for various K, and in first graph of table 1 are given the values $\bar{H}_p$ determined from these oscillograms.

Results of numerical investigation of the influence of K on the magnitude of losses during the searching for two types of control laws are listed in the following columns of table 1. It should be mentioned, that the value $\bar{H}_p$ depends upon what interval T_1 will be made the first step to γ. Because of this were introduced average values for the loss in tracing

$$\bar{\bar{H}}_p = \frac{1}{K} \sum_{1}^{K} H_p. \qquad (8)$$

It is evident from the table 1, that the losses for tracing have a minimum at K=3 or K=4 (for systems with control laws (2)). Further on the losses for tracing are reduced somewhat (for case (20), and for the law of control (1) they increase.

Losses for tracing for systems with law oc control (2) will be lower than for systems with law of control (1) at small (K=2,3) and high K $\geq$ 5) values of the multiplicity coefficient.

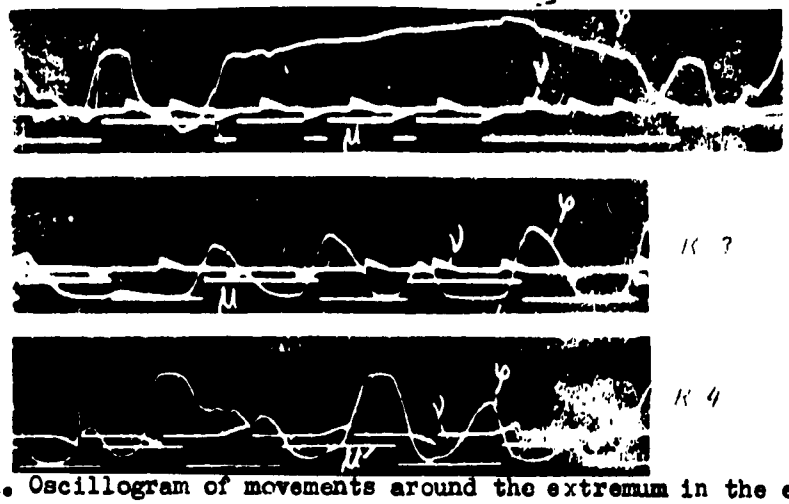

Fig.4. Oscillogram of movements around the extremum in the extremal step system with two controlling effects at various K.

Table 1

Loss for tracing	Magnitude of the Multiplicity Coefficient $K = \frac{T_2}{T_1}$					
	2	3	4	5	6	12
Experimental values $\overline{H}_p$	3,24	1,5	1,78	-	1,92	2,2
$\widetilde{\overline{H}}_p$ at control law (1)	2,63	1,44	1,25	1,5	1,62	--
$\overline{H}_p$ at control law (2)	1,75	1,4	1,75	1,46	1,16	--
$\overline{H}_p$ for the Gauss-Seidel method	1,5	1,5	1,5	1,5	1,5	1,5

By N_1 will be designated the period of oscillations around the extremum during the operation of the first channel of the system (μ) only, when ν = const, and by N_2 - the period of oscillations around the extremum during the operation of the second channel only (ν), when μ = const.

In [7] is shown that at zero initial conditions the minimum losses for tracing will be at N=4 and corresponding value of the control step. Calculations and experiments showed that in case of a system with two control effects the minimum loss for tracing will

be at $N_1 = N_2 = 4$.

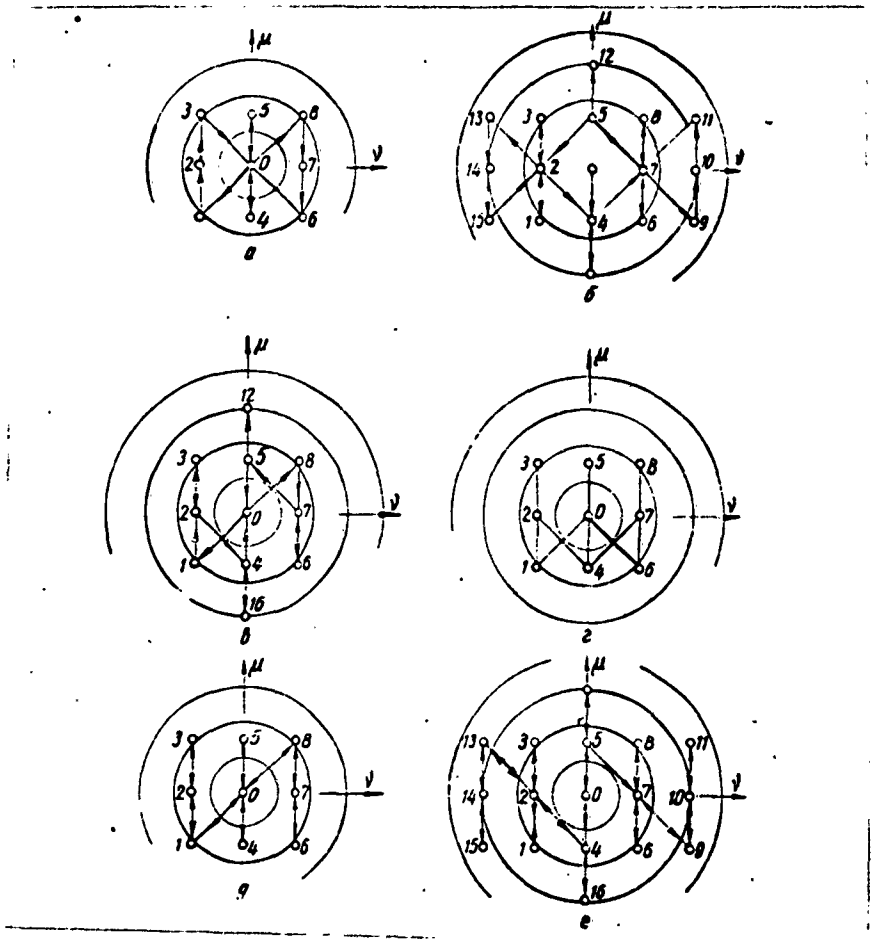

Fig.5. Movements around the extremum in the extremal step system for various initial conditions and various K.
$N_1=N_2=4$; a- at K = 2 the movement of the system will be: 0-1-2-3-0-4-0-8-7-7-6-0-5-0; b- at K = 2 the movement of the system will be: 0-4-7-8-7-9-10-11-7-6-7-5-12-5-2-1-2-13-14-15-2-3-2-4-16--4; c- at K=3 the movement of the system will be: 0-1-2-3-2-4-16-4-0-8-7-6-7-5-12-5-0; d- at K = 3 the movement of the system will be: 0-1-2-3-2-4-0-5-0-4-7-8-7-6-0; e- at K = 4 movement of system will be: 0-1-2-3-2-1-0-5-0-4-0-8-7-6-7-8-0-4-5-0; f- at K = 5 the movement of the system will be: 0-4-2-3-2-1-2-13-14-15-14-13-2-14-16-4-0-5--7-6-7-8-7-9-10-11-10-9-7-8-7-6-7-5-12-5-0.

The results of investigating [1, 2, 7] extremal step systems with one control effect can be utilized successfully with minimum losses of this tracing. Calculation results are given in table 2.

Table 2

PERIODS OF OSCILLATIONS

Tracing losses	$N_1 < N_2$ $N_1 = 4, N_2 = 8$	$N_1 = N_2 = 4$	$N_1 > N_2$ $N_1 = 8, N_2 = 4$
$\bar{H}_p$	2,72	1.44	2.93

In fig.5 is shown the direction of motion about the extremum for various K values and $N_1 = N_2 = 4$.

We compare the value of tracing losses during the Gauss-Seidel searchin method with the case discussed above. For zero initial conditions, figuring, that the control interval ν is by K times greater than T_1, we will obtain a term for tracing loss

$$\bar{H}_p = \frac{(4K+2)\,a_1 Q_1^2 + (2K+4)\,a_2 Q_2^2}{4(1+K)}, \quad (8)$$

provided we write $a_{12} = 0$. In last column of table 1 are given $\bar{H}_p$ values for various K for the very same values of system parameters. From table 1 is evident, that the method of multiple intervals has an advantage over the Gauss Seidel method at certain values of the multiplicity coefficient.

Transient Processes in the Extremal Step System with Two Control Effects

The condition of motion of an extremal step system at a considerable initial deviation from the extremum is characterised by the time of searching - time, within which the system reaches extremum [t_p]. The time of searching will be dependent upon the magnitude of the deviation from extremum and the initial conditions (ξ_0, η_0).

Under other equal conditions the time of searching for the method of multiple intervals will be proportional to the absolute value of maximum deviation coordinate from the extremum of the working point of the system μ_0 or ν_0 (when reading from the extremum). The system will arrive at the extremum by μ and ν respectively during the time

$$t_1 = \frac{|\mu_0|}{Q_1} T_1 \quad \text{та} \quad t_2 = \frac{|\nu_0|}{Q_2} T_2. \quad (9)$$

If $|\mu_0| > K|\vartheta_0|$, then the time of searching equals $t_p = t_1$, and if $|\mu_0| < K|\vartheta_0|$ the time of searching will be $t_p = t_2$. The time of searching by the Gauss-Seidel [4] method is determined by the total number of hours spent on searching for each control effect

$$t_n = \sum_i \frac{|\mu_i|}{Q_i} T_i. \qquad (10)$$

Comparisons of (9) and (10) show, that the time of searchingat the multiple intervals method is smaller than during the Gauss-Seidel method.

We will now discuss the results of experimental and numerical investigations of transient processes in an extremal step system with two controlling effects.

In fig.6 is given an example of the transient process, formulated in accordance with the oscillogram of the transient process in a model of an extremal system with two control effects.

A review of the oscillograms and numerical solutions of equations, which describe the behavior of the system (1)-(6) shows, that equations (9) and all conclusions connected with them are valid only in case when the signs of incremenets of regulation effects converge at the first moment with the signs lambda_X and lambda_Y.

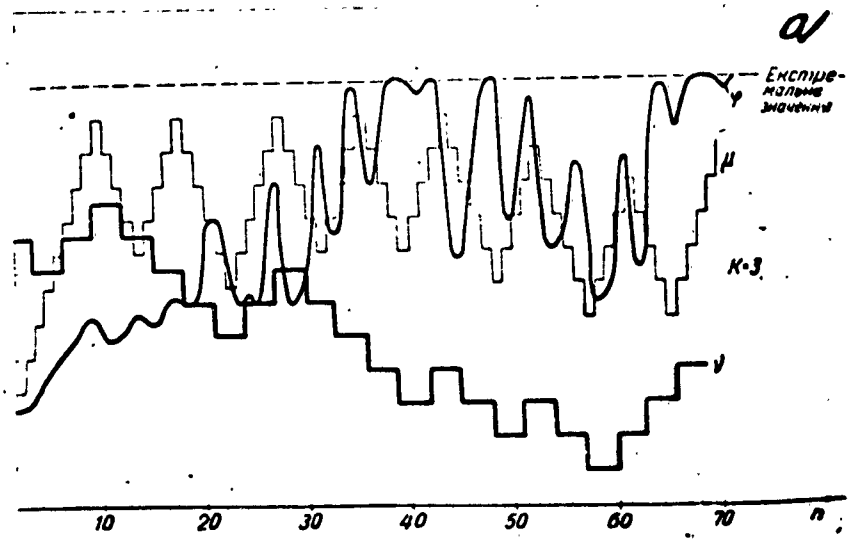

Fig.6. Search for extremum in an extremal-step system with two control effects at initial deviation from extremum. a-extremal values.

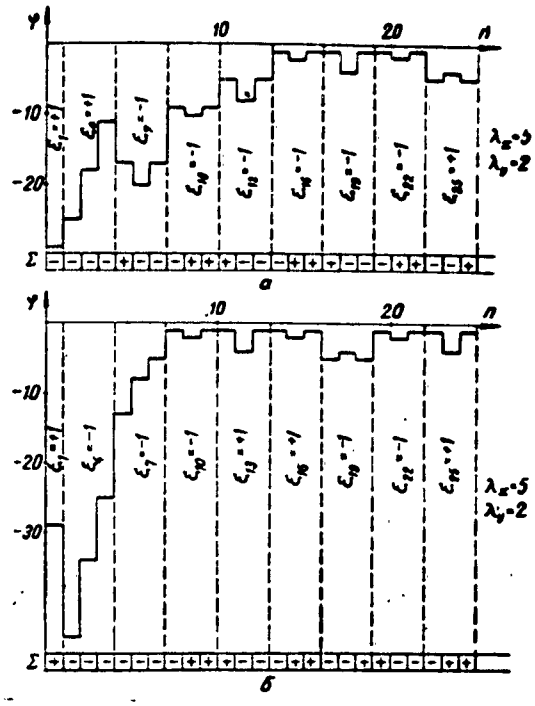

Fig.7. Search for extremum in extremal -step system.
a-at law of control (1); b- at law of control (2).

Equation (9) gives values of minimum possible time of searching. At other initial conditions are possible more complicated movements of the system (fig.6), at which the time of searching for the extremum will be greater. This is also due to the effect of one of the channels on the operation of the other.

A considerable improvement in the operation of the system will be attained when use is made of the integral law of control (2). In fig.7 is plotted the movement of the system to extremum for various laws of control, wherefrom it is evident, that the system with integral law of control is much faster.

Comparison of the obtained results with the results of applying the Gauss-Seidel method show, that even at maximum negative effect of the initial conditions the method of searching with multiple intervals of change in the controlling effects will be much faster. Experimental data and numerical examples of solving equations (1)-(6)

show that increases in the multiplicity coefficient K leads to a certain improvement in transient processes and to a reduction in searching time.

Drift of Extremum in an Extremal Step System with Two Controlling Effects.

Investigated is only the drift of the extremum with constant rate of change in outer disturbances

$$\lambda_x = \beta n, \quad \lambda_y = \gamma n, \quad \lambda = \varkappa n, \tag{11}$$

where beta, gamma and xi- rates of displacement of the extremum over coordinates μ, ν, φ, during the control interval T_1.

It is assumed, that the direction of the drift does not change. The magnitude, which characterizes the motional accuracy of the system beyond the extremum, is analogous to the error of watching in the following system

$$\bar{\bar{H}}_c = \frac{1}{K}\sum_1^K \bar{H}_c = \frac{1}{K}\sum_1^K \frac{1}{j-i}\sum_i^j (\varphi_n - \varkappa n), \tag{12}$$

where $\tilde{\bar{H}}_c$ - average error of watching (following) the extremum.

The effect of the multiplicity coefficient K on $\tilde{\bar{H}}_c$ is shown in table 3. Calculations were made for cases $Q_1 = Q_2 = \text{const}$, beta = gamma K, xi = 0 for two systems with control laws (1) and (2). Minimum of averaged error in following (watching) we have at K = 3. This result is in conformity with the selection of K for the case of constant autooscillations with minimum loss for tracing $\tilde{\bar{H}}_p$. The next investigations were carried out for the system K = 3.

Table 3

Averaged error of observing	Value of the multiplicity coefficient K					
	2	3	4	5	6	7
$\tilde{\bar{H}}_c$ at control law (1)	4,12	2,32	5.1	3,81	4,55	4.9
$\tilde{\bar{H}}_c$ at control law (2)	3,47	1.96	4,5	3,75	2,2	2.86

The effect of the rate of drift on the error $\tilde{\bar{H}}_c$ will be in nature the same as in the extremal-step system with one controlling effect [7]. At given parameters of the system there is a certain critical rate of drift beta_{cr}, gamma_{cr} at which the

system ceases to follow (observe) the displacements of the extremum, and the value $\tilde{H}_c$ rises continuously.

In [7] were brought out the correlations for parametric values of the system, at which exactly the same condition originates. The characteristic of the system with two control effects lies in the fact, that on account of the mutual influence of the control channels the system stops moving after the extremum at slightly greater than Q_{cr} values of the control step at the very same rates of drift.

The effect of control step value on $\tilde{H}_c$ is shown in fig.8. The dependence of $\tilde{\tilde{H}}_c = f(Q_1\ Q_2)$ is of extremal nature. The minimum value $\tilde{\tilde{H}}_c$ will be at a certain value of the control step. Increases and small decreases in magnitude of control step lead to a rise in $\tilde{\tilde{H}}_c$ and subsequent reduction in Q will lead to a loss in working ability of the system, when the extremal system does not move along the side of the extremum, but fluctuates (oscillates) around a certain central position, far away from the extremum.

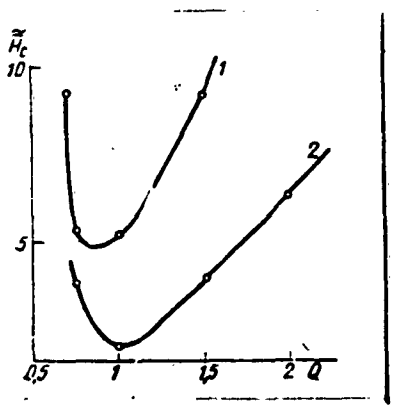

Fig.8. Effect of control step on the value $\tilde{H}_c$ at constant rates of drift beta=const. gamma=const. $Q_1=Q_2=Q$.

1-$\tilde{H}_c = f(Q)$ at control law (1); 2-$\tilde{\tilde{H}}_c = f(Q)$ at control law (2).

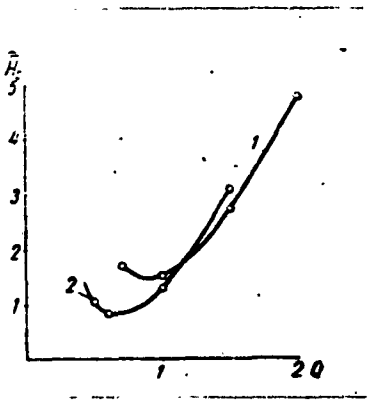

Fig.9. Effect of control step on value $\tilde{\tilde{H}}_c$ at constant rate of drift xi=const.

1-control law (1); 2- control law (2).

Considerable general improvements of the system is attained by applying the integral law of control; the error $\tilde{\tilde{H}}_c$ decreases by 2-3 times (see fig.8).

Calculations and experiments showed, that during the selection of the magnitude

of the control step for given rates of drift it is possible to utilize formulas [7], by raising the Q_{cr} values obtained from them by 10-15%.

We shall examine the influence of uniform drift $\lambda = \chi n$ on the performance of the system. The effect of drift $\lambda = \chi n$ on the extremal step system with one control effect was investigated in [2, 7]. It should be pointed out, that in the system with two control effects $\tilde{H}_c = f(Q)$ we will have extremum only at drifts of system characteristics along the side of the extremum.

The dependence of $\tilde{H}_c$ upon Q is given in fig.9 for systems with two control laws. As is evident from fig.9, the system with control law is superior only at small control step values. The optimum value of the control step should be selected experimentally or by subsequent approximations.

Conclusions

The extremal step system with two control effects discussed in this report and the proposed applications of the multiple intervals method assures the search of the extremum at limitations for the moments of change of one of the control effects with lesser errors, than the solely possible in this case method of Gauss-Seidel (at multiplicity coefficients K = 3).

Of the investigated control laws advantageous is the integral law (2) at which the system works with lesser errors $\tilde{H}_p$ and $\tilde{H}_c$.

Experiments and calculations confirmed the existence of optimum values of control step during drifts of object characteristics, at which $\tilde{H}_c$ is minimal.

Literature

1. A.G.Ivakhnenko, Technical Cybernetics, Gostekhizdat UkrSSR, Kiev, 1959
2. V.M.Kuntsevich. Certain Problems of the Theory of Extremal Step type Systems. Izvestiya Akademii Nauk SSSR, Otd.Tekhn.Nauk, Energetika i Avtomatika No.5, 1960
3. A.A.Fel'dbaum; Computers and Automatic Systems, GIFML, Moscow 1958
4. R.I.Stakhovskiy, On the comparison of Certain Search Methods for an Automatic Optimizer. Collection of Reports on the Theory and Application of Discrete Automatic Systems, Izdatel'stvo Akademii Nauk SSSR, Moskva 1958
5. R.H.Macmillan, N.W.Rees, Automatic Control Systems (Part 2) Process Control and Automation, vol.7 No.12, December 1960
6. S.L.H.Clarke, Correspondence, Process Control and Automation, vol.8, No.2, Ber.1961.
7. B.Yu.Mandrovskiy-Sokolov; Comparing Various Extremal Control Systems of

Controlling a Hydrominitor; Stable and Dynamic Working Conditions for Controlling a Hydromonitor, No.1.Avtomatika No.5,1961

8. B.Yu.Mandrovskiy-Sokolov. Comparing various Extremal Control Systems for Controlling a Hydromonitor. Report presented at the II All Union Conference on Hydromining Izdatel'stvo VNIIGidrougol', Novokuznetsk, 1960

Submitted,Febr.7,1961

Russian and English summaries included

On the Theory of Functional Generators with Cathode Ray Tubes

by

O.I.Petrenko

In This report is discussed the problem of transforming a graphic image of an analytical or exprerimentally obtained function of a certain variable in form electric load for subsequent utilization at measurements and adjustment of various equipment or for introduction into vomputers.

Among the developed devices probably the best known one is the photo-former [1-10] where the ray of the CRT, which is utilized as element of the follow up system, runs along the edge of mask profile, of the mask applied to the screen of the tube. The photo-former can be used wherever it is intended to generate electric pulses of some form or another, but basically it is used in electron modulating devices. Of the photometer is than required an accuracy of no less then 0.5 - 1%, as well as rapid action, which assures the time of increase of the output load of not more than 1% of the entire time of determination. This for example, at a determinst ion time of 10 msec requires the application of a photoformer with a pass band of more than 5 kc; for a satisfactory repetition of results the level of output noise should be 60-80 db of maximum output amplitude.

Equations of System Statics

Mode of Operation. The operation of the photoformer are in accordance with the following principle. In front of the screen of the CRT is placed a mask, the profile of which is made in conformity with a given nonlinear dependence for reproduction (fig.1).

The light from the spot on the screen through an optical system goes to a photomultiplier, connected over a amplifier to the vertical-deflecting plates of the tube. To the very same amplifier arrives the bias load V_0 necessary for pre-adjustment of

the beam (ray) along the so-called zero line of the photomultiplier, which is placed much higher than the edge of the mask in case, when the light does not reach the photo cathode. On the horizontal-deflecting plates of CRT is situated the enveloping load V_x.

The closed ring of screen-photomultiplier-amplifier-vertical-deflecting plates screen form an electron-optical follow system (follow-up system).

The polarity of the output amplifier is such that the output signal, if the photo cathode is illuminated, tries to lower the spot, moving same in direction of the mask. When approaching the edge of the mask further lowering of the ray causes reductions in the area of the point, which is illuminated on the screen, and together with it also reduction in photo stream of the photomultiplier, that is reduction in load V_f, which is on the amplifier.

These reductions last until, when the difference between the initial values of the load V_0 and load reduction from the photo stream V_f at an adopted amplification factor will assure on the vertical-deflecting plates a load, necessary for focusing the ray (beam) along the edge of the mask. If the load V_x is changed in accordance with the linear law, then the ray envelopes the entire profile of the mask, i.e., the load on the vertical-deflecting plates will change in conformity with the given nonlinear dependence.

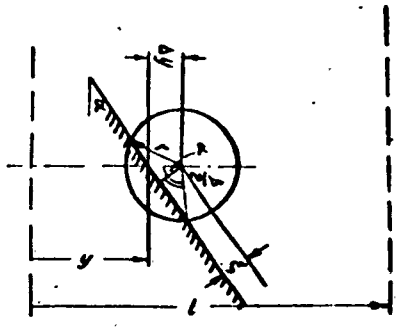

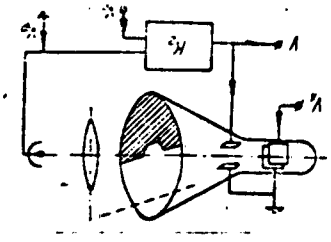

Fig.1 Block-Diagram of a Photoformer Fig. 2 Designations of Valu U

In Figure 1 is shown a tube with electrostatic control, that is why such a tube can be utilized with magnetic deviations. But if a high speed value is necessary, a tube with electrostatic control is considered the best.

The spot "runs" over the screen of the mask along the strech of the useful length of the scanner on the screen of the tube , but the light quantity, which is on the photocathode, will different for various positions of the spot. This means , that a part of the spot, which is covered by the mask, may change during the movement of the ray, and the error of the output signal will be different for various positions of the spot. The fact is, the edgeof the mask and the photomultiplier form and "error detector" in the servo system of the photoformerm i.e.there is a certain error signal, which controls the system. However,it is, as a rule, small in relation to the application of a sharp feedback. In addition to this error, which originates from the very mode of operation of the device, there are also other errors, which are causedby the imperfection of the system. As it will be shown later on , in principle they can be eliminated.

Linearity conditions of the system. We will assume ,turning to fig.2, that the spot is situated over 1 above the zero line of the mask (i.e.the distance between the zero line of the mask and the zero line of the photomultiplier equals 1) and the positionsof the line are such , at which its part S_T ($0 < S_T < \Omega r^2$) is covered by the mask.

A change in u designates the amplitude of the amplitude of the function in mm, and Δu - absolute error of its designations.

To continue the analysis, it is necessary to designate the value of the undarkened part of spot S, the light of which affects the photocathode. This can be done ,when assuming, that either the spot and the functional mask are situated in one area,which is only the light ray, perpendicular to the mask, may reach the photocathode.In practice such assumption will be valid, if the paralax of the optical system is made small.

The spot is characterized by a certain distribution of light intensity. If it

is well focused, then this distribution has an annular symmetry and its most important characteristics will be the maximum hermeticity of the flow j and the radius of the spot r.

We will designate the radius r as a radius of the spot with intensity J_0 which gives the very same luminous flux, as real luminous distribution. The mask is approximated with a straight line with inclination a, equal to the inclination of the tangent at the corresponding point.

As is known, the area of the segment equals

$$S_T = \frac{r^2}{2}(\beta - \sin\beta). \qquad (1)$$

By introducing designations $\frac{x_i}{\Delta y} = \cos\alpha$ and $\cos\frac{\beta}{2} = \frac{x_i}{r} = Z$ (fig.2) we will finally obtain

$$S_T = r^2(\arcsin\sqrt{1-Z^2} - Z\sqrt{1-Z^2}). \qquad (2)$$

The area of the undarkened part, standardized with respect to the area of the spot, equals

$$U = \frac{\pi r^2 - S_T}{\pi r^2} = 1 - \frac{1}{\pi}(\arcsin\sqrt{1-Z^2} - Z\sqrt{1-Z^2}). \qquad (3)$$

A painstaking analysis (fig.3) shows, that this dependence can be approximated by a straight line in the zone $-\frac{1}{2} \leq z \leq \frac{1}{2}$.

We will arrive to the vary conclution, if we will discussed other approximations, when the mask is approximated in such a rinf in radius, as well as the radius of curvature in the corresponding point, and the distribution of the luminous a spot is subject to the normal law of Gauss distribution with dispersion, equalling to the radius r[9].

In this way, in the main general case the dependence U = f(Z) can be approxima ted by a straight line

$$U = U_0 + mZ \qquad (1)$$

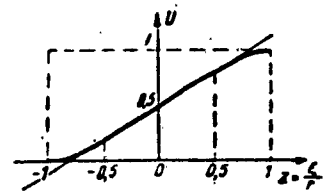

Fig.3. Linear approximation of nonlinear dependence U = f(z).

in the zone $|Z| \leq \frac{1}{2}$, for which is correspondingly $\frac{1}{4} \leq U \leq \frac{3}{4}$, if $U_0 = 0.5$ and m = 0.5. It means that the real nonlinear system is approximated by the linear depend-

ence in limited zone, which is accepted for effective.

On the other side, $$|Z| = \left|\frac{\xi}{r}\right| = \left|\frac{\Delta y \cos\alpha}{r}\right| < \frac{1}{2}, \quad 4a$$

hence the absolute error has the form of

$$\Delta y < \frac{r}{2\cos\alpha}. \qquad (5)$$

from the later expression, is individually evident:

a) the better the rays are focussed and lesser the dimension of the spot of the CRT, the smaller is the absolute errors of reproduction;

b) the greater the angle of inclinations of the mask, the greater is the errors. This points toward the fact, that when trying to generate high frequency in the performance of the system, creates additional difficulties and errors;

c) and finally, the value of the absolute error does not depend upon the value of the very ordinate of the y function.

Introduction of the basic equations of the system. When formulating the basic equations of the photoformer system, we must not forget that the ring of the feedback is made for the stable of the flow. Under the action of the spot in the zero linear of the photomultiplication decreases downward of the edge of the mask, i.e., in conformity of Figure 1.

$$UK = l - y - \Delta y, \qquad (6)$$

where K [mm] - general coefficient of the general transformation system, in general case equal to the product of three multiples.

$$K = K_1 K_2 K_3. \qquad (7)$$

The first multiple K_1, is equal

$$K_1 = \Phi_k \sigma M R_\phi, \qquad (8)$$

is the coefficient of amplification of transformation of the position of the ray in the electric signal. Here F_k - stream of light, which affects the photocathode of photomultiplier, σ sensitivity of photocathode of photomultiplier, -coefficient of amplification of photoamplifier along the stream, R_ϕ - anotic intension of photoamplifier, K_2 - coefficient of amplification of the applied electron amplifier, and K_3 is designated by the coefficient of amplification of the transformation of the electric signal in the displacement of the stream, i.e., the sensitivity of plates with $\left[\frac{\text{mm}}{\text{в}}\right]$ of a CRT.

along the stream, R_f - anotic intension of photoamplifier, K_2 - coefficient of amplification of the applied electron amplifier, and K_3 is designated by the coefficient of amplification of the transformation of the electric signal in the displacement of the stream, i.e. the sensitivity of plates with $\left[\frac{mm}{6}\right]$ of a CRT.

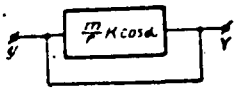

Fig.4. Block-diagram of a follow-up system of a photoformer

Substituting (4) in (6) and figuring, that $xi = \Delta y \cos a$, i.e. $(U_0 + m\frac{\Delta Y \cos a}{r}) K = 1 - y - \Delta y$, we will obtain a term for absolute error of the system -

$$\Delta y = -\frac{y - l + U_0 K}{1 + \frac{mK}{r}\cos a}. \qquad (9)$$

In view of the fact, that the zero line of the mask is our coordinate hight, then it is desired, that at $y = 0$ there should be no errors, i.e. $\Delta y = 0$. As is evident from (9), this is attained by a certain selection of load of initial displacement of the spot, namely

$$V_0 = \frac{l}{c} \approx \frac{0{,}5K}{c}. \qquad (10)$$

The initial establishment of the stream with the aid of simple limitation can be done automatically.

When realizing condition (10) the expression for the relative error is simplified into form

$$\frac{\Delta y}{y} = -\frac{1}{1 + \frac{mK}{r}\cos a}. \qquad (11)$$

On the basis of the latter expression the photoformer can be represented by a block diagram of a simple follow up system with one hundred percent feedback and amplification coefficient of open ring, equalling $A = \frac{mK}{r}\cos\alpha$ (fig.4). In conformity with this block diagram the general deviations of the spot from the zero line of the mask, which is designated by the output of the follow up system, equals

$$Y = \frac{A}{1 + A} y = \frac{\frac{mK}{r}\cos a}{1 + \frac{mK}{r}\cos a}. \qquad (12)$$

and the output load, which changes from plate

$$V = \frac{Y}{C}. \qquad (13)$$

These are the static equations of the photoformer.

Signal to Noise Ratios and Components of the general Error of the Device.

It is very important, that the noise level at the output of the photoformer should be low. The available level of noise and the nature of the latter ones may be divided into such groups:

a) the noise of a photomultiplier, which is the basic form of noise at the output and bears the nature of amplitude modulation;

b) changes in intensity of screen illumination, first of all, through actual loads of the tube, which produce the noise component mainly with a frequency of 50 c, on the other hand, through the heterogeneity of screen luminsphote. For example, at deviations of the order of ± 35 mm is evident a noticeable unfocusing of the ray, in connection with which the dimensions and intensity of the luminous spot changes with the length of the scanning.

To additional error sources can be referred the nonlinearity of the output characteristis of the deflecting plates of the tube, inaccuracies in the preparation of the mask, errors in optical system, changes in coefficient of amplification by the current of the photomultiplier in time, drift of zero and so on.

It was shown experimentally that the most important of these is the noise of the photomultiplier and changes in luminosity intensity of the screen. The latter can be reduced considerably when activating the tube with stabilized loas sources, and also by applying a local narrow band ring of feedback from the output of the additional element, situated between screen and mask, on the control grid of the tube , which controls the luminosity, as result of which the luminous intensity of the spot can be stabilized with limits of ± 1%.

We will discuss more definite noise of the very photomultiplier, As is evident [12], the signal-noise ratios for the stream of the photocathode are designated by expression

$$\frac{I_{cep}}{I_{ш}} = \sqrt{\left(\frac{I_{cep}}{2e\Delta f}\right)\left(\frac{1}{1+\frac{I_T}{I_{cep}}}\right)}, \qquad (14)$$

where I_{ser} and I_T - respectively the mean values of the useful signal and the dark current of the photomultiplier, Δf - frequency band pass of the system.

Expression (14) shows that the signal/noise ratios is greater at higher signal current, in spite of the fact, that the absolute value of noise rises. Another factor under the sign of the radical considers the decreases in signal/noise ratio through the dark current.

In accordance with the previously introduced designations $I_{ser} = \Phi_k \sigma$ and during their changes in the range $I_T \leqq I_{ser} \leqq \infty$ expression (14) is changed into form of

$$\frac{I_{cep}}{I_ш} = (0{,}7 - 1{,}0)\sqrt{\frac{I_{cep}}{2e\Delta f}} = (0{,}7 - 1{,}0)\sqrt{\frac{\Phi_k \sigma}{2e\Delta f}}. \qquad (15)$$

This term is valid for the photocathode, in the anode ring it will be different due to the fluctuation of the coefficient of secondary diode emission. Maximum reduction can be of the order $\frac{1}{3}$.

For reliable operation of the system it is necess ry to have certain signal/noise ratios (of the order of 8-10), which imposes conditions as during the selction of loads $R_н$ and working condition of the photomultiplier, as well as on the frequency characteristic of the equipment. The noise intensity at the output of the photoformer equals

$$V_ш = I_ш M R_ф \frac{K_2}{1 + A}, \qquad (16)$$

where the coefficient of noise intensity amplification was taken for a closed system.

Taking into consideration that $A = \frac{mK}{r} \cos\alpha \gg 1$ and utilizing expressions for K and I_{ser}, we will finally obtain

$$V_ш = \frac{r}{cm \cos\alpha}\sqrt{\frac{2e\Delta f}{\Phi_k \sigma}}. \qquad (17)$$

In this way, the higher the sensitivity of the photomultiplier and the greater the luminous stream, which reaches the photo cathode, the greater are the signal-noise ratios and the lesser is the noise intensity at the output. On the basis of (13) and (17) we obtain a corresponding expression

$$\frac{V_ш}{V} = \frac{r}{my \cos\alpha}\sqrt{\frac{2e\Delta f}{\Phi_k \sigma}}. \qquad (18)$$

STOP HERE

where it is the calculated parameter.

Minimum light stream of the spot. We will find the minimum value of the light stream, which gives the necessary signal/noise ratios at given band pass Δf.

It is evident from (18) that

$$\Phi_к = \frac{2e\Delta f}{\sigma}\left(\frac{I_{сер}}{I_{ш}}\right)^2. \qquad (19)$$

But the current, which reaches the photomultiplier, is only part of the general current Φ_{max}, irradiated by the spot of the electron ray tube ERT and weakened by the edge of the opaque mask, optical system, and also by the non-conformity in spectral ratio of the emission nature of the luminophore and spectral characteristic of photomultiplier, that is

$$\Phi_к = UTk\Phi_{макс}. \qquad (20)$$

In this term T - transmission coefficient of optical system, k -coefficient of interrelation of spectral characteristics, which in general case equals

$$k = \frac{\int_{\lambda_1}^{\lambda_2}\left(\frac{P}{P_{макс}}\right)_\lambda\left(\frac{\sigma}{\sigma_{макс}}\right)_\lambda d\lambda}{\int_{\lambda_1}^{\lambda_2}\left(\frac{P}{P_{макс}}\right)_\lambda d\lambda}, \qquad (21)$$

where $\left(\frac{P}{P_{max}}\right)$ - respective spectral emissive characteristic of the luminophore, P_{max} - maximu light current per unit of radiation length, $\left(\frac{\sigma}{\sigma_{max}}\right)_\lambda$ and σ_{max} - respective and maximum sensitivity of photocathode, λ_1 and λ_2 - boundaries of emissivity characteristics.

The maximum value of the light current Φ_{max} of the spot is measured by the focusing of the ray, accelerating intensity, type of luminophore, its effectiveness and maximum permissible loads, i.e. by the selected brightnesses and dimensions of the spot magnitude Φ_{max} is designated. In this way, equations (20) assist in the selection of the optical system.

Optical System. The task of the optical system is to reduce the parallax (and to justify the assumptions, made during the calculation of the expression for U) and transmission of maximum light current from the spot on the screen of the tube to the

photocathode which, as it was shown, decreases the noise level at the output of the device.

An apparent way of nullifying the parallax lies in the arrangement of the spot (or in the mentioned image) in the plane of the functional mask. This can be done perhaps ideally in the system, where the spot is focused on the mask with the aid of a lens and the undarkened light from the latter is picked up with the aid of another condensation lens on the photocathode (Figure 5a).

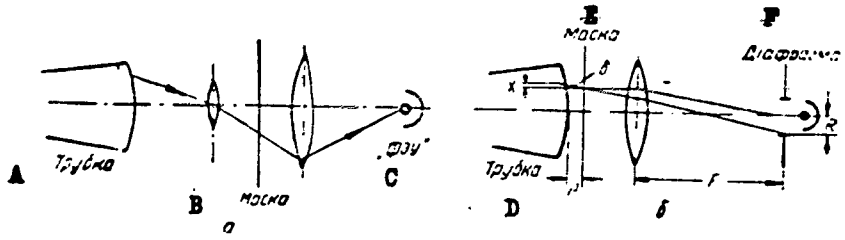

Figure 5 - Types of optical systems; a-tube; b-mask; c-"FZU"; d-tube; e-mask; f-diaphragm.

The transmission coefficient of such a system for a single optical modification equals

$$T=\frac{1}{16}\left(\frac{D}{F}\right)^2 T', \qquad (22)$$

where $\frac{D}{F}$ - respective lens aperature; T' - transmission coefficient of condansation lenses, which is characterized by losses due to repulsion and absorption in the optics and it equals normally 0.75. Practically the value T can be of the order of $(2\text{-}5)\cdot 10^{-3}$.

The disadvantage of such a system is its high sensitivity as to the disposition of lenses.

The fact is,there is no real necessity for removing the entire parallax,because there are more real factors which bring in the error.

It is therefore reasonable to try a simple system (Fig.5b) with the mask situated directly along the screen of the tube, for which

$$T=\left(\frac{R}{F}\right)^2 T', \qquad (23)$$

where R - radius of the diaphragm along the photomultiplier, F - focal distance of the lens.

Maximum values of the parallax, x, which is characterized by maximum angle δ between the optical axis and the ray from the screen, which passes through the opening of the diaphragm, equals

$$x = p \operatorname{tg} \delta = p \frac{R}{F}, \qquad (21)$$

where p - distance between spot and functional mask.

By a compromise solution it is possible to obtain a value T of the very same order as in the system, shown in fig.5a, and do away with the value x, which can be disregarded. The adjustments of the system in this case are noncritical.

Dynamic Characteristic of the Device

General aspects. When discussing the dynamic operational condition of the device we utilize the method of radical (basic) hodograph and the analysis of distributing zeros and poles of the transmission function of the system, which assures simultaneous control over frequency and transient characteristics of the system [14, 15].

At the beginning we shall establish an accurate form of this transmission function. The frequency-dependent member is introduced thanks to the luminophore of tube screen. All fluorescent screens have a certain time of afterglow, which is characterized by the average life span of the carrier charges.

In consequence of the afterglow additionally to the light from the element of the screen, which is being irradiated at the given moment, the photocathode of the photomultiplier is also affected by the light from the point of the screen, which has already been abandoned by the ray. A highly important factor is the form of the damping characteristic. For many luminophores this characteristic is subject to an exponential law of constant time T_0, which gives a drop in frequency characteristic - $\frac{20 \text{ db}}{\text{dek.}}$

Encountered are also luminophores with drop in illumination governed by a

hyperbolic or any other complex law, which is made up of a number of exponents [17].

The electron part of the feedback link, which cuts in ordinarily one or two amplification cascades (stages), brings in its time constant T_p, but for the most part

$$T_n < T_e. \tag{25}$$

Considering the above stated, the amplification coefficient of the open link equals

$$A = \frac{A_0}{T_e T_n} \cdot \frac{1}{\left(p+\frac{1}{T_e}\right)\left(p+\frac{1}{T_n}\right)}. \tag{26}$$

The basic equations of the photoformer (15) acquire the form of

$$y = \frac{A_0}{T_e T_n} \frac{1}{\left(p+\frac{1}{T_e}\right)\left(p+\frac{1}{T_n}\right)+\frac{A_0}{T_e T_n}} = \frac{A_0}{T_e T_n} \frac{1}{p^2+2\xi\omega_n p+\omega_n^2}, \tag{27}$$

where

$$2\xi\omega_n = \frac{T_e+T_n}{T_e T_n} \tag{28}$$

and

$$\omega_n^2 = \frac{A_0+1}{T_e T_n} = \frac{\frac{mK\cos\alpha}{r}}{T_e T_n}. \tag{29}$$

As is evident from [14] the frequency as well as the transient characteristic of such a system are fully designated by the values ω_n and ξ, which characterize the parameters of complex poles of transmission functions.

For example the band pass of the system, which is designated as a frequency, at which a 3 db amplification is lower than the zero frequency amplification, equals

$$\Delta f = 2\pi\omega_n \sqrt{1-2\xi^2+\sqrt{2-4\xi^2+4\xi^4}}. \tag{30}$$

At xi $<$ 0.707 the frequency characteristic has a projection (rise) in frequency

$$\omega_m = \omega_n \sqrt{1-2\xi^2}, \tag{31}$$

equalling

$$M = \frac{1}{2\xi\sqrt{1-\xi^2}}. \tag{32}$$

In the latter case the transient process in the system is also characterized by

FIRST LINE OF TEXT

considerable overcontrol. In this case the half period of oscillation damping, of oscillations which are superimposed, equals

$$t = \frac{\pi}{\omega_n \sqrt{1-\xi^2}}; \tag{33}$$

the time constant of their attenuation is $\frac{1}{\xi\omega_n}$, and the maximum value of overregulation with respect to the amplitude of the gradual input function has the form of

$$M_p = \frac{\xi\pi}{\sqrt{1-\xi^2}}. \tag{34}$$

In immediate systems rapid action is designated by time necessary to attain at the output of the system a value, which differs by a certain percentage from the statical. For example, a difference of 2% between the mentioned values is attained within the time

$$\tau > 4\frac{1}{\xi\omega_n}. \tag{35}$$

Consequently, the rapid action of the photoformer system according to (28) and (29) at selected value xi = 0.707 is designated by the term

$$\tau \cong 5{,}7\sqrt{\frac{T_e T_n r}{mK\cos\alpha}}. \tag{36}$$

Frequency Characteristic of Photoformer. In a real photoformer the working frequency is designated not by expression (30), but by the conditions of realizing linear approximation of the system $|Z|\angle\frac{1}{2}$.

The fact is, by utilizing expression (11), it is possible to write

$$Z = \frac{\xi}{r} = \frac{Ay\cos\alpha}{r} = -\frac{\cos\alpha}{r(1+A)}y, \tag{37}$$

hence

$$\frac{Z}{y} = -\frac{\cos\alpha}{r}\frac{\left(p+\frac{1}{T_e}\right)\left(p+\frac{1}{T_n}\right)}{\left(p+\frac{1}{T_e}\right)\left(p+\frac{1}{T_n}\right)+\frac{A_0}{T_e T_n}} = \frac{\cos\alpha}{r}\frac{\left(p+\frac{1}{T_e}\right)\left(p+\frac{1}{T_n}\right)}{p^2+2\xi\omega_n p+\omega_n^2}. \tag{38}$$

Distribution of zeros and poles of given function in a complex area is shown in fig.6,a. As is evident, the closest to the origin of coordinates is zero in point $\frac{1}{T_e}$; it will characterize the behavior of the system at lower frequencies.

Because of the fact, that the analytical expression for the frequency characteristic in this case is very complex, we will construct an asymptotic frequency characteristic of the entire system, applying the law, that zros give a raise in the characteristics of $\frac{20db}{dek}$, and complex poles a reduction by $-\frac{40db}{dek}$ at a frequency ω_n.

The general fom of such characteristic is shown in fig.6 b.

In the most complex case $y = \pm y_{max}$ the characteristic can be utilized only below the line $\left|\frac{Z}{Y}\right| = \frac{1}{2Y_{max}}$, which takes place at a frequency

$$f_0 = \frac{1}{2\pi T_e}\frac{m}{2}\frac{K}{y_{макс}}, \qquad (39);$$

if both time constants T_e and T_i are separated considerably

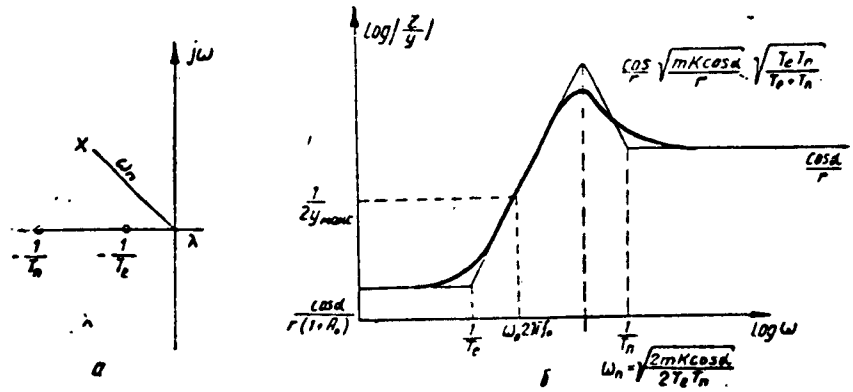

Fig.6. Distribution of zeros and poles for function (38) and approximate form of frequency characteristic.

Taking into consideration (11) and (5) at a condition, that $m = 0.5$ and $\frac{mK}{r}\cos\alpha \gg 1$, expression (39) is reduced into simple form

$$f_0 \approx \frac{1}{2\pi T_e}. \qquad (40)$$

In this way, the frequency range of linear operation of the system f_0 is characterized by maximum time stability in the system.

This frequency range should not be mixed up with band pass (30), which designates the rate of transient processes in the system.

When frequencies are greater than f_0, during the reproduction appear nonlinear distortions, causing "cut offs" of various parts of the functional mask.

When constructing a photoformer the values T_c, T_p and K are selected so, that the system should be linear; the time of rapid action is short; the noise level characterized by the band pass, moderate, not affecting the capability of the spot to track the profile of the mask.

Further reduction in the noise level is attained by placing a filter behind the feedback link, i.e. at the output contour.

Compensating the effect of the screen's afterglow. Known methods of improving the characteristics of immediate systems [16] for the photoformer allow to increase its rapid action, but do not affect the frequency range of the linear operation of the system.

Possible solutions are the introduction into the transmission function of an open system of quadripoles with frequency characteristic, which grows with the rate $\frac{20db}{dek}$, which in the complex area corresponds to the introduction of "zero", compensating the undesired pole for the effect of screen's afterglow.

Practically this can be easily determined by means of the cascade fig.7 oriented directly behind the photomultiplier which has in the cathode ring an RC-linkage of constant time, which equals exactly T_c.

As a matter of fact, the amplification factor of such cascade upon the fulfillment of condition $SZ_k \gg 1$ in the entire frequency range, which interests us, equals

$$Ky = \frac{SR_2}{SZ_k} = \frac{R_2}{R_k}(1 + pT_c). \qquad (41)$$

We shall briefly examine , how the compensation, which is being introduced, affects the signal/noise ratio

See Page 41a for Figures 7 - 8

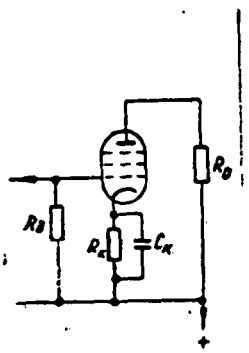

FIG. 7 Circuit of Compensation Cascade

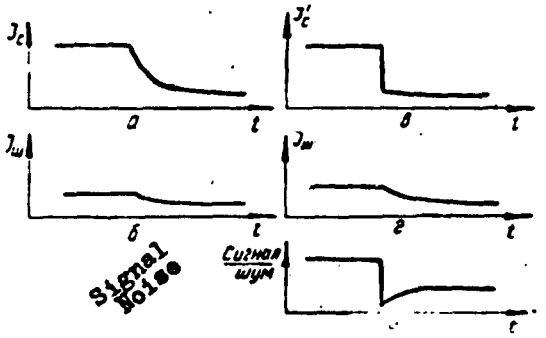

FIG. 8 Formation of "Noise Obliteration" When Spot Changes From White to Black

FIRST LINE OF TEXT

First of all, noises, which are characterized by an integral spectrum, are amplified by the compensation cascade, which has an amplification factor, growing with frequency proportional with the term $\sqrt{1+\omega^2 T_e^2}$.

For the noise stream of the photocathode we will obtain a new expression

$$I_ш \sim \sqrt{2ef_{макс}(1+f^2_{макс}T^2_e)}, \qquad (42)$$

where the frequency f_{max} designates the band pass of the system. At $f^2_{max}T^2_e \gg 1$ the signal to impedance ratio acquires the form of

$$\frac{I_{сер}}{I_ш} = \frac{1}{T_e\Delta f}\sqrt{\frac{I_{сер}}{2e\Delta f}}. \qquad (43)$$

Another undesired consequence of compensation is the so-called phenomenon of "noise obliteration". When the light beam passes over from the luminous zone into the dark one as results of screen's afterglow the current at the photomultiplier will decrease exponentially with time (fig.8,a), the noise level in itself decreases (fig. 8 b).

With the aid of a compensation cascade is restored the form of the signal current (fig.8b), but the noise level remains unchanged (fig.8 d). Consequently in the next moment of time directly behind the transition of the ray from "white" in "black", the signal/noise ratio will be at its lowest (fig.8.e).

In case of a sharp change over from "black" to "white" we will obtain a reverse effect; for the initial moment the signal/noise ratio will be maximum. This is especially important for the photoformer, which functions with a mask in form of graph lines on paper or photo film [10].

The application of a tube with short T_e is more desirable than the introduction of a compensation for the screen's afterglow effect.

4

3

Requirements for elements of the system

The given analysis allows to formulate a number of specific requirements relative to the selection of basic elements of the system.

1

STOP HERE

Cathode Ray Tube. Tube is the main element of the arrangement and the least accurate part of the system; errors, introduced through the imperfection of the tube, are not removed by the feedback linkage. The most important disadvantage of the tube is the nonlinearity of the deflecting system, which appears in the change of sensitivity coefficient along the length of the screen.

This drawback can be removed by introducing a nonlinear compensation beyond the feedback link: by changing the scale of the mask or by applying at the input a correcting gamma-cascade with corresponding characteristics, which was made in accordance with the principle of lump-linear approximation with the aid of diodes.

Another important characteristic is the radius of the spot r. Since the feedback factor of the system is inversely proportional r (11), and the noise level is directly proportional r (16), it is thus very important to obtain the least spot.

The small dimension allows the spot also to track all the details of the mask. The screen should be flat to reduce the distance between spot and mask, and of course, of the parallax.

As pointed out before, the selection of the type of luminophore is also an important factor. On one hand, the amplification factor of the system is directly proportinal to the light stream from the screen Φ_{max}; on the other hand - the noise level is inversely proportional $\Phi^{1/2}_{max}$. Consequently it is necessary to select tubes with greater accelerating intensity and high effectiveness of the screen. In addition, the spectral characteristics of the screen and photomultiplier must be compatible and the screen's afterglow time - short.

Most suitable for this purpose are tubes 18L047A, 13L037M, 13L037A and others.

Photomultipliers. First and above all, the sensitivity of the photocathode should be high to reduce the noise level and to obtain a high signal/noise ratio (14) and (16).[3]

Next, the photocathode should be in one plane with the screen and the area of the cathode should be sufficient to cover the opening of the diaphragm (fig.5 b).

FIRST LINE OF TEXT

This points toward the advisability of utilizing photomultipliers of end type (FEU-25, FEU-31, FEU-35 and others). In finally to raise the signal/noise ratio the dark current of the photomultiplier should be small, which places limitations not only on the selection of FEU but also on the requirements as to its arrangement: anode and diode intensities should be properly selected, the optical system and FEU should be well screened, the photomultiplier and input linkages of the amplifier distributed in an electromagnetic screen. As mentioned, one of the sources of the common error of the installation is the change in amplification along the current of the photomultiplier in the process of operation.

It is necessary to create a stabilization scheme maintaining the general amplification factor within intervals of 10% regardless of time.

Functional mask. It was assumed before that the mask is exactly the necessary thing for the reproduction of the function. But during the manufacture of same there arises a series of difficulties. First of all is selected the material of the mask. It should be nontransparent, easily machineable material without jagged edges and stable to temperature and humidity changes.

Usually black paper or aquadag is used, which is applied directly on the screen of the tube.

In first case the mask is cut out with an a curacy of up to 0.1 mm which gives a relative errors of 0.25%. But, if the mask was made with changed scale for compensation of nonlinearity of the deflecting system, then the requirements for same are increasing.

The best method of manufacturing the mask is the photographic one, when a picture is taken of the function, painted beforehand in larger scale.

Error compensation, error caused by tube, can be attained by such modification of the coordinate system of the mask, which corresponds to the reproduction of the image, which is brought in by the tube. But such a mask can be used only with that particular tube.

STOP HERE

For the possibility of rapidly changing the function during the operation a so-called controlled mask was proposed [11, 13], which represents a rubber bar on adjusted stretchers.

Example of Calculation. It is necessary to built a photoformer with an accuracy of 2% in amplitude and 1% in time.

Total time equals 10 microseconds, which stipulates a rapid action system of 100 microsec.

Output voltage 50 v; noise level lesser than 60 mv.

First we select tube 13L037A with 2% linearity of deflecting system and 90°±3° angle between the lines. The luminophore of the screen of type A has spectral emissivity in the range of 4000-6000 Å with maximum at 4300 Å.

Afterglow time last for 50 microsec, sensitivity of deflecting plates c = 0.37 mm/v.

When the load on the third anode U_a = 3 kv the current of the screen becomes 90 mka; the radius of the spot equals 0.5 mm, which assures a light stream $\Phi_{max} = 10^{-2}$ lum.

Next we select the photomultiplier FEU-24 with end type flat cathode with photocathode sensitivity σ = 25 microamp/lum.

The zone of spectral characteristic is in the range of 3000-6000 Å with maximum of more than 4100 Å, the conformity coefficient of spectral and emission characteristics is approximately equal to k = 0.88.

The dark current of the photomultiplier equals $5 \cdot 10^{-7}$ amp at an anode load of 1800 v, total amplification of current is approximately $3 \cdot 10^6$.

The mean current at the output I_{aver} = 250 microamp at an anode load R_{an} = 56 k.

On the basis of the necessary output signal amplitude and sensitivity of the deflecting plates, we evaluate the dimension of the mask:

$$y = cV = 50 \cdot 0.37 = 18.5 \text{ mm}.$$

Through the curvature of tube screen the useful plane area of the latter is limi-

FIRST LINE OF TEXT

ted to 25-30 mm in vertical and 30-40 mm in horizontal.

Figuring in the transmission coefficient of the disconnecting cathode repeater, we select u_{max} = 20 mm. According to (11) as the given relative error $\frac{\Delta y}{y}$ = 0.02 we will designate A_0=49, which at r = 0.5 mm, m = 0.5 and cos α = 0.25 gives a value K = 196.

The light stream, reaching the photocathode and assuring the selected condition of the photomultiplier, equals $\Phi_k = \frac{I_{aver}}{\sigma M} = 3{,}3 \cdot 10^{-6}$ lm, then the transmission coefficient of the optical system is designated as $T = \frac{\Phi_k}{UK\Phi_{max}} = 7{,}6 \cdot 10^{-4}$ at $U \simeq 0{,}5$.

When selecting the optical system fig.5,b and at a distance between screen and mask of p = 2 mm we will obtain: F = 110 mm, R = 6 mm and maximum error of parallax x = 0.1 mm.

Due to the fact, that $K = I_{aver} R_k K_2 c$, we find the value of the amplification coefficient of the electronic part of the system K_2 = 38.

The frequency range of the arrangement according to (39) equals

$$f_0 = \frac{mK}{2y_{макс}} \frac{1}{2\pi T_e} = 8 \text{ кгц.} \qquad 44$$

It is desired that the electron part of the arrangement should have no smaller band pass, which designates the value of the time constant

$$T_u \leq \frac{1}{2\pi f_0} = 20 \text{ мксек.} \qquad 45$$

At such selection of T_p according to formula (36) we will obtain the rapidity of the system ao 26 microsec.

There is a certain reserve which allows to apply at the input a filter to reduce noise, the level of which according to (17) and according to given values equals 200 mv.

This concludes the basic calculation of the photoformer. Calculation of the electronic part is more simple; especially at given values K_2 and T_p this part can be made with the aid of one differentiation cascade.

2

1

STOP HERE

LITERATURE

1. D. M. MacKay, A high-speed electronic function generator, Nature, vol. 159, March, 1947, p. 406.

2. D. J. Mynall, Electronic function generator, Nature, vol. 159, May, 1947, p. 743.

3. D. J. Mynall, Electrical analogue computing, Electronics Eng., vol. 19, June-Sept., 1947.

4. D. E. Sunstein, Photoelectric waveform generator, Electronics, vol. 22, Febr. 1949, p.100.

5. A. B. Macnee, An electronic differential analyzer, PIRE, November, 1949, p. 1315.

6. H. W. Shultz, J. E. Calvekt, E. L. Buell, The photoformer in Anacon Calculations, Proc. NEC, vol. 5, 1949, p. 40.

7. E. J. Hancock, Photoformer design and performance, Proc. NEC, vol. 7, 1951, p. 228.

8. N. Hamby, A Function generator, Electronic Eng., vol. 30, February 1958, p. 91.

9. E. Elgeskog, Photoformer Analysis and Design, Trans. of Chalmers University, Sweden, 1957.

10. C. N. Pedeksov, A. A. Geklach, R. E. Zennek, A precise electronic function generator, Proc. NEC, vol. 7, 1951, p. 216.

11. A. B. Macnee, A high-speed product integrator, Tech. Report 136, Research Laboratory of Electronics, M. I. T., 1949.

12. M. O. Chechik; S.M. Faynteyn; T. M. Lifshits; Electronic Multipliers, GITTL, 1957.

13. G. Korn, T. Korn; Electronic Modulating Devices, Foreign Literature, Moscow, 1955.

14. D. Traksel; Synthesis of Automatic Control Systems, Mashgiz, Moscow 1960.

15. English

16. Fundamentals of Automatic Control (Edited by V. V. Solodovnikov), Mashgiz, Moscow, 1954.

17. M. M. Gratsianskaya; Visibility of the Signal on the Screen of a Cathode Ray Tube. Scientific Reports of Higher Educ. Inst. Radiotekhnika i Elektronika No. 4, 1958, p. 189.

18. L. Benes; Electrooptical Observation Lines. Automation, No. 6, 1960.

Submitted October 18, 1960.

Russian and English Summaries Included

FIRST LINE OF TEXT

Supporting Structures of Irrigation Channels as Objects of Control

by

Ya.T.Dub

Irrigation systems are often provided with supporting installations for the purpose of maintaining a high water level at certain sections of the channels to assure maximum delivery of water to minor channels. To fully automate irrigation systems it is also necessary to automate these installations. The problem here is to automate the control of the water level at the upper water level of supporting structures. To solve this problem it is necessary to know their static and dynamic qualities. Irrigation channel supports are formed with the aid of sluice-gates, similar to those seen at water reservoirs (main installations) channels.

When the water flows through the sluice-gate openings there is a drop in water pressure, the magnitude of which depends upon the height of opening the sluice-gate and loss of water. A change in height of sluice gate opening of the supporting structure has practically no effect on the magnitude of water delivery into the channels and on its level at low water level of the structure, but only causes a change in the drop and water level at the upper limit of the structure. Consequently, the supporting structure can be considered as an object of control, for which the input value is the change in height of opening the sluice gate, and the output value - the change in water level at the upper boundary of the structure.

The dynamic properties of water heads as objects of control can be determined with the aid of known hydraulic dependences and electrohydrodynamic analogies [1,2]. The electric circuit, analogous to the supporting structure, consists of two in-series connected electric transmission lines L_1 and L_2 (fig.1), to which is hooked up the voltage source E_0, and between which is cut in in-series an ohmic resistor R_q. DC-

LAST LINE OF TEXT

current i_c reduces the value of water delivery into the channels Q_0. In the drawing fig.1. the input value of the control object is presented by the change in resistance value R_d, the output value by the change in voltage U_1 at the end of the first line L_1. It is necessary to determine the transmission and transfer function of the control object. For this we must determine the change in voltage U_1 in the drawing of fig.1. caused by the uneven change in resistance R_d by an inconsiderate value ΔR_d, for example by shunting of part ΔR_d of resistance R_d (see fig.1).

At the time of the transient process the electric power transmission line without windings becomes a certain transient resistance Z(p), which according to [3] equals

$$Z(p)=\sqrt{\frac{R_0+pL_0}{pC_0}}=\rho\sqrt{1+\frac{2a}{p}}, \qquad (1)$$

where rho $=\sqrt{\frac{L_0}{C_0}}$, $a=\frac{R_0}{2L_0}$, R_0, L_0, C_0 - allocated parameters of the line (respectively resistance, inductance and capacitance); p -differentiation operator.

At the initial moment of the transient, at which $p=\infty$, the electric line forms an ohmic resistance, with a magnitude q and, in this way, at an uneven change in magnitude of resistance R_d all parameters of the circuit change by leaps and jumps. The equivalent electric circuit for this case is shown in fig.2 and its consists of three in-series connected resistances R_d, rho_1 and rho_2 through which passes current i_0. Index 1 pertains to the upper level, index 2 - to the lower.

At the moment of closing the contact, shunting a small section of the resistance R_d, the current in the circuit fig.2 changes by leaps and jumps by a value

$$\Delta i_0=\frac{E_0}{\rho_1+\rho_2+R_d+\Delta R_d}-\frac{E_0}{\rho_1+\rho_2+R_d}\approx\frac{\Delta E_0}{\rho_1+\rho_2+R_d}, \qquad (2)$$

where $\Delta E_0 = -i_0\Delta R_d$, $(\Delta R_d < 0)$.

The change in voltage in this circuit is determined by dependences

$$\Delta U_{10}\approx\frac{-\rho_1}{\rho_1+\rho_2+R_d}\Delta E_0$$

and

$$\Delta U_{20}\approx\frac{\rho_2}{\rho_1+\rho_2+R_d}\Delta E_0. \qquad (3)$$

As is evident from the obtained dependences uneven increases in the opening of sluice gates of the supporting structure causes at first an uneven reduction in water level in the low boundaries, and vice versa.

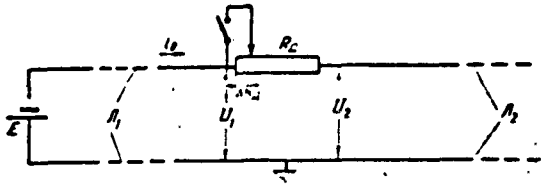

Fig.1 Equivalent electric circuit for supporting structure

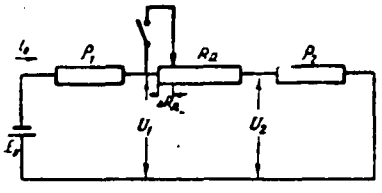

Fig.2. Equivalent electric circuit to determine changes in values at the initial moment of the transient process.

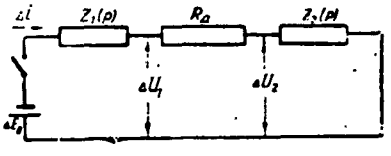

Fig.3. Equivalent electric circuit to determine transmission function of supporting structure.

To determine in the circuit fig.1. the total transient process after shunting part of resistance R_d it is necessary to solve the problem - cutting in constant voltage ΔE_0 to the circuit with in-series connected resistances $Z_1(p)$, $Z_2(p)$ and R_d (fig.3).

The term for the current in operational form is

$$\Delta i(p)=\frac{\Delta E_0}{Z_1(p)+Z_2(p)+R_\Delta}=\frac{\Delta E_0}{\rho_1\sqrt{1+\frac{2a_1}{p}}+\rho_2\sqrt{1+\frac{2a_2}{p}}+R_\Delta}. \qquad (4)$$

Taking into consideration the fact that we are interested in the dynamic characteristic of the control object in the initial period of the transient process, to which high values of operator p do correspond expression (4) can be changed (modified) by approximation

$$\Delta i(p)\approx\frac{\Delta E_0}{\rho_1\left(1+\frac{a_1}{p}\right)+\rho_2\left(1+\frac{a_2}{p}\right)+R_\Delta}=\Delta i_0\frac{p}{p+a}. \qquad (5)$$

where

$$a=\frac{\rho_1 a_1+\rho_2 a_2}{\rho_1+\rho_2+R_\Delta}. \qquad (5a)$$

STOP HERE

The solution of expression (5) has the form of

$$\Delta i(t) = \Delta i_0 e^{-at} = \Delta i_0 e^{-\frac{t}{T}}. \qquad (5b)$$

where T is the time constant.

In this way, at the beginning of the transient process the current at circuit fig.3 changes with in accordance with the law, close to exponential, with constant time

$$T = \frac{\rho_1 + \rho_2 + R_д}{\rho_1 a_1 + \rho_2 a_2}. \qquad (6)$$

The change in voltage $\Delta U_{1д}$ representing the output value of the control object, takes place after the initial jump also with exponential dependence with such time constant T.

After the transient process has been completed in the circuit fig.1 is restored the initial value of the current i_0 and voltage U_2, and voltage U_1 changes by a value $\Delta U_1 = - i_0 \Delta R_д = \Delta E_0$. Consequently, the transmission function of the supporting structure with sufficient practical accuracy can be described by term

$$W(p) = K \frac{ATp + 1}{Tp + 1}, \qquad (7)$$

where $A = \frac{rho_1}{rEo_1 + rho_2 + R_д}$, and T is calculated by formula (6). With that formula we receive easily the transient function, which has the form of

$$h(t) = K\left[1 - (1 - A)e^{-\frac{t}{T}}\right] = K\left(1 - \frac{\rho_2 + R_д}{\rho_1 + \rho_2 + R_д} e^{-\frac{t}{T}}\right). \qquad (8)$$

Dependences (7) and (8) are identical to the ones obtained by us previously [2] for mentioned structures.

The order of magnitudes, which are included in dependences (6)-(8), can be determined for specific structures, by substituting in the formula analogous hydraulic values and their known numerical values.

On the basis of electrohydraulic analogies [2] we will obtain dependences

$$L_0 = \frac{\gamma}{g\omega}, \quad R_0 = \frac{\gamma l}{Q_0}, \quad C_0 = \frac{B}{\gamma}, \quad R_д = \frac{2\gamma z}{Q_0}, \quad \rho = \frac{\gamma}{\sqrt{g\omega B}}, \qquad (8a)$$

where gamma- specific weight of water, g - acceleration force of terrestrial gravi-

tation, ω - area of lateral cross section of the flow . I - slope of free surface of water (piezometric slope), Q_0 - restoration of delivery value in channel, B-width of water stream on its surface, z- difference in levels between upper and lower borders of the structure (fig.4).

The magnitude of the slope of the free surface I_1 at the upper border, where irregular movement of water takes place , equals [1]

$$I_1 = I_0 - \frac{dh_1}{dl}, \qquad (9)$$

where I_0 - inclination of channel bottom, l - distance along horizontal, h_1-depth of stream.

For the irregular movement of the liquid accoding to [1] can be written a differential equation

$$\frac{dh_1}{dl} = \frac{I_0\left[1-\left(\frac{Q_0}{Q}\right)^2\right]}{1-\left(\frac{h_{0\,kp}}{h}\right)^3}, \qquad (10)$$

where Q_0-actual delivery of water at the channel, Q-delivery which corresponds to uniform movement of the liquid at the channel at level h; $h_{0\,crit}$-critical height of flow at delivery Q_0

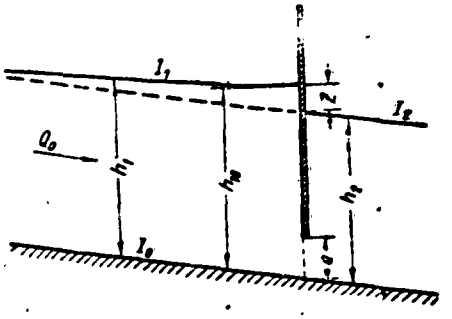

Fig.4. Principal diagram of supporting structure

Taking into consideration the fact that for a majority of irrigation channels the denominator of term (10) is close to unity and by comparing the dependences (9) and (10) between each other, we will obtain a term

$$I_1 \approx I_0\left(\frac{Q_0}{Q}\right)^2. \qquad (11)$$

At the lower border the movement of the water is uniform and, consequently, I_2 =

I_0. Substituting these dependences in formula (6) will obtain after transforms a term for time constant of supporting structures

$$T=\frac{1}{I_0}\cdot\frac{2Q\left(\frac{1}{\sqrt{g\omega_1 B_1}}+\frac{1}{\sqrt{g\omega_2 B_2}}\right)+4Z}{\left(\frac{Q_0}{Q}\right)^3\sqrt{\frac{g\omega_1}{B_1}}+\sqrt{\frac{g\omega_2}{B_2}}}. \qquad (12)$$

All the values, included in formula (12), are the function of the level at upper border h_{10} and delivery of water at the channel Q_0. Calculation shows, that for supporting structures, mounted on irrigation channels of trapezoidal cross section of mean value, time constants, calculated by formula (12), have an order of from hundreds to thousands of seconds.

But for one and the same channel they change to considerable extents. At ranges of change of water delivery to the channel, equalling to three, the time constant of the object can change by ten times or more, whereby greater values correspond to lesser water deliveries. The process of controlling is affected by value A, which is numerically equal to the respective magnitude of the jump in water level at the initial moment of the transient process.

It is evident from formula (7) that the value A is of maximum importance at maximum deliveries of water, for which resistance R_d is minimum, and close to zero at minimum deliveries of water into the channels.

The magnitude of the amplification factor of the control object depends also upon the condition of its operation.

The range of its change can be determined on the basis of the known dependence for the guard opening [1]

$$Q=\mu ab\sqrt{2gz}, \qquad (13)$$

where μ- coefficient of delivery, a-height of opening the sluice gate; b-width of sluide gate opening.

Considering, that at slight deviations from equilibrium state the coefficient μ remains unchanged and figuring, that after completion of the transient process Δ

= 0, we will obtain

$$\frac{\Delta Q_-}{Q_0} = \frac{\Delta a}{a} + \frac{1}{2} \cdot \frac{\Delta z_-}{z} = 0$$

$$\Delta z_- = \Delta h_{1-} = \frac{-2z}{a} \Delta a, \qquad (14)$$

where ΔQ_-, ΔZ_- and Δh_{1-} -inserted values ΔQ_0, ΔZ and Δh_1

On the basis of (14) it is possible to write the dependence

$$K = K_0 \frac{2z}{a}. \qquad (15)$$

To determine the range of change in the amplification factor K it is necessary to know, how the delivery coefficient μ changes in relation to the parameters of sluice gate opening. In [4] is given the dependence $\mu = f\left(\frac{2z}{a}\right)$ for the sluice gate opening, from which it is evident, that for very small values of the parameter $\frac{2z}{a}$ the coefficient μ is close to one. With a rise in parameters $\frac{2z}{a}$ the coefficient decreases and goes down to a value of $\mu = 0.62$, which it attains already practically at $\frac{2z}{a} \gg 2$. To examine the boundary conditions of the operation of the supporting structure we can take the extreme values of the delivery coefficient, because at maximum deliveries $\frac{2z}{a} \ll 1$, and at minimum ratios $\frac{2z}{a} > 2$.

Considering from formula (13) the height of opening the sluice gate and substituting same in (15) and taking the ratios of values K for boundary cases, we will obtain

$$\frac{K_2}{K_1} \approx 0{,}62 \frac{Q_1}{Q_2} \left(\frac{z_2}{z_1}\right)^{1/2}, \qquad (16)$$

where the index 1 corresponds to maximum, and index to minimum deliveries of water at the channel.

If the rate of the change in water delivery at the channel equals three and the drop thereat changes by five times, then the amplification factor of the object on the basis of (16) changes by more than 30 times.

Approximate calculations show, that the parameters of the individual supporting structures do change in very broad intervals. The most favorable conditions of

of controlling the water level in the upper boundary of the structure correspond to the passing by channels of maximum deliveries. In this case the time constant and the amplification factor of the object have minimum values, and the parameter A - maximum. With reduction in water delivery at the channels the controlling conditions worsen: the time constant and the amplification factor rise sharply, and the parameter A goes straight down to zero. Consequently, at minimum water deliveries at the channel the supporting structures can be considered as aperiodic links.

Literature

1. N.N.Agroskin, G.T.Dmitriyev, F.I.Pikalov, Gidravlika, Gosenergoizdat 1950.
2. Ya.T.Dub; Control objects on Irrigation Systems AVTOMATIKA, No.3, 1960
3. K.A.Krug; Transient Processes in Linear Electric Circuits, Gosenergoizdat, 1948
4. V.Ya.Popova, Delivery coefficients during outflow from under flat sluice gates Gidrotekhnicheskoye Stroitel'stvo No.10, 1948

Submitted December 16, 1960

Russian and English summaries included

FIRST LINE OF TEXT

Static Characteristics of AC Throttle Drives

by

Yu.M.Rozov.

The results of laboratory and industrial testing of asynchronous throttle type electric drives showed that static characteristics of drives with throttle control require serious study and radical improvement of their quality. Statism coefficients because of different troubles for throttle type drives with feedback for speed as well as with control for current and voltage differentials [1, 2] are complex nonlinear functionsof speed, moment, voltage of the source and feedback coefficients. As a rule , the given speed of a motor controlled by a saturation choke is realized in one point only.

The accepted and relatively simple statism coefficients of a throttle type drive are observed during change in load and voltage moments of the source in narrow limits, whereby with the reduction in the established speed of the motor these limitation become even more narrower.

Throttle drives are ordinarily adjusted to a certain stable load characteristic of the object and do nit satisfy the requirements of "unstable " loads with a reduction in the load moment the speed of the controlled motor rise relative to the given, and at a rise in load the circuit does not provide the motor with overloading ability - it looses speed and at sufficiently high overloads it may stop completely. As will be shown the cause for these shortcomings of throttle type drives is the incompatibility of the nonlinear nature of a controlled motor and saturation choke on one hand, and linear correlations in feedback wheel, on the other.

This report is devoted to study and establishment of possibilities of improving the static characteristics of a throttle AC-type drive with control of current and voltage differentials (see arrangement [1, 2]) and with utilization of a rotor of an

asynchronous motor, developed by the author [3.4].

Rough mathematical descriptions of laws governing elements of throttle drives differ with exceptional complexity. During the derivation of equations for saturation coil and motor with induction rotor support, which correspond with practical requirements were utilized empirical laws of certain summary physical processes, in which participate only the equivalent parameters of elements and the basic effects in the system under consideration.

To obtain these laws were approximated the results of experimental investigations of throttle drive elements under real working conditions of the saturation coil in an asynchronous motor and feeding the motor from the saturation coil. Of three type of trouble inherent to throttle drive (loading moment, source voltage fluctuations and thermal change of parameters) in the equations of drive elements and in the entire system we utilized only the changes in load moment and source voltage fluctuation, which are the basic trouble effects.

In the throttle drive arrangement the asynchronous motor, being alternating by the value of the complex support, is connected to the source through the complex alternating resistance of the saturation coil. The components necessary for the derivation of equations for these resistances should be in conformity with the accepted numerical vectors or with the utilizations of the theory of functions of complex variable.

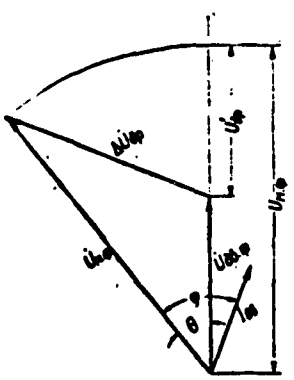

Fig.1. Vector diagram of voltages of an AC throttle drive.

The following considerations allow to operate with equations of elements of the system with considering phase displacement of voltages and currents. The controlling effect in the system, with which the moment of the motor will be designated, is the load (voltage) magnitude on its stator. As shown by investigations the magnitude of that voltage and the lagging

of the motor's voltage vector from the voltage vector of the source are synonymously determined by the correlation m.r.s of choke magnetization and current of the motor at constant value of source voltage.

We shall examine the vector diagram of motor and choke voltages for a single phase (fig.1). Transfers of vector values of source voltage on the vector line of motor voltage allow to determine the value U_{mot} by a simple subtraction from source voltage values of a certain fictitious voltage drop value on the choke.

$$\Delta U'_{xp} = I_{xp} \cdot Z'_{xp}, \qquad (1)$$

That is

$$Z'_{xp} = \frac{\Delta U'_{xp}}{I_{xp}}. \qquad (2)$$

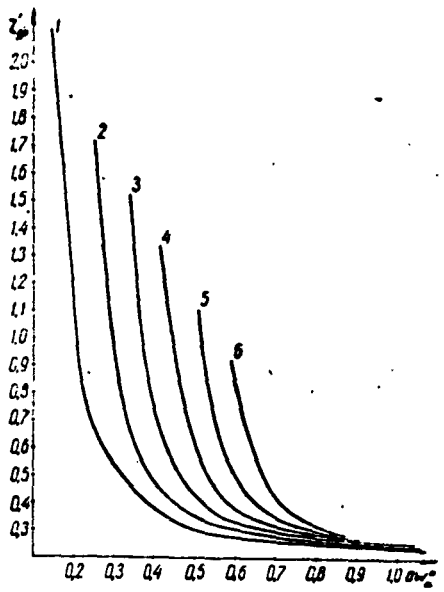

Fig.2. Dependence of saturation coil resistance upon m.r.s. of magnetization at various current loads. 1 - 0.3 I_{nom}; 2-0.5 I_{nom}; 3-0.7 I_{nom}; 4- 0.9 I_{nom}; 5- 1.1 I_{nom}; 6- 1.3 I_{nom}.

This value is a fictitious value of choke resistance, which fully determined by the magnetomotive force of choke magnetization and the current of the motor (fig.2.). Phase displacement of motor voltage relative to source voltage Θ does not take part in determining the moment of the motor and that is why it is of no interest to us. The power coefficient of the motor with induction support at various speeds and loads changes slightly, and it can be considered as stable. Consequently on the diagram fig.1. the angle φ is also entirely determined by the magnetic state of the magnetic drive of the choke , which is valid in expressions (1), (2) and can be further operated with scalar values .

In the following investigation was accepted a system of relative units. The relative units are given in table 1.

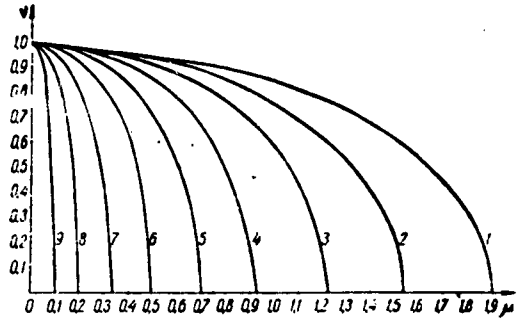

Fig.3. Curves of equal voltages of an asynchronous motor with induction rotor support.
1-1.0 U_{nom}; 2-0.9 U_{nom}; 3-0.8 U_{nom}; 4-0.7 U_{nom}; 5- 0.6 U_{nom}; 6-0.5 U_{nom}; 7-0.4 U_{nom}; 8- 0.3 U_{nom}; 9- 0.2 U_{nom}

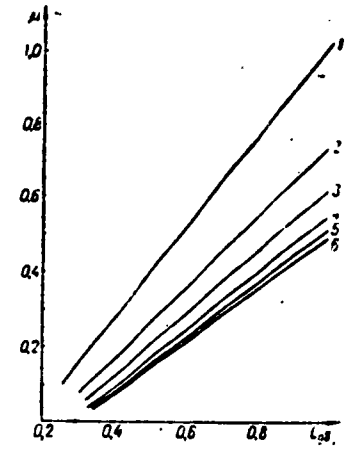

Fig.4. Dependence of motor moment upon current at various rates of rotation
1- 1200 rpm; 2 - 1000 rpm; 3- 800 rp.; 4- 600 rpm; 5- 400 rpm; 6- 200 rpm.

In conformity with the stated facts the equations of elements of the system will be written in form of

$$v^2 = 1 - \frac{A\mu^2}{\upsilon_{zs}^4} \quad \text{при } \mu > 0 \text{ і } v > 0, \tag{3}$$

$$\mu = (B + Dv^2)\upsilon_{zs} - C, \tag{4}$$

$$\zeta_{zs} = E + Fv^2 - G\upsilon_{zs}, \tag{5}$$

$$\zeta'_{zp} = \frac{L}{aw^*_- - N\upsilon_{zs}} \quad \text{при } aw^*_- - N\upsilon_{zs} > 0, \tag{6}$$

$$aw^*_- = a^*_i \upsilon_{zs} - a^*_g \upsilon_{zs}, \tag{7}$$

$$\upsilon_{zs} = \upsilon_u - \sqrt{3}\upsilon_{zs}\zeta'_{zp}, \tag{8}$$

$$\upsilon_{zs} = \upsilon_{zs}\zeta_{zs}. \tag{9}$$

Equations (3) were obtained by approximating the experimental dependence , shown in fig.3, which is presented by the known diagram of voltage equations in the "speed - moment " axes. Curves of equal voltages are approximated by quarters of ellipses. The coefficient A depends upon the ratio of the support of rotor phase of

controlled motor and the parameters of the induction additional support at the rotor wheel.

Equations (4) are the result of approximation of experimental dependence of motor moment upon the rate of rotation (rpm) and the current of the motor (Fig.4).

TABLE 1

SYSTEM OF RELATIVE UNITS

RELATIVE VALUE	DESIGNATION	RATIO	REFERRED TO
Source voltage	$v_м$	$\frac{U_м}{U_{м.ном}}$	$U_{M\ nom}$-rated source voltage
Motor voltage	$v_{дв}$	$\frac{U_{дв}}{U_{дв.ном}}$	$U_{mot.nom}$-rated motor voltage
Motor current	$v_{дв}$	$\frac{I_{дв}}{I_{дв.ном}}$	$I_{mot.nom}$-rated motor current
Absolute equivalent of motor resistance	$z_{дв}$	$\frac{Z_{дв}}{Z_{дв.ном}}$	$Z_{mot.nom}$-nominal absolute equivalent resistance of motor phases
Absolute fictitious choke resistance	$z'_{др}$	$\frac{Z'_{др}}{Z_{дв.ном}}$	$Z_{mot.nom} = \frac{U_{mot.nom}}{I_{mot.nom}}$
Motor rpm	v	$\frac{n}{n_c}$	n_c - synchroneous rate of rotation of motor
Moment of motor	μ	$\frac{M}{M_{ном}}$	M_{nom} - rated moment of motor
M.r.s. of choke magnetization (ampere-turns of DC current)	aw^*_-	$\frac{aw_-}{aw_{-н}}$	aw_{-n} - m.r.s. of magnetization which corresponds to practically total saturation of choke
Relative coefficient of current feedback	s^*_i	$\frac{aw_i}{v_{дв}\, aw_{-н}} = \frac{s_i}{aw_{-н}}$	
Relative coefficient of voltage feedback	s^*_u	$\frac{aw_u}{v_{дв}\, aw_{-н}} = \frac{s_u}{aw_{-н}}$	

In essence, these are equations of known curves of equal currents [1]. Expression (5) characterizes the change of equivalent motor support, which are executed by the parameters of the motor and e.r.s. of rotation, depending upon the rate of rotation and the current of the motor (Fig. 5). The constant coefficients B,C,D,E,F and G are also determined by the ratios of the induction parameters of the rotor support and the rotor itself.

The dependence of the "fictitious" support of the saturation coil upon m.r.s.

of magnetization and current load is described by equation (6) which approximates curves fig.2. Equqtion (7) is the law of controlling the system. Term (8) characterized the dependence of motor voltage upon source voltage and fictitious voltage drop on the choke. Equation (9) links voltage, current and total equivalent resistance of the motor. Equations of static characteristic of throttle drive, which forms the function of the output coordinate (speed ν) of disturbances (moment of load μ and source voltage ν_{M}), can be obtained by exclusion of intermediate variables ν_{mot}, U_{mot}, $zeta_{mot}$, $zeta_{dr}$, aw^{*}=.

The transform of the system of equations (3) - (9) leads to equationsof sixth power, which in turn by substitution leads to a cubical equation with coefficients in formof multimembered. The derivation of equation and its roots is very difficult, they do not submit to true simplification and are not mentioned in this report. More simple equations of static characteristic of the system can be obtained by replacing equations (6) and (8) with one expression, which was obtained by approximation of voltage dependence at the output of the choke, or on the stator of the motor, upon the magnetization ampere-turns and current load (fig.6).

$$U_{дв}^{*}=0{,}9\nu_{м}^{*}(aw_{-1}^{*}-Q\nu_{дв}) \quad \text{при} \quad (aw_{-}^{*}-Q\nu_{дв})>0. \qquad (10)$$

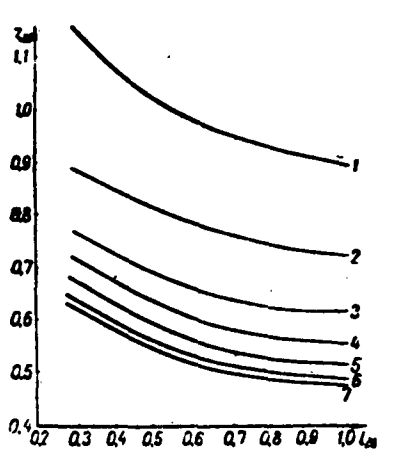

Fig.5. Dependence of total equivalent support of motor with induction rotor support at various rates of rotation. 1-1200 rpm; 2-1000 rpm; 3-800 rpm; 4-600 rpm; 5-400 rpm; 6-200 rpm; 7-100 rpm

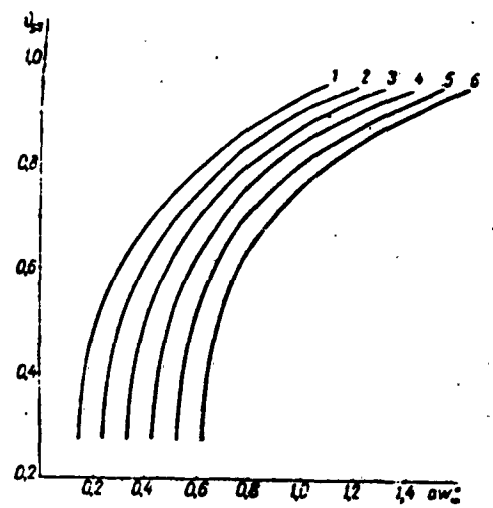

Fig.6. Dependence of motor voltage upon choke magnetization m.r.s. at various motor currents. 1-0.3 I_{nom}; 2- 0.5 I_{nom}; 3- 0.7 I_{nom}; 4 - 0.9 I_{nom}; 5-1.1 I_{nom}; 6-1.3 I_{nom}.

Excluding in the system of equations the variables U_{mot}, αw_2^*, U_{mot} $zeta_{mot}$ we will obtain equations of the fourth order (magnitude).

$$\nu^2 = 1 - \frac{A\mu^2(B+D\nu^2)}{0{,}9\upsilon_m^4(\mu+C)(\alpha_i^* - E\alpha_g^* - F\alpha_g^*\nu^2 - Q)}, \qquad (11)$$

which by substituting the term

$$\nu^2 = 1 - y \qquad (12)$$

is reduced to a square root equation

$$0{,}9F\alpha_g^*\upsilon_m^4(\mu+C)y^2 + \{0{,}9\upsilon_m^4(\mu+C)[\alpha_i^* - \alpha_g^*(E+F) - Q] + AD\mu^2\}y - A(B+D)\mu^2 = 0. \qquad (13)$$

The roots of this equation have the form of

$$y_{1,2} = -\frac{0{,}9\upsilon_m^4(\mu+C)[\alpha_i^* - \alpha_g^*(E+F) - Q] + AD\mu^2}{1{,}8F\alpha_g^*\upsilon_m^4(\mu+C)} \pm$$

$$\pm \frac{\sqrt{\{0{,}9\upsilon_m^4(\mu+C)[\alpha_i^* - \alpha_g^*(E+F) - Q] + AD\mu^2\}^2 + 3{,}6AF(B+D)\alpha_g^*\upsilon_m^4\mu^2(\mu+C)}}{1{,}8F\alpha_g^*\upsilon_m^4(\mu+C)}. \qquad (14)$$

Thanks to the fact that $[\alpha_i^* - \alpha_m^*(E+F) - Q] > 0$, $\nu^2 \leq 1$ and $y > 0$, the root with minus sign between two parts of this expression has no physical sense. Consequently

$$\nu = +\sqrt{1-y} =$$

$$= \sqrt{1 + \frac{0{,}9\upsilon_m^4(\mu+C)[\alpha_i^* - \alpha_g^*(E+F) - Q] + AD\mu^2 - \sqrt{\{0{,}9\upsilon_m^4(\mu+C)[\alpha_i^* - \alpha_g^*(E+F) - Q] + AD\mu^2\}^2 + 3{,}6AF(B+D)\alpha_g^*\upsilon_m^4\mu^2(\mu+C)}}{1{,}8F\alpha_g^*\upsilon_m^4(\mu+C)}}. \qquad (15)$$

Further on in order to simplify the statements all calculations are conducted for a concrete throttle drive, manufactured and tested at the Institute of Electrical Engineering of the Academy of Sciences Ukr-SSR, with a capacity of 2.8 kw.

The constant coefficients in the system of equations for this drive have such values: A = 0.26; B=0.61; C=0.18; D=0.69; E=0.52; F=0.58; Q = 0.47.

The value of the intermediate variable y for this drive, which will be utilized by us below, will be written as follows

$$y = \sqrt{\left[\frac{0{,}86\alpha_i^*}{\alpha_g^*} - \frac{0{,}4}{\alpha_g^*} - 0{,}95 + \frac{0{,}17\mu^2}{\alpha_g^*\upsilon_m^4(\mu+0{,}18)}\right]^2 + \frac{0{,}65\mu^2}{\alpha_g^*\upsilon_m^4(\mu+0{,}18)}} -$$

$$- \left[\frac{0{,}86\alpha_i^*}{\alpha_g^*} - \frac{0{,}4}{\alpha_g^*} - 0{,}95 + \frac{0{,}17\mu^2}{\alpha_g^*\upsilon_m^4(\mu+0{,}18)}\right]. \qquad (16)$$

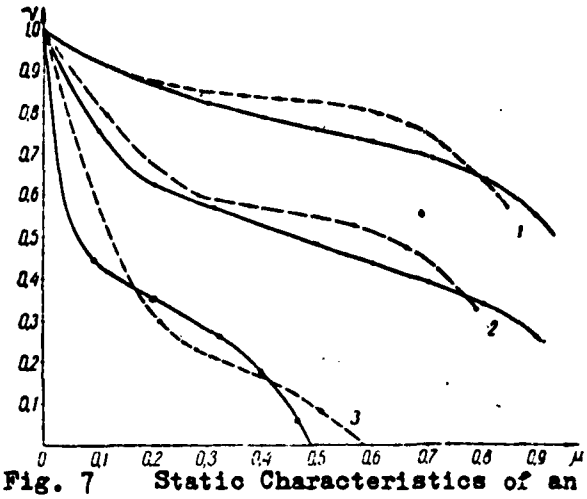

Fig. 7 Static Characteristics of an AC-Throttle Drive at Various Adjustments

1-$a_i^* = 1.a_u^* = 0.4$; 2-$a_i^* = 1, a_u^* = 0.65$; 3-$a_i^* = 0.77; a_u^* = 0.47$

_____calculated characteristic; —— experimental characteristic

Equations of static characteristic for the investigated 2.8 kw throttle drive have the form of

$$\nu = \sqrt{1 + b - \sqrt{b^2 + \frac{0{,}65\mu^2}{\alpha_\mu^* \upsilon_u^* (\mu + 0{,}18)}}}, \qquad (17)$$

Where

$$b = \frac{0{,}86\alpha_i^* - 0{,}4}{\alpha_u^*} + \frac{0{,}17\mu^2}{\alpha_\mu^* \upsilon_u^* (\mu + 0{,}18)} - 0{,}95. \qquad (17a)$$

The calculated static characteristics in comparison with the experimental ones are shown in Figure 7. The disagreement between results of calculation and investigation, which amounts to 10-20%, should be attributed to linearization of certain non-linear dependences on account of disregarding during the derivation of equation of secondary factors and a certain inaccuracy in approximation.

Term (12) was written with deviations at small values of same

$$2\nu\Delta\nu = -\Delta y. \qquad (18)$$

Increments in the complex function in (16) at certain increments of arguments μ and μ_m will be written as

$$\Delta y = \frac{\partial y}{\partial \mu}\Delta\mu + \frac{\partial y}{\partial \upsilon_u}\Delta\upsilon_u. \qquad (19)$$

Having taken the partial derivatives and calculating (18)we will obtain an

expression

$$\Delta\nu = -\frac{\Delta y}{2\nu} = -\gamma_{\mu}\Delta\mu + \gamma_{\upsilon_{\text{н}}}\Delta\upsilon_{\text{н}}. \qquad (20)$$

Here γ_{μ} and $\gamma_{\upsilon_{\text{н}}}$ - statism coefficients for corresponding disturbances, which equal

$$\gamma_{\mu} = \frac{1}{2\nu}\cdot\frac{\partial y}{\partial\mu} =$$

$$= \frac{\mu\ (\mu+0{,}36)\,\upsilon_{\text{н}}\left[0{,}29\alpha_i^{*}+0{,}33\alpha_{\text{н}}^{*}-0{,}14-0{,}34\sqrt{(0{,}86\alpha_i^{*}-0{,}95\alpha_{\text{н}}^{*}-0{,}4)^2+\frac{(0{,}29\alpha_i^{*}+0{,}33\alpha_{\text{н}}^{*}-0{,}14)\,\mu^2}{\upsilon_{\text{н}}^{4}(\mu+0{,}18)}}\right]}{4\alpha_{\text{н}}^{*}\nu\upsilon_{\text{н}}^{3}(\mu+0{,}18)^2\sqrt{(0{,}86\alpha_i^{*}-0{,}95\alpha_{\text{н}}^{*}-0{,}4)^2+\frac{(0{,}29\alpha_i^{*}+0{,}33\alpha_{\text{н}}^{*}-0{,}14)\,\mu^2}{\upsilon_{\text{н}}^{4}(\mu+0{,}18)}}}; \qquad (21)$$

$$\gamma_{\upsilon_{\text{н}}} = \frac{1}{2\nu}\cdot\frac{\partial y}{\partial\upsilon_{\text{н}}} =$$

$$= \frac{4\mu^2(\mu+0{,}18)\left[-0{,}29\alpha_i^{*}-0{,}33\alpha_{\text{н}}^{*}+0{,}14+0{,}34\sqrt{(0{,}86\alpha_i^{*}-0{,}95\alpha_{\text{н}}^{*}-0{,}4)^2+\frac{(0{,}29\alpha_i^{*}+0{,}33\alpha_{\text{н}}^{*}-0{,}14)\,\mu^2}{\upsilon_{\text{н}}^{4}(\mu+0{,}18)}}\right]}{4\alpha_{\text{н}}^{*}\nu\upsilon_{\text{н}}^{3}(\mu+0{,}18)^2\sqrt{(0{,}86\alpha_i^{*}-0{,}95\alpha_{\text{н}}^{*}-0{,}4)^2+\frac{(0{,}29\alpha_i^{*}+0{,}33\alpha_{\text{н}}^{*}-0{,}14)\,\mu^2}{\upsilon_{\text{н}}^{4}(\mu+0{,}18)}}}. \qquad (22)$$

The common denominator of statism coefficients

$$S = 4\alpha_{\text{н}}^{*}\nu\upsilon_{\text{н}}^{3}(\mu+0{,}18)^2\times$$

$$\times\sqrt{(0{,}86\alpha_i^{*}-0{,}95\alpha_{\text{н}}^{*}-0{,}4)^2+\frac{(0{,}29\alpha_i^{*}+0{,}33\alpha_{\text{н}}^{*}-0{,}14)\,\mu^2}{\upsilon_{\text{н}}^{4}(\mu+0{,}18)}} \qquad (23)$$

is proportional to the rigidity of the system, which establishes the measures of its reaction to any kind of disturbances. The nonlinearity of static characteristics, functional dependence of statism coefficient and the magnitude of proportionality of the system's rigidity upon the rate and magnitude of disturbances was obtained from the constancy condition of the feedback coefficients α_i^{*} and $\alpha_{\text{н}}^{*}$, or from the

condition of constructing feedbacks by linear law. This is confirmed by experiment.

Since an asynchronous motor, during its operation at higher slips, and the saturation coil are nonlinear by their nature, the only permissible way of actually improving the quality of static characteristics of AC throttle drives is the application in the system of such feedbacks, the coefficients of which are in a certain functional dependence upon the output coordinate (speed ν) and upon the magnitude of disturbances.

We will analyze the terms of statism coefficients (21) and (22). The numerators of these expressions possess identical multiples (multiple values), taken at the square arc, and differ only by the sign. The equality of these multi members to zero is an invariance condition of static error of the system pertaining to disturbances - load moment and oscillationsof source voltages. The system having zero statism for the load moment and source voltage fluctuations at

$$0{,}29\alpha_i^*+0{,}33\alpha_u^*-0{,}14=$$

$$=0{,}34\sqrt{(0{,}86\alpha_i^*-0{,}95\alpha_u^*-0{,}4)^2+\frac{(0{,}29\alpha_i^*+0{,}33\alpha_u^*-0{,}14)\mu^2}{\upsilon_u^*(\mu+0{,}18)}}. \qquad (24)$$

After certain transforms with the utilization of (4) we will obtain

$$\frac{3{,}3\alpha_i^*\alpha_u^*-1{,}56\alpha_u^*}{0{,}3\alpha_i^*+0{,}33\alpha_u^*-0{,}14}=\frac{[\upsilon_{as}(0{,}61+0{,}69\nu^2)-0{,}18]^2}{\upsilon_u^*\upsilon_{as}(0{,}61+0{,}69\nu^2)}. \qquad (25)$$

It is evident, that equality can be attained at various combinations of dependences α_i^* and α_u^* upon U_{mot}, ν and U_M. The following deliberations lead to the selection of really feasible dependences of feedback coefficients. The dependence of any one of these coefficients upon source voltage U_M should be assured by the introduction into the system of a compound connection with the voltage source, which would considerably complicate the entire drive system, the main value of which lies in simplicity and reliability. As is shown by terms (22), (23) and (25), total elimination of static errors without cutting in the voltage source is impossible.

Figuring, that deviations of voltage source, as a rule, does not exceed 5% and that only one part in the drive system is of negative connection, the voltage of the motor raises the rigidity of the system by many times, it is then possible to draw

a conclusion regarding the possibility of considerably decreasing static errors without compound connection with scurce voltage.

Since in our system there is no tachogenerator and the fixing element is situated along side the feedback for the voltage, it is safe to assume α_u^* as dependent upon speed, consequently the fixing element should be made with a certain functional dependence upon the necessary rate of rotation of the motor. Finally, by linking with a current dependent coefficient the simplest thing of all is to establish connection with the current. Consequently, equation (25) can be realized at $U_{bl}=1$ and at laws of change of α_u^* and α_i^* in the form of

$$\alpha_u^* = \frac{l+mv^2}{nv^4+pv^2+q} \qquad (26)$$

1a

$$\alpha_i^* = a\upsilon_{zs}^3 + b\upsilon_{zs}^2 + c\upsilon_{zs} + d. \qquad (27)$$

Substitution of last expressions in (25) and solving of same with respect to coefficients a, b, c, d, l, m, n, p and q gives a formula for calculating the dependences of feedback coefficients upon the speed and current of the tested 2.8 kw drive

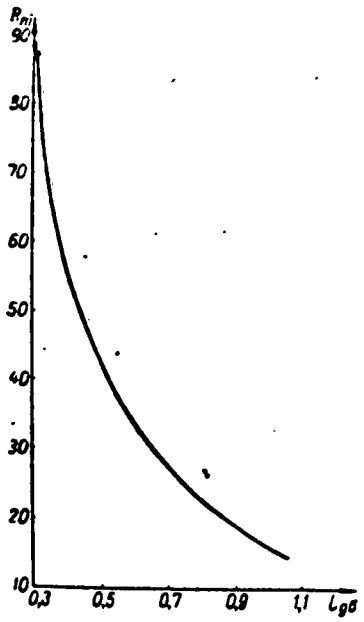

Fig.8. Characteristic of nonlinear subsequent support in the vicinity of feedback for the current.

$$\alpha_u^* = \frac{0,65-0,2v^2}{1,1v^4+0,08v^2+0,5}; \qquad (28)$$

$$\alpha_i^* = 585\upsilon_{zs}^3 + 91\upsilon_{zs}^2 + 16\upsilon_{zs} + 0,22. \qquad (29)$$

Realization of dependence α_i^* upon current can be derived, e.g. by introduction along the linkage behind the current a following correcting nonlinear element. Such an element can be a choke, which becomes automatically saturated or magnetized, connected in-series to a current transformer.

Investigations carried out at the Institute of Electrical Engineering at the Academy of Sciences Ukr-SSR, showed, that static error

due to change in load moment can be practically reduced to zero by connection of an artificial nonlinearity into the feedback circuit for the current. Experimental dependence of the support of the successive correcting element in the circuit of the current feedback upon the current of the motor, which assures a considerable reduction in static error, is shown in fig.8. Problems of synthesizing correcting elements and their practical realization with assurance of maximum rigidity of the system will be explained in the following reports.

Literature

1. A.G.Ivakhnenko. Automic Controlling the Speed of Asynchronous Low Capacity Motors. Izdatel'stvo Akademii Nauk Ukr-SSR, 1953

2. I.K.Parra, Yu.M.Rozov, E.G.Chugunniy; Results of Industrial Testing of AC 10 kw Drives with Choke Control. Avtomatika No.5. 1960

3. Yu.M.Rozov; Throttle Electric Drive. Author Certificate No.138657 (class 21c 59/35) with privelege from Oct.9.1959 "Byulleten' Izobreteniy "No.11,1961

4. Yu.M.Rozov; New Type of Rotor for Asynchronous Motor used in a Throttle Type Drive System. Energetika i Elektrotekhnicheskaya Promyshlennost', No.4,1960

5. Yu.M.Rozov; Investigation and Calculation of an Induction Auxiliary Type Rotor Support for an asynchronous Motor,controlled by a Saturation Coil. Avtomatika No 2.1961

Submitted Sept.30,1961

Russian and English summaries included

Tri-Phase Reversive Drive with Magnetic Semiconductor Amplifier

by

N.V.Khrushchova

Known are numerous circuits [3] of contactless reversive operational devices with two-and three-phase motors, where the output cascades are built on electron tubes. But the application of tubes in similar arrangements is undesirable. In [4] is described the circuit of a two-phase drive with input cascades on semiconductor triodes and rate feedback with tachometer generator. Feedback can be executed without tachometer generator, e.g.with the aid of current and voltage transformers [1, 2]

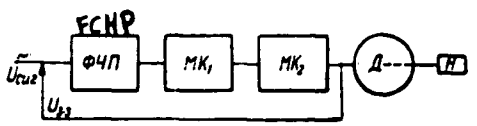

Fig .1. Block diagram of reversive tri-phase drive
FCHP - phase sensitive amplifier; MK_1 and MK_2 - magnetic cascades No 1 and 2. D-motor; N-loads.

In this report is described the circuit of a tri-phase reversive drive without electron tubes with stabilizing feedback for speed without a tachometer generator.

The block-diagram of an asynchronous throttle drive with tri-phase motor AOL 11/4 capacity 0.12 kw is shown in fig.1. and the principal circuit diagram in fig.2. The first phase sensitive is built on P4-A triodes, the third and second - on magnetic amplifiers. The third - power amplification stage (cascade) consists of five or six magnetic amplifiers for direct (MP_3, MP_4, MP_5) and reverse (MP_6, MP_7, MP_8) rotation of the motor.

Former amplification is realized on two single-tact magnetic amplifiers or

dual tact amplifier with DC output, e.g. MP_1 and MP_2 (see fig.2). Rate of rotation stabilization is attained by the application of a positive feedback for current and negative for voltage.

Summing up was realized at AC current on the primary winding w_1 of input transformer TR_1 of the semiconductor cascade FCHK. Primary winding of current transformer TC and voltage transformer TN are connected in phases 1 and 3 of the motor (see fig.2). To cordinate the feedback phases U_{st} with the phase of the input signal U_{sig} there is a phase changing device (FOP), connected to the output of current and voltage transformers.

The feedback voltage U_{st} at the input of the phase changing device equals

$$U_{ст}=U_{тн}-U_{тс}=k_1U_{1-3}-k_2(I_{ф_1}-I_{ф_3}). \qquad (1)$$

where $I_{ф_1}$ and $I_{ф_3}$ - currents of first and third phases, U_{1-3}- line voltage.

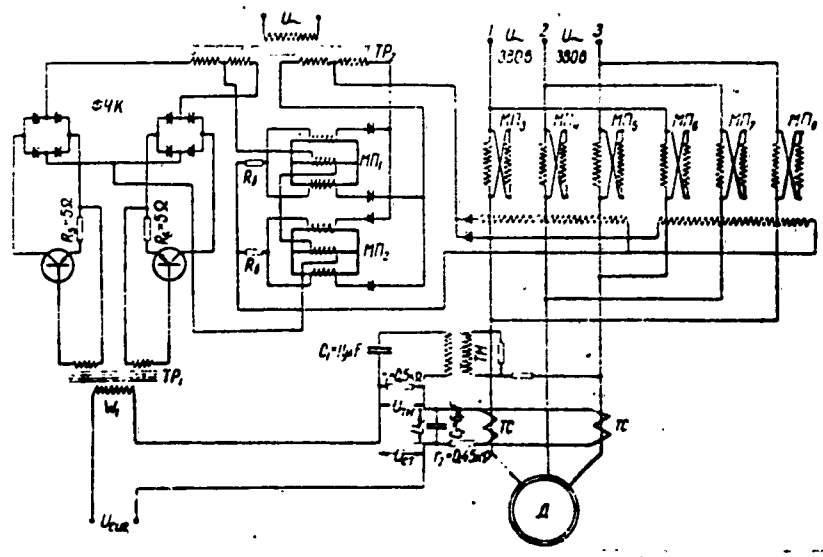

Fig.2. Principal Circuit diagram of a reversive tri-phase drive

The parameters of phase turning device are selected so, that at a motor speed equalling zero (n = 0), the voltage at its output U_{st} would be close to zero

$$U_{ст}=U_{тн}-U_{тс}=0. \qquad (2)$$

The output of the feedback sensing element U_{st} connected in the ccunterphase with

controlling signal U_{sig} at the input of the phase sensitive cascade (FCHK). Upon a change in sign of the control signal, i.e. during the reversing of the motor, the voltage phase U_{st} changes by 180°.

The phase turning device can be made with the aid of an arrangement on active resistances and capacitances. The configuration of the FOP circuit depends upon the phase displacement between voltages at outputs of current U_{ts}, voltage U_{tn} transformers and the input signal U_{sig}. The calculated parameters of FOP correspond to the distribution of vectors U_{ts}, U_{tn} and U_{sig} shown in fig.3. But there is also possible another arrangement of these vectors.

In further considerations the angles φ_1 and φ_2 between the voltages at output of current transformer U_{ts}, voltage transformer U_{tn} and U_{sig} are accepted as constant in the entire range of motor speeds. Such assumptions are possible for the motor with Shenfer rotor.

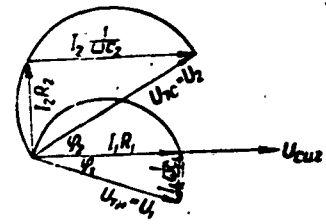

Fig.3. Vector diagram for calculation of phase turning device of feedback stabilizing element.

To the phase rotating device, shown in fig.2, corresponds a displacement circuit fig.4. The resistance r_n and voltage U_{st} in this arrangement are the input parameters of a semiconductor cascade FCHK, r_n is accepted as active, negligible inductance of TR_1 transformer. Having fixed the resistances

$$r_1 = \frac{1}{\omega C_1} = 0{,}1\, r_n. \tag{3}$$

and coming out from the vector diagram fig.3, we will determine the FOP parameters

$$c_1 = \frac{1}{r_1 \omega \operatorname{tg} \varphi_1}, \tag{4}$$

$$c_2 = \frac{1}{\omega 0{,}1 r_n}, \tag{5}$$

$$r_2 = \frac{1}{\omega c_2 \operatorname{tg}(90 - \varphi_2)}. \tag{6}$$

Currents I_1, I_2 and voltages on the secondary windings of current and voltage transformers U_1 and U_2 can be determined from equations

$$I_{10}r_1 - \frac{1}{\omega C_2} I_{20} = 0, \qquad (7)$$

$$I_1 r_1 - \frac{1}{\omega C_2} I_2 = U_{ст}. \qquad (8)$$

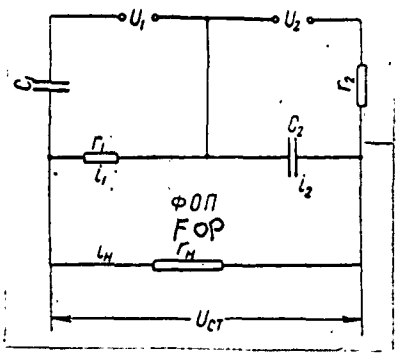

Fig.4. Scheme of displacement of phase rotating device of feedback stabilization element.

Equation (7) corresponds to the working condition of FOP at the braked motor (n=0), when condition (2) should be fulfilled. The current I_{10} and I_{20} designate the current at outputs of voltage and current transformers under this condition.

Equation (8) is complex for the condition of nominal rate ($n = n_{nom}$), current I_1 and I_2 indicate currents at outputs of current and voltage transformers in this condition.

When formulating equation (8) no consideration was given to feedback current I_n at the output of the circuit. Such assumptions are valid because, according to ratio (3), resistances r_1 and $r_2 = \frac{1}{\omega C_1}$ are much lower, than the output resistance FOP (marked on the displacement circuit bt r_N).

The system of equations (7) and (8) with four unknowns can be solved, if it would be supplemented by ratios

$$\frac{I_{10}}{I_1} = b \text{ та } \frac{I_{20}}{I_2} = a. \qquad (9)$$

The relationships (9) between currents at the output of current and voltage transformers remain valid (at a condition of constancy of their transformation coefficient with change in motor speed) and for currents and voltages of the motor, which can be determined from its curves of identical currents and voltages. Knowing the values a and b it is possible to solve the system of equations (7), (8) and (9) with respect to the currents I_1 and I_2

$$I_1 = \frac{U_{ст}}{r_1} \cdot \frac{a}{a-b}, \qquad (10)$$

$$I_2 = U_{ст} \omega C_2 \frac{b}{a-b}. \qquad (11)$$

The voltage U_1 and U_2 on the secondary windings of voltage and current transformer are stipulated from formulae

$$U_1 = I_1 \sqrt{\left(\frac{1}{\omega C_1}\right) + r_{2}^{1}}.$$
$$U_2 = I_2 \sqrt{\left(\frac{1}{\omega C_1}\right) + r_{2}^{11}}. \qquad (12)$$

Values I_1, I_2, U_1 and U_2 are the basic data for the calculation of currents and voltages of transformers [1].

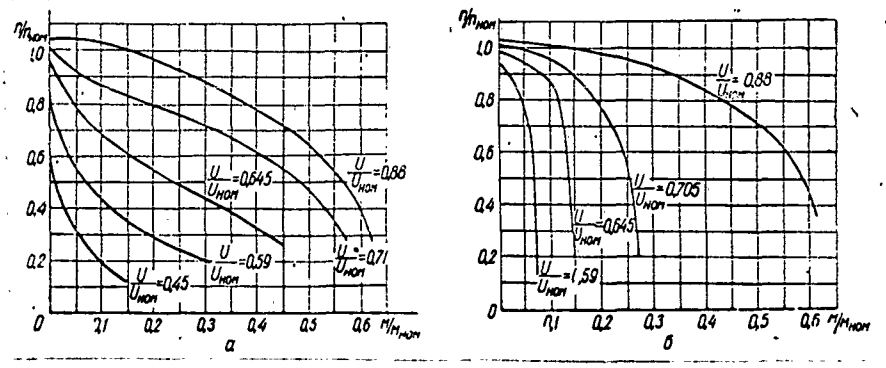

Fig.5. Experimental mechanical properties of drive with and without feedback. a- with feedback; b - without feedback.

The function of the feedback in the circuit of the drive with semiconductor input cascade (see fig.2) was checked experimentally. Tests showed, that feedback broadens the zone of linearity, in which the rate of motor rotation depends upon the magnitude of the controlling signal and raises the rigidity of the mechanical characteristics.

For the purpose of comparison fig.5 shows the mechanical characteristics of a motor with and without feedback.

Literature

1. A.G.Ivakhnenko; Automatic Speed Control of Asynchronous Low Power Motors. Izdatel'stvo Akademii Nauk Ukr-SSR.1953.

2. A.G.Ivakhnenko; Device for Controlling a Reversive Asynchronous Electric Motor Author thesis No.104432, MEP No.3756 dated Aug.14.1951.

3. B.I.[illegible]; S.M.Domanitskiy; Contactless Operational Devices of Industrial Auto-

mation, Gosenergoizdat Moscow, 1960.

4. V.S.Volodin; Ye.D.Larin; M.A.Rozenblat; G.V.Subbotina; High Speed Push-Pull Magnetic-Semiconductor Amplifier for a Power Follow-Up Drive "Avtomatika i Telemekhanika" No.3, 1959

Submitted: September 19, 1961.

Russian and English summaries included.

Electronic Differential System for Automatically Measuring the Rate of Rolling

by

P.I.Dekhtyarenko; S.F.Kozubovskiy; A.M.Meleshev; S.R.Raykhman

At the Automatic Control Lab of the Institute of Electrical Engineering at the Academy of Sciences Ukr-SSR was developed an electron variant of a differential system for automatically measuring the rate of rolling by the correlation method. The correlation method of measuring the rate of rolling was described in [1], and the bases of its automation system - in [2, 3]. We shall briefly review the mode of operation of the correlation metering device measuring the rate of rolling.

Two points of a metal strip, are situated over a fixed distance l in direction of rolling, are illuminated by two sharp luminous dots. The brightness of the luminous dots during the movement of the metal strip changes as result of presence of structural heterogeneities on the surface of the metal, cracks and dross. The images of lines are perceived by two photomultipliers , from the outputs of which is taken down an electric signal, proportional to the brightness of the lines. Amplified signals are fed to the correlator.

The output signal of the correlator (intercorrelation function) is maximum in case, when the control of lagging, which is introduced into the channel of the first signal, is equal to transportation lag τ_T from the moment the metal passes a distance between two points (lines).

The magnitude of lag, which is introduced, is synonymously bound with the rate of the metal by the dependence $v = \frac{l}{\tau_T}$, which allows to use this method for measuring the rate of rolling. The controlled lagging block (BRZ) is calibrated directly in rate values.

The system is automated with the aid of an extremal regulator, connected to the output of the correlator, which finds automatically the maximum of the correlation function, acting against the BRZ.

Differential circuit. The process of finding the maximum with the aid of ordinary extremal control circuits is connected with searching oscillations, which reduce the rapid action of the system. The differential circuit has no such shortcoming, which governs the basis for the developed electronic system.

The specific charactristic of the differential circiut is the presence of a "model of the control object" - of another correlator channel with additional constant laggings

The characteristic of the model has exactly the same form as the characteristic of the object, but it is displaced along axis γ by the value of this constant lag. A comparison of output signals of the object and "model" allows to obtain error signals, which assures the entry of the system into the zone of extremum, after which the system is mainteined in the point of intersection of object and model characteristics.

The differential circuit of automating the correlation metering device is easily distinguished from ordinary circuits by its simplicity and greater sensitivity, because the differential characteristic in the zone of system equilibrium has greater curvature, than the characteristic of the object in the zone of the extremum. The function of the differential circuit is more thoroughly described in [3].

The characteristic of the developed system is also the application of the relay correlation function

$$R_T^{\text{sign}}(\tau) = \frac{1}{T}\int_0^T \text{sign}\,[f(t)]\,\text{sign}\,[f(t-\tau)]\,dt \qquad (1)$$

instead of the ordinary

$$R_T(\tau) = \frac{1}{T}\int_0^T f(t) f(t-\tau)\,dt. \qquad (2)$$

Consequently, the correlation function of the continuous output function f(t) will be substituted by the correlation of the corresponding to it "relay function" sign[f(t)] which is designated by the moment of transition through zero of this output function (fig.1). As is shown in many investigations, this can be done at normal

correlations of the output process and by normal distribution of its momentary values. The relay correlation function depends only upon the probability of the alternation of signs (zeros) of the output process [6].

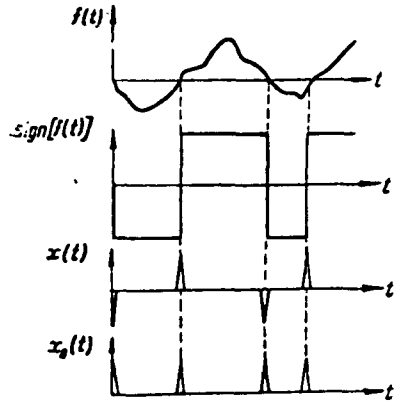

Fig.1. Transformation of input signal in measuring device. We will examine a circuit relay function and pulse, which correspond to zeros of output function. f(t)-signal at output of phototransmitter; sign[f(t)]-relay function at output of forming line; x(t)-differentiated pulses; $x_0(t)$-output signal of converter (monopolar pulses which correspond to zeros of output function).

The utilization of relay correlation functions makes it possible to considerably simplify the correlator apparatus. Especially, ERZ for the relay function is much simpler than than for the signal of general form, because the task is reduced to the delaying of short pulses, which correspond to zeros of the output signal (or corresponding relay function[1]).

Instead of the multiplying device of the correlator is utilized a relatively simple coincidence circuit.

Circuit-diagram of a correlation velocity diagram of a correlation velocity measuring device (fig.2). The signals coming from photomultipliers FP_1 and FP_2 are amplified with the aid of amplifiers P_1 and P_2 and fed to the forming (F_1 and F_2) and transforming (P) links for the transformation of input signals into a relay function and into a short monopolar potential pulses, which correspond to zeros of the output function (see fig.1). These pulses with the aid of an electronic ERZ are delayed for a time τ, the magnitude of which depends upon the control load applied to the ERZ. The controlled lag block includes as an element of alternating delay τ (the ERZ proper) as well as elements of constant delays τ', τ_1 and τ_2.

The delayed pulses with the aid of triggers-formers T_1 and T_2 (triggers with calculated input) are again converted into rectangular pulses (relay function) and delivered

to multiplying devices I (of the coincidence circuit). The difference in delays in elements τ_1 and τ_2 deisgnates the displacement of characteristics of two differential circuit channels (output signals of coincidence circuits I). Signals from the output of coincidence circuits through cathodic repeaters KP are fed to the electron keyer EK and through a memory device PP to the controlled lagging device.

Input, forming and transforming links. Amplified signals from the output of phototransmitters * approach the forming and transforming links through the normally open contacts $1P_1$ and $2P_1$. Relay R_1 is cut in by contact of relay R_2. Relay R_2 has two windings, one of which is fed rectified signal voltage of the phototransmitter of the first channel, and the other one control the operational threshold of the system (nonsensitivity zones).

In the absence of signal from the fascimile transmitter FP_1 the winding of relay R_1 is currentless and to the input of the former do not come in weak impediment signals, which in the absence of the basic signal would lead to wrong operationsof the circuit.

The input sign-changing signal of general form, which exceeds the zone of insensitivity of relay R_2, with the aid of forming and transforming links is transformed into a sequence of monopolar pulses, which correspond to zeros of the output signal (see fig.1). These transformations are realized with the aid of the forming cascade (L_2 and 1/2 L_3), phase invertor (1/2 L_3) and amplifier (1/2L_4). All this is evident from fig.3.

As a forming cascade was utilized a diode-regenerative scheme with pulse transformer[7]. The input amplified load f(t) is fed through relay contacts $1P_1$ and TR_1 pulse transformer winding to the cathode of right diode L_2. The left diode L_2 and resistance R = 68 kohms serve for the purpose of symmetrizing the charge and discharge currents of the input capacitor. Rectangular load pulses on the anode of tube L_3 sign[f(t)] are differentiated when passing through capacity C = 750 micromicrofarads.

* The optical system and phototransmitters made by engr T.D.Kravets

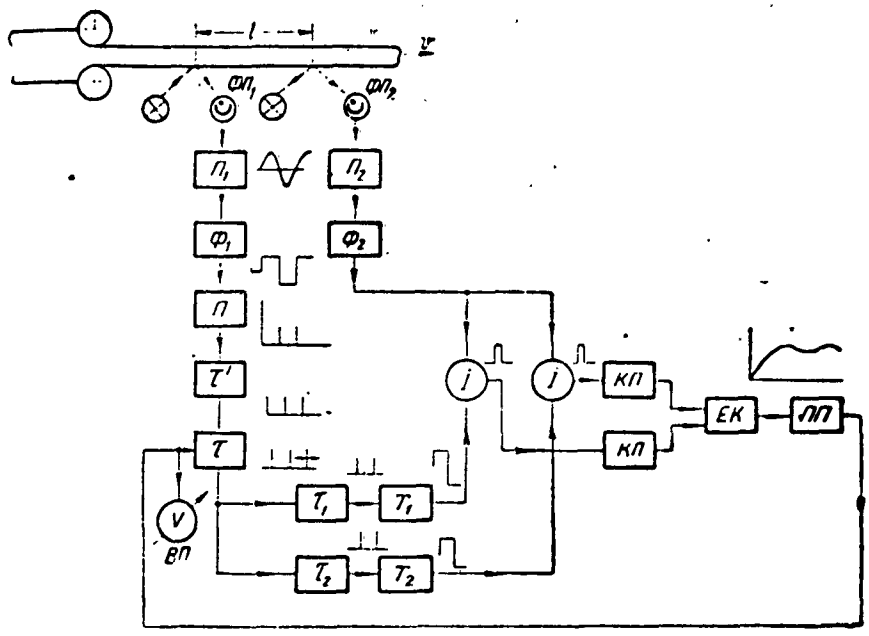

Fig.2 Circuit Diagram of Correlation Measuring the Speed of Rolling Mills
FP_1 and FP_2 - Photomultipliers; P_1 and P_2 - input signal amplifiers; F_1 and F_2 - formers of rectangular pulses (of relay function); P - converter of relay function into pulses corresponding to zeros of input signal; τ_1', τ_1, τ_2 - constant lag elements.

T_1 and T_2 - triggers with calculated input; I - coincidence circuit; KP-cathode repeater; EK-electron key; PP-memory device; VP-measuring device, calibrated in speed values.

See Page 78a for Figure 3

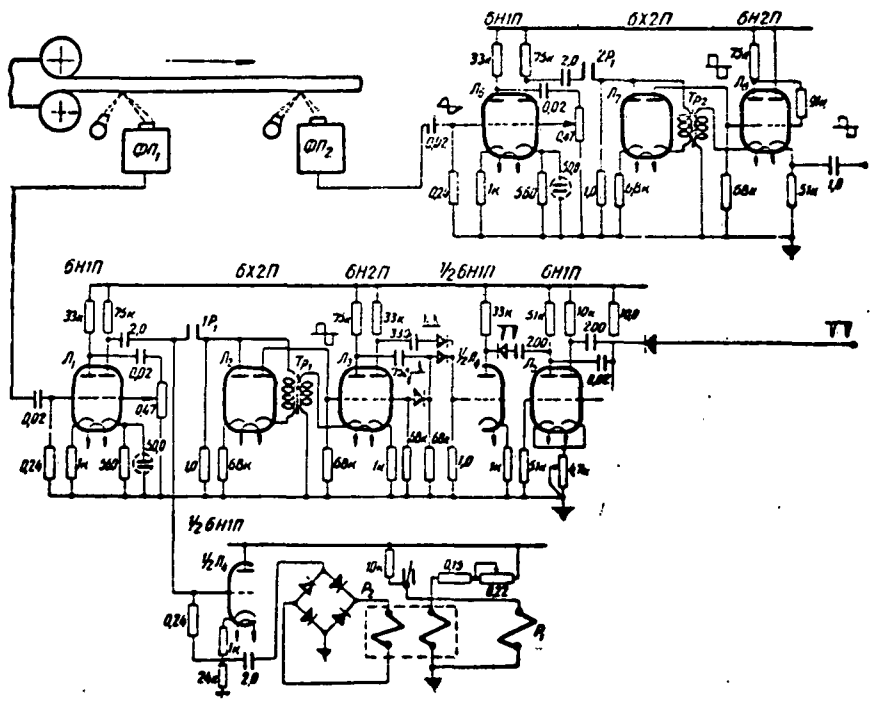

Fig. 3 Principal Diagram of Input Forming and Transforming Links

The pulses x(t) obtained after the capacitance are divided by polarity by point diodes and delivered to the input of the amplifier 1/2 L_4. Negative pulses are alternately passed through the phase inversion cascade. After amplification from the anode of the right half of tube L_4 are taken down the negative polairy pulses $x_0(t)$, which are fed to rhe delay block (τ', τ_1, τ_2 in fig.2).

Delay block. The delay block assures the delay of monopolar pulses for a time, corresponding to transport delay τ_T and depends upon the distance between the lines l and the rate of motion of the rolling mill v (fig.2).

The delay elements are controlled by monovibrators, which can be alternately commutated to obtain the necessary delay time. The total delay is a combination of previously selected constant delays (τ', τ_1, and τ_2) and alternating delay τ, the magnitude of which is controlled by the load, which is fed to the grid of left half of tube L_2 (fig.4).

As is known, the time of delay of a monovibrator is designated by circuit parameters R and C and by the conditions of the tubes in open state. In our case for monovibrators with constant time changing the delay time corresponds to $T_1=T_2=T_3=T_4=8$ microsec.

The experimental dependence of pulse delay time upon the magnitude of the controlling load, which is fed to the grid of left half of the tube L_{12} is depicted in fig.5. It is evident from the drawing, that it is approximately linear.

From the monovibrator plate with alternating pulse duration L_{12} (Block of controlled delay τ on fig.2) the signal after amplification from 1/2 L_{13} appears at the separated inputs of the monovibrator with various interchange time (blocks of constant delay τ_1 and τ_2 on fig.2). The time of changing the monovibrator, assembled on L_{14} tubes, equals $\tau_1 = 7$ msec, monovibrator on L_{15} tubes - $\tau_2 = 5$ msec. The difference in delays $\Delta\tau = \tau_1 - \tau_2 = 2$ msec.

The delayed pulses of negative polarity from tube plates of monovibrators are fed to the input of triggers with calculated input L_{16} and L_{17} (T_1 and T_2 in fig.2).

From the loads of cathode repeaters L_{18} is removed the voltage, the form and frequency of which are analogous to the voltage after the former, but it is displaced in time by a magnitude, which is designated by elements L_{19} and L_{20} (fig.6) by coincidence circuits ("of the multiplying device " I in fig.2.)

Coincidence Circuit. The coincidence circuit is built on double triodes with common load anodes. In the absence of signals or when positive signals are fed to both grids the tubes are open. The circuit parameters are selected so that during the closing of one of the tubes the current through resistance of plate load and the voltage on it remain practically unchanged.

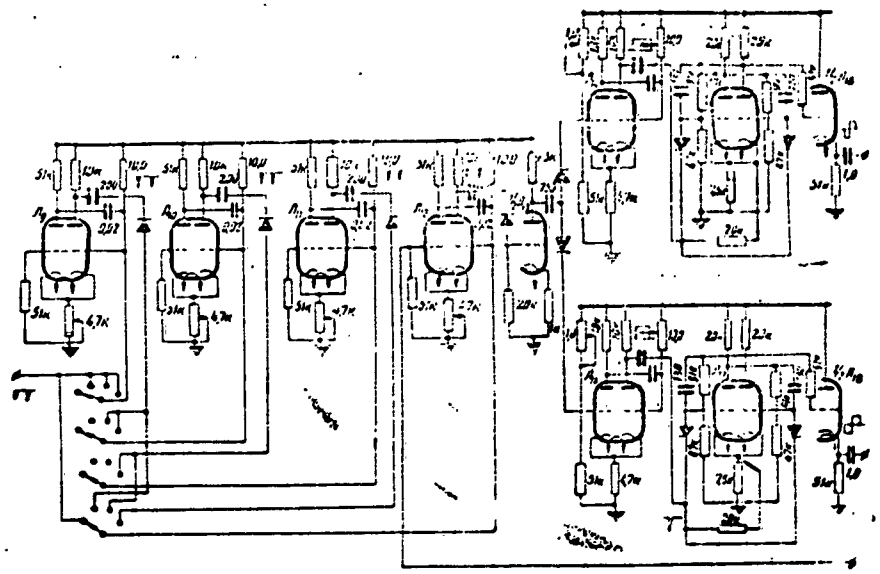

Fig.4. Principal circuit diagram of delay block U_{51} of 6N1P type tube

During simultaneous feeding of negative signals to both grids the triodes close. This causes a rise in plate voltage to the magnitude of the anode source, and from the output load is removed a pulse of positive polarity, the duration of which depends upon the phase displacements of the voltages which are fed to the grid of the coincidence circuit.

In our case to the right grid of thecoincidence circuit is coming in a signal

from the former of the second channel - sign$[f(t-\tau)]$, and to the left grid- signals of first channel delayed by the time τ_1 and τ_2. If the delays τ_1 and τ_2 would be equal and coincide with the time of transporting the delay τ_T, then the output pulses of both coincidence circuits would have an identical duration. But the delays differ from each other by the time $\Delta\tau = \tau_1 - \tau_2$ and consequently during the equality of one of them to the time of transporting τ_T the other one differs from this value by the magnitude $\Delta\tau$ and the output signals of the coincidence circuit (duration of output pulses) is different. The equality of output signals of coincidence circuits is possible only in case of system equilibrium, when both delays τ_1 and τ_2 differ from τ_T by the value $\frac{\Delta\tau}{2}$.

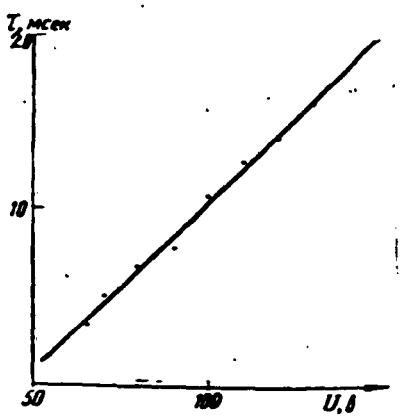

Fig.5. Experimental characteristic of BRZ (dependence of time of delay upon magnitude of control voltage)

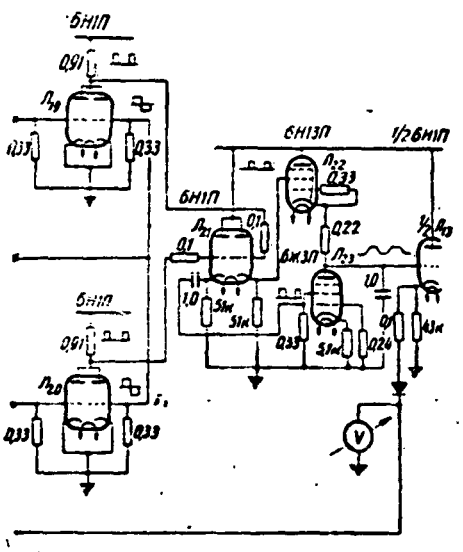

Fig.6. Coincidence circuit and electron key

When the rate of rolling is changed the delay time appears to be unequal to the transport delay and the duration of pulses at the outputs of coincidence circuits will be different.

Positive pulses, taken from plate loads of coincidence circuits, through cathodic repeaters L_{21} are fed to the electron key, in the circuits of which is included a capacitor C = 1 microfarad. The voltage on the capacitor is designated by the duration

of the pulses, which arrive at the electron key.

When the pulses appear at grid screen of tube L_{22} the capacitor becomes charged; when the pulses arrive at L_{23} the capacitor is discharged. The circuit parameters are selected so, that the time constants near the charge and discharge of the capacitor are identical. The mean value of the potential on the capacitors is designated by the difference in the duration of the pulses, which arrive at the electron key. The greater the pulse duration, of pulses taken from L_{22}, the greater is the voltage on the capacitance and, vice versa, that voltage is lower, the greater the duration of pulses taken from L_{23}.

Finally the magnitude of the potential on the capacitors is designated by the rate of motion of the rolling mill. When this load is delivered through cathode repeater 1/2 L_{13} in the vicinityof the grid of the monovibrator L_{12} takes place a change in delay controlling time, and subsequently in each case the change in rolling rate brings about a change in signal delay time in the first channel.

The output load, taken from capacitor through cathodic repeater, is measured by the voltmeter, calibrated in values of rate of motion of the rolling mill. By the indications of the installation, included in the monovibrator grid, it is possible to determine the rate of motion of the rolling mill.

Literature

1. N.Bremli, S.Carlyle, R.Sims. Certain Trends in Automating Rolling Mill Industry (report at First International Congress IFAK) Transactions of I International Congress of IFAK, Moscow 1960.

2. S.F.Kozubovskiy; Automation of Systems Measuring The Rate of Hot Rolling by the Correlation Method " Avtomatika " No.3, 1961

3. S.F.Kozobovskiy; Automating Correlation Measuring of Rolling Rate with the Aid of Differential Circuit, "Avtomatika" No.1, 1962

4. O.G.Ivakhnenko; Technical Cybernetics, Gostekhizdat Ukr-SSR Kiev, 1959

5. O.G.Ivakhnenko; Correlation Methods in Cybernetic Systems of Automatic Control "Avtomatika" No.2, 1960

6. S.N.Bernshteyn. Theory of Probabilities, ONTI, Gostekhteorizdat, 1934

7. Generation of Electric Oscillations of Special Form, Izdatel'stvo Sovetskoye Radio, Moscow, 1951

Submitted May 12, 1961

Code Frequency-Combination System for Telemetering

by

B.S.Didyk, F.O.Katkov

In code systems of telemetering the transmission of discrete values of a primarily measured magnitude is realized by the formation and sending into the channel of a group of signals, which make up the code, the necessary number of which is determined by the permissible discreteness error.

At proper formulation of the code systems of telemetering, the code systems can be reliable at a considerable level of interferences in the channel (communication channel). That is why already known devices are characterized by considerable complexity, relatively low operational reliability and low rate of speed.

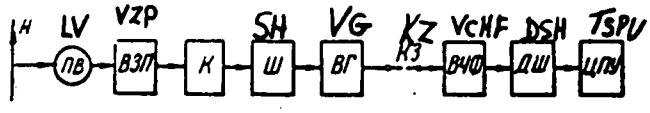

Fig.1. Block-diagram of a telemetering code frequency-combination system A-measured value, PV-primary measuring device; VZP-indicator unit; K-Commutator; SH- coder; VG-generator unit; KZ-communication channel; VCHF-unit of frequency filters; DSH-decoder; TSPU - digital receiver.

The code frequency-combination system of telemetering developed at the Faculty of Automatics and Telemechanics of the Kiev Polytechnicum, does not have these short comings.

A simplification of the arrangement, and increase in speed and reliability were attained on account of parallel coding from the application of frequency characteristics.

Codes are formulated by compiling combinations of n through m frequencies, which are sent simultaneously.

In contrast to code-pulse systems the high frequency signal , which corresponds to the given value of the primary measured value, is sent by a transmitter and continuously fixed by the receiving device. In consequence the apparatus is considerably simplified , and any failure of components in the device or channel of communication is revealed practically at the moment of its origination.

The block-diagram of the telemetering code-frequency-combination system is shown in fig. 1.

The primary metering devices (PV) transforms the measured value into an angle of rotation or linear displacements. The indicator unit (VZP) connects the primary measurement device with commutator K, which through coder (SH) affects the frequency signal generators of the VG generator unit.

On the receiving side the high frequency signal is picked up by frequency filters (VCHF), which control the decoder (DSH). To the outputs of the decoder is connected a receiving device with digital reading TSPU.

Each discrete value of measured magnitude, measured with the aid of the primary measuring device, of the indicator, commutator, coder and generators is transformed into a high frequency code. At the receiving end the block of frequency filters, decoders and device with digital reading, fixes the obtained signal.

The developed telemetering system is entirely contactless.

The indicator unit shown in fig.2 is situated in the primary measuring device and consists of several photoelectric transformers, the number of which depends upon the permissible discreteness error

$$N_{transf} = \frac{50}{\beta\%}$$

where N_{transf} - number of photoelectric transformers, $\beta\%$ - permissible discreteness error.

As photoelectric transformers were used photo-triodes of the Institute of Automation of the State Plan Ukr-SSR.

It is also possible to apply photodiodes with subsequent signal amplification.

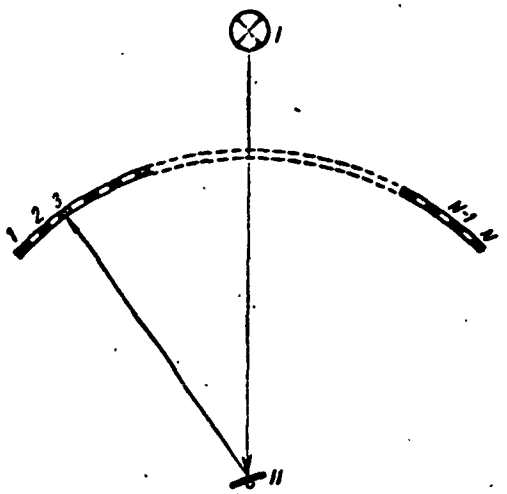

Fig.2. Indicator Unit; 1,2,3...N - photoelectric transformers, I-light emitter, II-mirror.

On the axis of the set up is situated a mirror, illuminated by a narrow stream of light. Under the effect of the light stream, coming from the mirror, is released one of the photoelectric converters, depending upon the position of the movable system of the primary measuring device. With its beam it affects the corresponding input zone of the commutator.

The commutator (fig.3) is made up of a number of triggers connected with each other by valves. The output voltages are taken from load resistances R_L.

To set the triggers of the circuit in initial position (with open left triodes) is applied a droppable system which consists of T_1, C_1, R_1 elements. At the moment the commutator is connected to the power source, the emf of which is induced on the secondary winding of transformer T_1 and is made up of power voltage U_{power}.

Around the bases of left triodes of each trigger are passing negative current pulses, which exceed the currents of bases of right triodes. In consequence of this all the left triodes find themselves in open state, and the output rings of the commutator are currentless.

When signals from the indicator arrive at the commutator there is subsequent commutation of triggers. At each moment of time the output voltage is taken from one trigger only, in which the left triode is closed. The balance of triggers is situated in reverse state and the voltages at their outputs are equal to zero.

The output voltage of the commutator through a matrix coder (fig.3) supplies a corresponding group of generators. At the receiving side the multifrequency signal affects the frequency filters (CHF), the output voltages of which are sent to the input of the matrix decoder DSH (fig.4).

The output rings of the decoder are shunter by triodes, in open state; on account of the displacement current which passes resistance R_3. Upon the approach of a dual frequency telemetering signal proper triodes of the circuit close and the load voltage (bulb of light tableau) rises sharply. The decoder can be applied practically at any number of frequencies in the multifrequency signal.

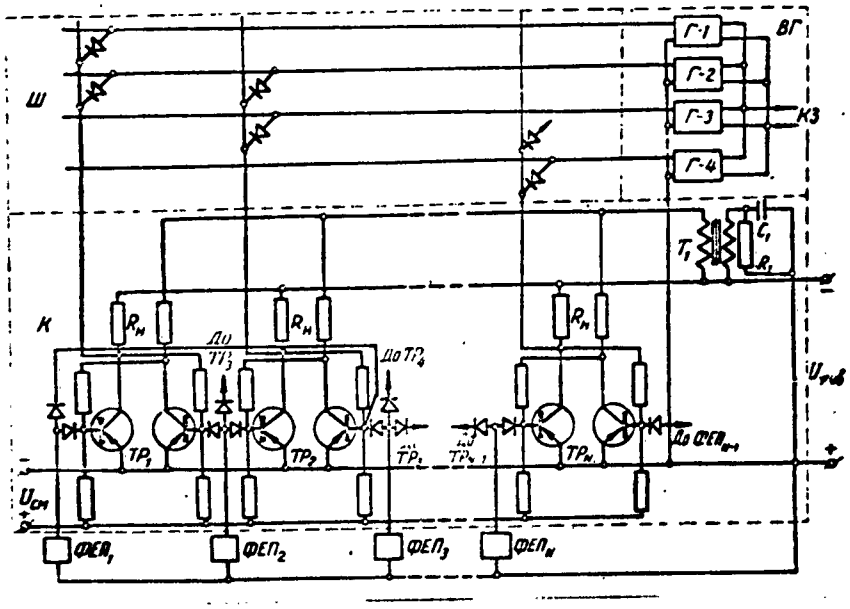

Fig.3. Circuit of transmitter; FEP-photoelectric converters, K-commutator, VG-generator unit; SH-coder.

The developed frequency-combination system of telemetering possesses high speed and interference resistance. Application of the system is perspective for operation at high frequency, as well as radio channels with high level of interferences.

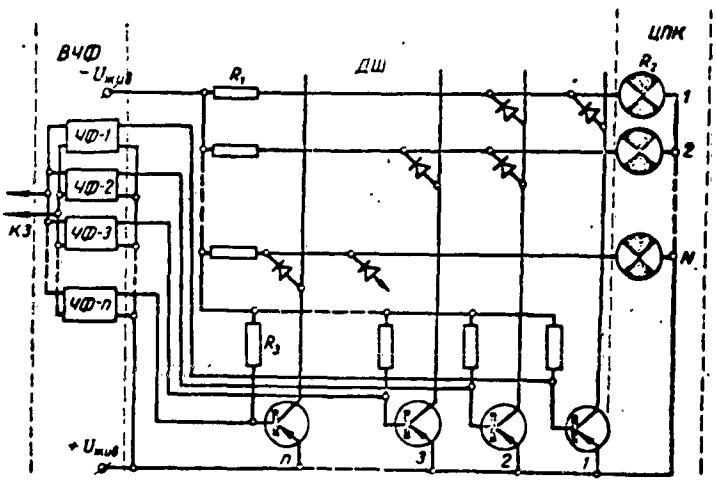

Fig.4. Circuit of receiver; VCHF-Block of frequency filters; DSH-decoder; TSPU-Digital receiving device.

Literature

1. F.A.Katkov; Contactless Coders and Devoders of Frequency-Combination Telemetering Systems. Izvestiya Vysshikh Uchebnykh Zavedeniy, Energetika, No.12, 1959.

2. F.A.Katkov; Multifrequency Narrow Band Telemetering Systems. Gostekhizdat Ukr-SSR, 1960

Submitted: July 5, 1961.

Symmetrical Mono-Frequency Forced Oscillations in Nonlinear Automatic Control Systems

by

V.V.Pavlov

Great attention is attached to the study of symmetrical mono-frequency forced oscillations in automatic control systems with truly nonlinear element, [1, 3, 4]. The basis for approximate determination of forced oscillations in nonlinear systems is the term for equivalent linearization of the nonlinear member $F(x, px)$, obtained by N.M.Krylov and N.N.Bogolyubov [2] for the case, when the nonlinear member is proportional to the small parameter ξ.

For the vital nonlinear member, which is not proportional to the small parameter ξ, in report [5] is given a more defined expression for equivalent linearization

$$F(x, px) = -\left\{\frac{q'(a)}{\omega} px + \left[-q(a) + \frac{\lambda}{\omega} q'(a) + \left(\frac{q(a)}{2\omega}\right)^2 + \left(\frac{q'(a)}{2\omega}\right)^2\right] x\right\}, \quad (1)$$

where lambda and omega - attenuation decrement and the frequency of the "originated solution" * $q(a) = \frac{1}{\pi a}\int_0^{2\pi} F(a\cos\psi, -\lambda a\cos\psi - \omega a\sin\psi)\cos\psi\, d\psi$ and $q'(a) = \frac{1}{\pi a}\int_0^{2\pi} F(a\cos\psi, -\lambda a\cos\psi - \omega a\sin\psi)\sin\psi\, d\psi$ the application of which for studying transient processes gives a much more accurate result, than during the application of the term for equivalent linearization [2].

We shall discuss the question of applying term (1) for the examination of forced monofrequency oscillations in systems with vital nonlinear member. The equation which

* "Originating" solution found from initial equation $F(x, px) \equiv 0$.

describes any kind of a system, will be

$$Q(p)x + F(x, px) = S(p)f(t). \quad \left(p \equiv \frac{d}{dt}\right). \tag{2}$$

where Q(p) and S)p)- multiples of any kind of a degree with true constant coefficients, whereby the degree Q(p) is by one degree higher than S(p); f(t) = B sinΩt .

If the linear part of the automatic control system has the property of a filter [4] then in first approximation it is possible to seek a solution for fixed forced oscillations in form of

$$x = A\sin(\Omega t + \varphi). \tag{3}$$

Equation (2) will then acquire the form of [4]

$$\left[Q(p) - S(p)\frac{B}{A}\left(\cos\varphi - \frac{\sin\varphi}{\Omega}p\right)\right]x = -F(x, px). \tag{4}$$

For linearization - F(x, px) with term (1) it is necessary first to determine the values λ' and frequencies ω of the solution of the "originated" equation, which we will obtain from (4) at F(x, px) = 0

$$\left[Q(p) - S(p)\frac{B}{A}\left(\cos\varphi - \frac{\sin\varphi}{\Omega}p\right)\right]x = 0. \tag{5}$$

It is apparent, that solution of equation (5) will have the form (3)*; it is evident herefrom, that the values, which characterize the "originating" solution can be written as

$$\lambda = 0, \quad \omega = \Omega. \tag{6}$$

Then

$$F'(x, px) = -F(x, px) = -\left\{-\frac{q'(A)}{\Omega}px + \left[q(A) + \left(\frac{q(A)}{2\Omega}\right)^2 + \left(\frac{q'(A)}{2\Omega}\right)^2\right]x\right\}. \tag{7}$$

where

$$q(A) = \frac{1}{\pi A}\int_0^{2\pi} F(A\cos\psi, -A\Omega\sin\psi)\cos\psi\, d\psi.$$

$$q'(A) = \frac{1}{\pi A}\int_0^{2\pi} F(A\cos\psi, -A\Omega\sin\psi)\sin\psi\, d\psi. \tag{7a}$$

It is evident herefrom, that the difference between the defined term for equivalent linearization (7) and the approximation according to [2] lies in the corrective member Δq

* We are interested only in the establishment of a solution.

$$\Delta q = \left(\frac{q}{2\Omega}\right)^2 + \left(\frac{q'}{\Omega}\right)^2. \qquad (8)$$

the magnitude of which actually depends upon the frequency of forced oscillations Ω and upon the values q(A) and q'(A).

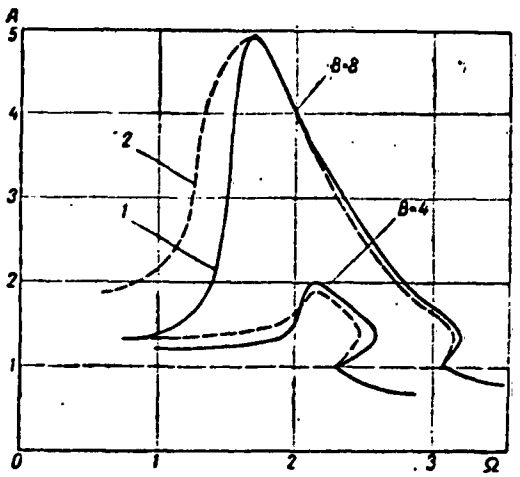

Drawing; Approximate amplitude-frequency characteristic of an automatic control system, described by equations $x'' + x' + 1.96\,x + F(x) = B \sin \omega t$. 1 - with consideration of correction; 2-without consideration of correction.

Next, by substituting (7) in (4), we arrive at a defined term to investigate mono-frequency forced oscillations

$$A\,\frac{Q(j\Omega) + (\varsigma - \Delta\varsigma) - i\varsigma'}{S(j\Omega)} = Be^{j\varphi}. \qquad (9)$$

Whereby its change from the terms ordinarily applied in this case lies only in the correcting member Δq.

As an example was drawn an amplitude-frequency characteristic after term (9) for cases where $\Delta q \neq 0$ and $\Delta q = 0$ for automatic control systems, which are described by equations

$$\frac{d^3x}{dt^3} + \frac{dx}{dt} + 1{,}96x + F(x) = B \sin \Omega t, \qquad 9a$$

where

$$F(x) = \begin{cases} 5 \text{ при } x > 1 \\ 0 \text{ при } -1 < x < 1 \\ -5 \text{ при } x < -1 \end{cases} \qquad 9b$$

As is evident from the drawing, a vital correction takes place in the zone of lower frequencies. However, as already mentioned before, the magnitudeof the correction depends not only upon the frequency,but also upon the value q and q', i.e.upon the concrete form of the linearization coefficient, which must be included in each concrete case.

Literature

1. L.S.Col'dfarb. About certain nonlinearities in Automatic Control Systems "Avtomatika i Telemekhanika" vol. 8, No.5, 1947

2. N.M.Krylov, N.N.Bogolyubov; Introduction into Nonlinear Mechanics,Kiev,1937

3. I.I.Krinetskiy. Controlling Internal Combustion Engines,Mashgiz,1960

4. Ye.P.Popov, I.P.Pal'tov; Approximation Methods of Investigating Nonlinear Automatic Systems, Fizmatgiz, Moscow, 1960

5. V.V.Pavlov; Finding Approximate Solutions for Nonlinear Differential Equations, describing transient processes in automatic Control Systems, Avtomatika, No.6, 1961.

Submitted March 3, 1961.

Automatic Potential (Voltage) Regulator to Protect Underground Installations against Corrosion.

by

I.K.Parra; N.V.Petina

One of the effective methods of combatting corrosion of underground installations is cathodic protection, the nature of which lies in the fact, that the construction, which is being protected is subjected to cathodic polarization from an outer source of DC-current by forming the necessary potential difference between construction and the surrounding medium.

The magnitude of the protective potential, created by nonautomatic cathode stations SKZ inserted, for example, along the underground pipe line within certain distances, depends upon the condition of the ground, magnitude of anodic grounding, presence of stray currents etc.

At the Electrotechnical Inst. of the Academy of Sciences Ukr-SSR was developed a staticpotentials regulator (Automatic Station of Cathodic Protection (ASKZ), the tasks of which are to maintain the protective potential at a given level.

The principal circuit diagram of the ASKZ is shown in fig.1. In contrast to previously developed sample of potentials regulators [1, 2] this arrangement is contact less, built on magnetic boosters and germanium diodes, it has no rotating parts, it is simple and reliable in operation.

The basic parameters of ASKZ-1 are as follows:

Calculated power of regulator P_{max} = 550 watts and it is attained at a load resis-

ance $R_L = R_a/3 + R_T/3 = 1.0$ ohms, whereby $I_n = 23.5$ amp.

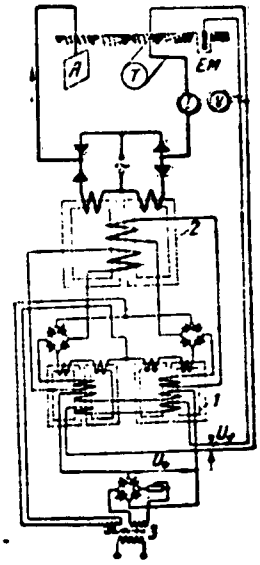

Fig.1. Principal circuit diagram of automatic cathodic protection station.

The input resistance of regulator R_{inp} = 4000 ohms.

Given are the permissible deviations of the potential at drainage point ± 0.1 v, i.e., $U_{inp} = 0.2$ v:

$$I_{вх} = \frac{U_{вх}}{R_{вх}} = \frac{0.2}{4000} = 50\,\mu A, \quad P_{вх} = \frac{U_{вх}^2}{R_{вх}} = \frac{0.2^2}{4000} = 10^{-5}\,вт. \qquad (1)$$

The amplification factor of the regulator for the power is

$$a_p = \frac{550}{10^{-5}} = 55 \cdot 10^6. \qquad (2)$$

The amplification factor of the regulator for current is

$$a_i = \frac{23}{50 \cdot 10^{-6}} = 46 \cdot 10^4. \qquad (3)$$

The multiplicity of the current at regulator output is

$$\frac{I_{макс}}{I_{мин}} = \frac{23.5}{0.5} = 47. \qquad (4)$$

Maximum value of the potential, which may be formed by the regulator of given power, depends upon the magnitude of the anode-ground resistance $R_{a/z}$ and the resistance of pipe line insulation $R_{T/z}$

$$U_{рег\,макс} = I_{макс} \cdot R_{т.з.} \qquad (5)$$

Fig.2 contains curves for maximum values of positive potentials for the pipe lines $U_{T/z}$, which at given values $R_{a/z}$ and $R_{T/z}$ can be worked out by the regulator, having formed the protective potential (at drainage point), equalling $U_p = -0.8$ v (with an accuracy of ± 0.1 v).

The ASKZ-1 potentials regulator was tested in 1960-1961 along the path of the

gas pipe line in the vicinity of Moscow and Dnepropetrovsk.

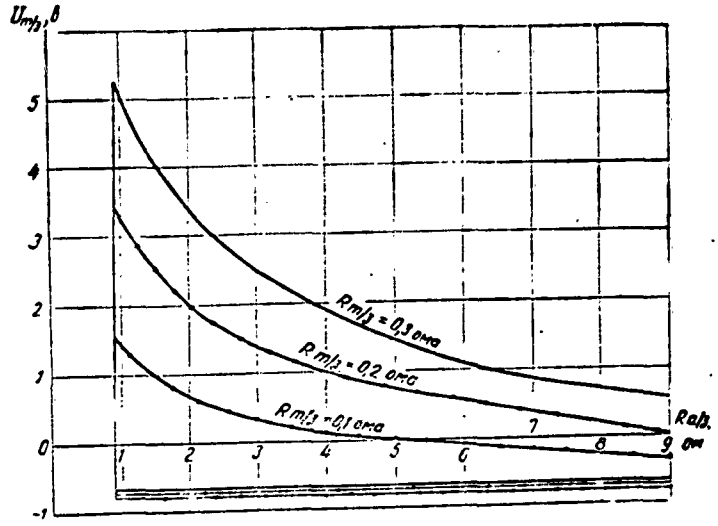

Fig.2. Zone of Operation of regulator at given $U_{T/z}$, $R_{a/z}$, $R_{T/z}$ and U_{ψ}

Fig.3 presents a graph for the change in pipe line potential without cathodic protection and after connection of ASKZ-1. The fixed value of the potential $U_{\psi} = -1.0$ v is maintained with an accuracy of $\pm$ 0.1 v at a change in pipe potential $U_{T/z} = +2 \div -0.7$ v. The time constant of the regulator is 0.7- 0.9 sec (at a change in controlling effect from minimum to maximum).

SEE PAGE 94a FOR FIGURE 3

The ASKZ regulator may find application at all communications, where cathodic corrosion protection is used; particularly advisable is its application in zones of action of stray currents. Right now the ASKZ-1 is in industrial application along pipe lines in the regions of Dnepropetrovsk.

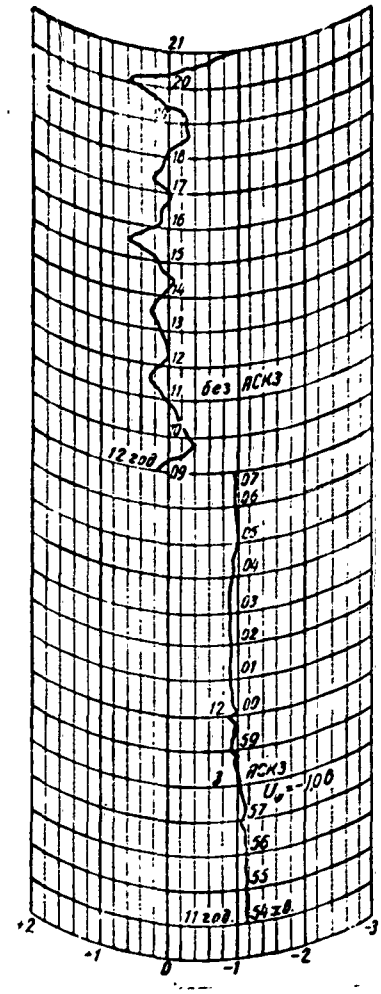

Fig. 3 Graph Showing the Change in Pipeline Potential Without Protection and After Connection of ASKZ

Literature

1. V.I.Ivanenko; A.D.Pushchalovskiy; Automatic Protective Potential Regulator for Pipe Lines, Avtomatika No.1. 1957

2. V.I.Ivanenko; Yu.V.Krementulo; A.D.Pushchalovskiy; Automatic Protective Potential Regulator for Pipe Lines, Avtomatika, No.4,1958

3. I.N.Alekseyev; V.I.Ivanenko; A.D.Pushchalovskiy; Automatic Protective Potential Regulator for Pipe Lines, Gazovaya Promyshlennost' No.11, 1957.

Submitted: December 12, 1961.

Optimum Speed Regulator of River Boats

by

O.F.Chernish

Beginning with 1960 the Automatic Controls Laboratory of the Electrotechnical Institute of the Academy of Sciences Ukr-SSR and the Department of ship Hydromechanics of the Hydrological and Hydrotechnical Inst. of the Academy of Sciences Ukr-SSR are conducting research operations on the development of an automatic indicator and regulator of optimum speed of river boats.

The tasks of seeking and maintaining optimum speed of river boats can be solved as systems with feedback, as well as systems of open type- trouble control systems [1, 5] For practical realization was selected the latter system. The basic advantage of this system is the rapid action, promoted by the fact, that the inertia of the ship's body does not affect the action of the system.

In this report is discussed a trouble control system designed and manufactured at the Automatic Control Lab of the Electrotechnical Inst. of the Academy of Sciences UKR-SSR by the author together with a group a lab co-workers* in cooperation with the Department of Ship's Hydromechanics and the Inst.of Hydrology and Hydrotechnique of the Academy of Sciences Ukr-SSR (solution of theoretical problems concerning the hydromechanics of the ship and automation of River Ship Transportation, executed by Academician of the Acad.of Sc.Ukr-SSR G.E.Pavlenko).

The system realizes "optimum compounding characteristic" $n_{opt} = f_1(h)$ - dependence

of optimum number of revolutions upon the depth of ship's travel [1].

An approximate calculation of this characteristic was made by the known method of G.E.Pavlenko [3,4]

The calculation results are shown in Fig. 1.

One of the basic units of the regulator is the functional converter. To calculate the functional converter it is necessary to have such dependences, which are either given analytically or graphically.

1. The dependence of the optimum number of revolutions upon the depths for various values of the parameter p (see fig.1)

$$n_{opt} = f_1(h, p). \quad p = 3 \div 7. \tag{1}$$

2. Characteristic of tachometer generator

$$U_{TG} = an. \tag{2}$$

3. Characteristic of converting installation [6]

$$U_{conv} = f_2(h). \tag{3}$$

4. Characteristic of potentiometer of feedback of depth follow up system

$$U_{z.z} = bs. \tag{4}$$

On the basis of dependences (1) - (4), it is possible to calculate the characteristic of the functional converter

$$U_{f.p.} = f_3(s). \tag{5}$$

Here in the formulae (1) - (5) were introduced such designations: n_{opt} - optimum number of revolutions of ship's power plant, h - depth of ship travel, Y_{Tg} - voltage at tacho generator outputs, n - number of revolutions of ship's engine, U_{conv}-load at output of converting installation to echo depth finder, $U_{z.z}$ - feedback voltage of the depth follow-up system, s-angle of rotation of feedback potentiometer slide, $U_{f.p.}$-load at output of functional converter, a and b - constant coefficients.

#Footnote for page 96...The development of the regulator was assisted by engr.L.I. Chugunnaya, the unit was assembled by mechanic V.V.Korochinskiy.

The functional converterconstitutes a functional potentiometer, which realizes dependence (5). In the role of functional potentiometer in the regulators is utilized a linear wire potentiometer R_1, in which individual sections of windings were shunted by resistances R_2-R_6 (see fig.2).

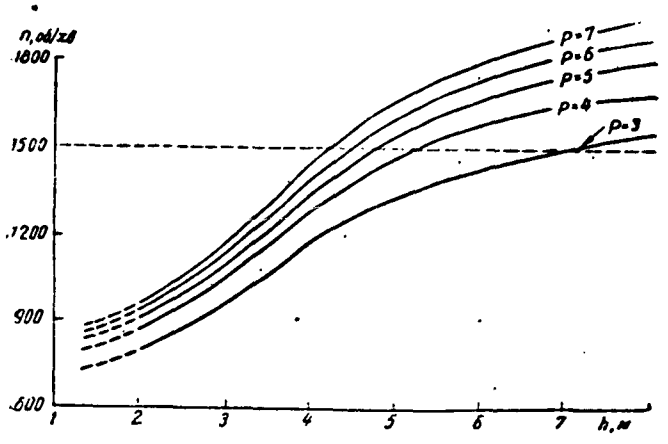

Fig.1.Dependence of optimum number of revolutions of ship's engine upon depth for various values of the parameter p.

In fig.3 and 4 is given the structural and principal arrangement of the regulator controlling the rate of motion of river boats.

Prior to mounting the regulator on board the ship it is adjusted for the least optimum number of engine revolutions at any given depth (e.g.1.5 m). In this case there should be an equality $U_{f.p} \approx U_{Tg.}$

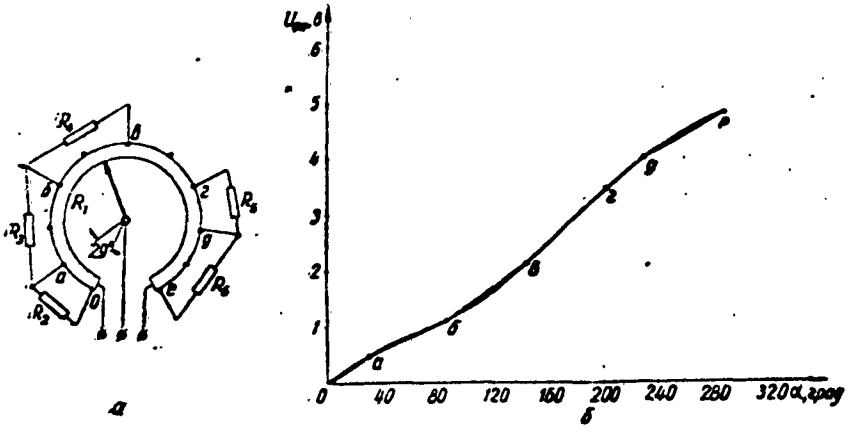

Fig.2.Schematic and characteristic of functional converter a-schematic of functional converter; R_1 = 18 kohm, $R_{2,3}$ = 3 kohm, R_4 = 9.1 kohm, R_5=10 kohm, R_6 = 4.7 kohm; b- characteristic of functional converter; straight line -calculated curve, broken cabcdef - approximating curve.

During the movement of the ship and change of depth in ship's travel the depth indicator (EX and PP) emits a DC-voltage, which is fed to the input of the depth follow-up system (in fig.3. the system is shown by dotted line). The operating engine VD_2 together with depth action shift the slide of the functional potentiometer FP. The voltage of the FP (switch $P_{r.r}$ should be in positionA) is parallel with the voltages of the tachometer generator and the forcing device (PF). The obtained voltage differential is amplified and sent to the VD_1, which shifts the lever of the Diesel fuel pump into necessary direction. The operating engine VD_1 is cut off upon the attainment of $U_{f.p} \approx U_{Tg}$.

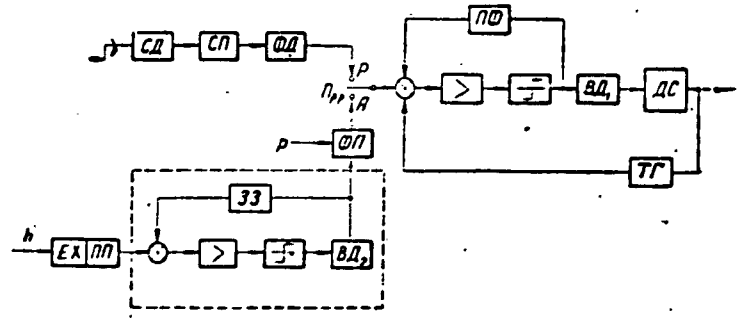

Fig.3. Structural scheme of regulator governing optimum speed of river boats SD-selsyn-transmitter, SP - selsyn-receiver, FD-phase discriminator; $P_{r.r}$ - type of operations switch, EKH-echo depth finder, PP-converter installation, ZZ-feedback, VD_2-operating engine; FP-functional potentiometer; PF-forcing device, VD_1-operating engine, TG-tachometer generator, DS-- ship's power plant.

To improve control quality, the regulators employ a forcing device, which in fig.4. is designated by dotted line (see [12], pp.380-398).

Control of the operational motor VD_1 and VD_2 is realized through transistors T_2-T_5. With the aid of switch P_4 is fixed a certain condition of the ship, which is characterized by the given value of the parameter p [4].

The regulator arrangement is provided with the possibility of manual remote control of fuel feeding into the power plant of the ship. In this case the type of work

switch $P_{r \cdot r}$ (on the principal diagram P_1) must be shifted into position P. In addition the regulator allows a rapid and simple change over to manual cable control which exists on board the ship. To bring such a change over into realisation, the ship's engineer should disconnect only the power of the electromagnetic coupling (EM) using circuit breaker VK_1, mounted on the handle of fuel feeding device.

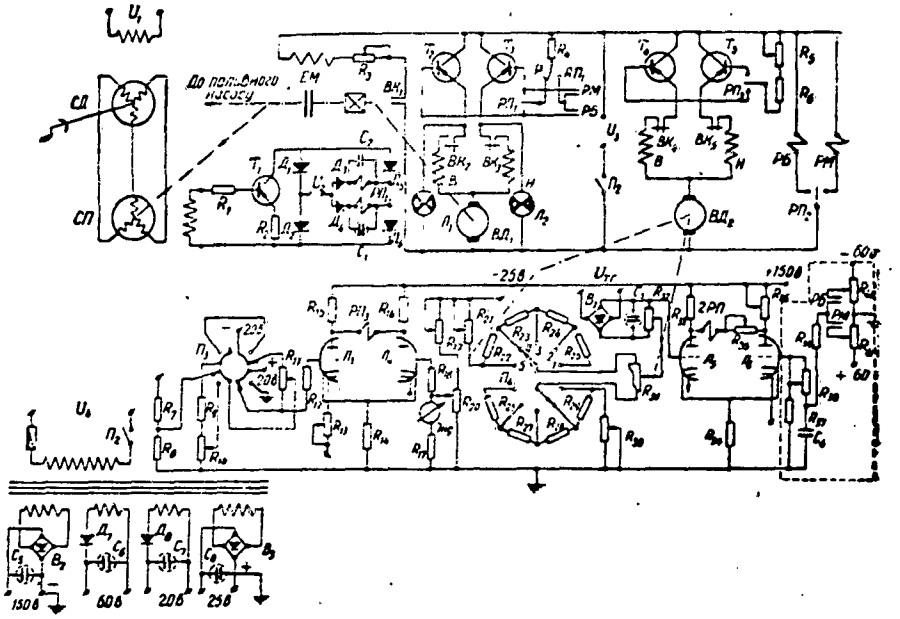

Fig.4. Principal diagram of optimum speed regulator of river boats

R_1=2 kohm, $R_{2,3}$=100 ohm, $R_{4,14,34}$=240 ohm, R_5= 4 kohm, $R_{6,25,29}$=1.8 kohm, $R_{7,8}$=500 kohm, R_9=1.5 megohm, R_{10}=1 megohm, $R_{11,32,38}$=470 kohm, $R_{12,37}$=110 kohm, R_{13}=50 ohm, $R_{15,16,33}$=15 kohm, R_{17}=40 kohm, $R_{18,21}$=100 kohm, $R_{19,30,35,36}$=22 kohm, R_{20}=3 kohm, $R_{22,23,26,27}$=680 ohm, $R_{24,28}$=750 ohm, R_{31}-functional potentiometer, R_{39}=150 kohm, $R_{40,41}$=4.7 kohm, $C_{1,2}$=4.0, $C_{3.7}$=50.0, C_4=1.0, C_5=20.0, C_6=100.0, C_8=1000.0; SD and SP - selsyns types SGSM-1, D_{1-6}-diodes, DG-TS27, $D_{7,8}$-diodes, DG-TS24, T_{1-5} - P4V type triodes, VK_{1-5}-terminal circuit breakers KV-6A, VD_1- operating motor MU-50, VD_2-operating motor MS-160, $L_{1,2}$-SM31 type signal lights, L_{3-6}-6N3P tubes, RB, RM-RKM-1 type relays, RP_1,RP_2,RP_5- RP-5 (high ohmic) relay types, P_{1-2}-TP1-2 type switches; P_3-range switch, P_4-5P8N-K-13 type switch, Ind-M592 type microammeter, B_{1-3}-semiconductor rectifiers; U_1=100 v, 400 c; U_2=40 v, 400 c; U_3=24 v; U_4=127 v, 400 c.

See Page 100a for Figure 5

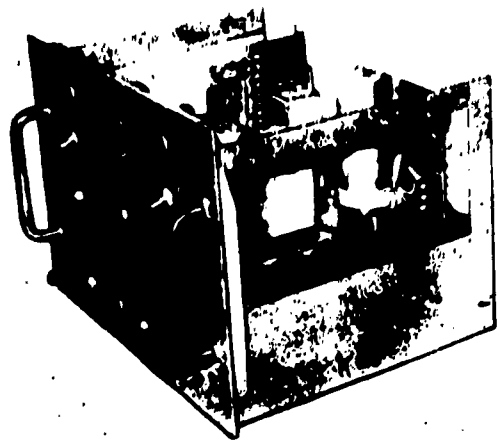

Fig. 5 General View of Optimum Speed Regulator Of River Boats

General view of regulator is shown in fig.5. Regulator less depth feeler, power source and operational motor, mounted directly along the power plant of the ship weighs nearly 10 kg and has overall dimensions of 230X330X250 mm. On the forward panel are mounted all basic regulator adjustment levers.

The regulator was tested toward the end of 1961 navigation on a typical Dneper river boat covering a water distance of 3.5 km in two turns which constitutes 20% of the entire length of the section.

The depth along the section was changed from 1.7 to 3 m. Testing results are listed in table

No. of run	Fuel consumption g	Fuel consumption per km	Fuel combustion %	Time of operation sec	Speed of boat km/hr	Reduction in speed %	Remarks
1	5248	1,50	—	697	18,23	—	Ship controlled by ship's master
2	5121	1,46	—	635	19,91	—	
3	5464	1,56	—	689	18,28	—	
Average	5228	1,51	56	673,6	18,81	—	
1	3090	0,883	—	684	18,4	—	Ship controlled by regulator
2	3580	1,023	—	721	17,48	—	
3	3384	0,967	—	676	18,65	—	
Average	3352	0,958	—	694	18,19	3	

The described regulator was especially developed for the steamer "Laboratory" but it can also be installed on any one river steam boat with main motors type D6, and by modifying same also on other Diesel outfits. To mount and adjust regulator on any one such ship will require slight resolderings at the functional converter and replacement of certain components. The principal arrangement of the regulator remains unchanged.

As was shown by tests, normal operation of the regulator depends basically upon the reliable operation of the depth feeler. Good depth feelers for optimum speed regulators of river boats can be echo depth finders of the REL-6 and "RIKA" types.

Literature

1. A.G.Ivakhnenko. Technical Cybernetics, Gostekhizdat, Ukr-SSR, 1959

2. A.G.Ivakhnenko, Elektroavtomatika, Gostekhizdat, Ukr-SSR, 1957

3. G.Ye.Pavlenko; Method of Determining Permissible Condition of Ship Movement on Rivers and channels. Izdatel'stvo Acad.Nak Ukr-SSR, Kiev,1959

4. G.Ye.Pavlenko; Controlling the Conditions and Automation of Ship Guidance on Rivers. Izdatel'stvo Acad.Nauk.Ukr.SSR, Kiev,1961

5. O.F.Chernish; On the Problem of Cybernetically Controlling the Rate of Motion of River Boats. Avtomatika,No.3, 1961

6. O.F.Chernish; Transformer units of depth feelers for river boats,Avtomatika No.1. 1962

Submitted,October 28, 1961

Using Negative Static Characteristics of a Source-Arc System For Welding With Nonconsumable Electrode

By

Ye. M. Yesibyan

For the arc welding process is highly important the constancy of the melting effect of the arc on the welded item,which is defined by three parameters of the arc,current I, voltage U_d as well as length L.

The length of the arc due to the technological features of welding and physical properties of the arc does not remain unchanged during the welding process and varies within certain intervals.

At an unchanged power of the arc with an increase in its length there is an increase in the dispersion of the thermal stream and its fusing (melting) effect decreases.

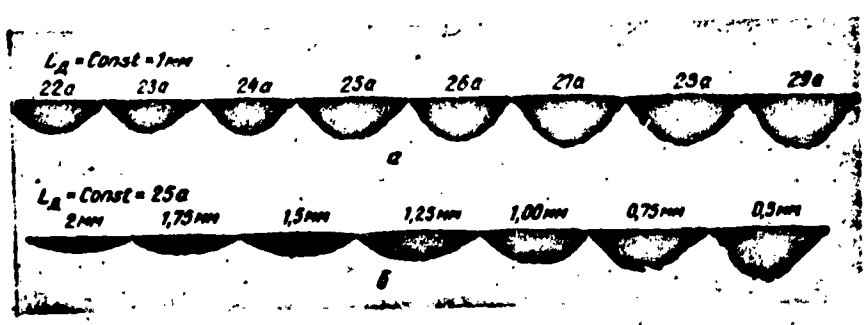

Fig. 1. Lateral microsections of plates fused with tungsten electrode in an Argon medium at various arc current (a) and at its various length (b).

At arc length fluctuations there are also fluctuations in its electric parameters - current and voltage. Arc voltage is established by the physical properties of the arc

and changes with change in its length in accordance with the linear law [1]

$$U_d = A + BL$$

where A - sum of anodic and cathodic voltage drops at the arc, [b]; B - potential gradient at the column of the arc [v/mm].

For numerous arc types thanks to the small potential gradient at the column of the arc the voltage changes are not much higher than the nature of the inverse dependence of the smelting action of the arc upon its length.

This is confirmed by experimental data. In fig.1.a is shown an illustration of a lateral macrosection of stainless steel plates fused together by a tungsten electrode arc in an argon medium at unchanged current and various length (and relative load) of the arc.

The dependence of the melting effect of the arc upon the change in its current is straight. In fig.1 b is shown an analogous illustration of a lateral macrosection of a plate, welded under the very same conditions at unchanged length and various arc currents.

The nature of current change at change in arc length is determined by the properties of the power source and principally it can be arbitrary. The characteristic of power sources of the welding arc is in reverse to the dependence of the current upon the length of the arc (fig.2,a).

The dependence of the current upon the length of the arc I=f(L) can be considered as a static characteristic of the source-arc system, and its dropping nature - as a positive auto-equilibration or statism of the system. The statism coefficient of the system in this case is

$$K_c = \frac{dI}{dL} > 0.$$

Positive autoequilibration is a natural quality of feedback-less power systems and it proved to be very profitable for consumable electrode arc, being the fundation of the known arc auto-control principle. Thanks to the inverse dependence of current upon arc length at arc length variations there is a corresponding change in rate of

electrode melting (consumption) and, in this way, the welding condition is maintained constant. When welding with a consumable electrode arc length variation remain unavoidable and at an inverse dependence I = f(L) the variations of the fusing effect of the arc are intensified.

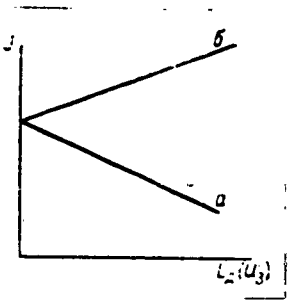

Fig.2. Static characteristics of source-arc system. a-positive; b-negative

Up until recently the technology of welding with consumable electrode with intent of stabilizing the welding process has employed measures of artificially maintaining the unchanged length of the arc with the aid of automatically controlled (by the load of the arc) welding heads.

Proposed is a principally different way of stabilizing the melting effect of the arc on account of obtaining a direct dependence of current upon arc length, i.e. negative static characteristic of source-arc system (fig.2,b).

As is shown by investigations, at a certain negative deviation of the characteristic I = f(L) the opposite deviations of the melting effect of the arc with current deviations and arc length deviations, the latter are mutually compensated, and the melting effect of the arc, as well as the welding condition remain unchanged.

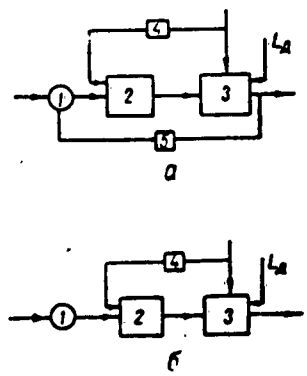

Fig.3. Structural schemes of devices with negative static characteristic of source-arc system. a-at compensating current stabilization; b-at parametric current stabilization; 1-current source;

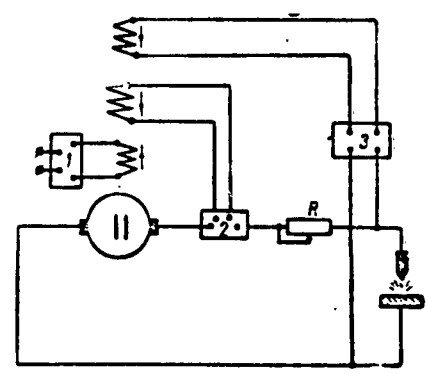

Fig.4. Principal scheme of a combination current control system by arc length 1-tasks; 2-current linkage; 3-voltage linkage.

2-regulator;3-control object (arc);4-voltage linkage (disturbed L_d); 5-current linkage.

The advantage of the proposed method lies in the fact, that the development of trouble due to arc length is realized practically inertialess by the very power source without additional complicated and inertia regulators governing arc length. This reveals new possibilities for mechenized or manual welding with a consumable electrode, especially the ability of welding of metals of very small thickness.

Astatic or negative static characteristic can be obtained by introducing into the power source of the welding arc automatic control elements, e.g. by using a combined or differential control systems [2,3].

In fig.4 is given the principal diagram of a combined current control system in accordance with arc length by utilizing a DC generator with three control windings as power source. A corresponding structural diagram is given in fig.3.a. In this arrangement, in addition to the control principle with feedback 5 (compensating stabilization of arc current), is also used the principle of controlling by the distortions in arc length (compound link 4 with arc voltage, proportional to its length).

Another quite simple variant for the obtainment of astatic or negative static characteristic of the source-arc system was developed at the Electrotechnical Institute of the Academy of Sciences Ukr-SSR [4] by inserting into the head of the welding ring a semiconductor triode 1 in series with arc 2 and the DC-source 3 (fig.5). In the arrangement shown in fig.5,a is realized parametric stabilization of arc current, equalling the collector current of triode I_k. Here the arc current at unchanged basic current I_b remains unchanged in broad intervals of voltage oscillations of DC current source (network voltage oscillations) and variations in length (voltage) of arc.

In this case

$$\frac{\partial U_a}{\partial l} \to \infty, \quad K_c \to 0. \qquad (1)$$

where $\frac{\partial U_a}{\partial l}$ - dynamic resistance of the source.

The characteristic of the system is close to astatic.

To obtain a negative static characteristic it is necessary to introduce, in addition

to the stabilizing, arc currents an element (in our case a semiconductor triode), an additional compounding link 4 of the base ring with arc voltage, as is shown in fig.5,b. Consequently

$$\frac{\partial U_1}{\partial l} > 0, \quad K_c < 0. \qquad (2)$$

A corresponding structural scheme is shown in fig.3,b.

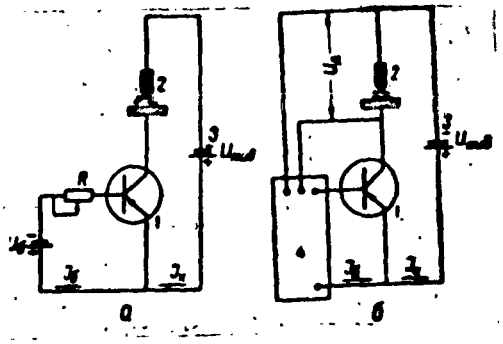

Fig.5. Principal Diagram of an arrangement with Semiconductor Triode in the ring of the arc; a-with arc current stabilization; b-with arc current control.

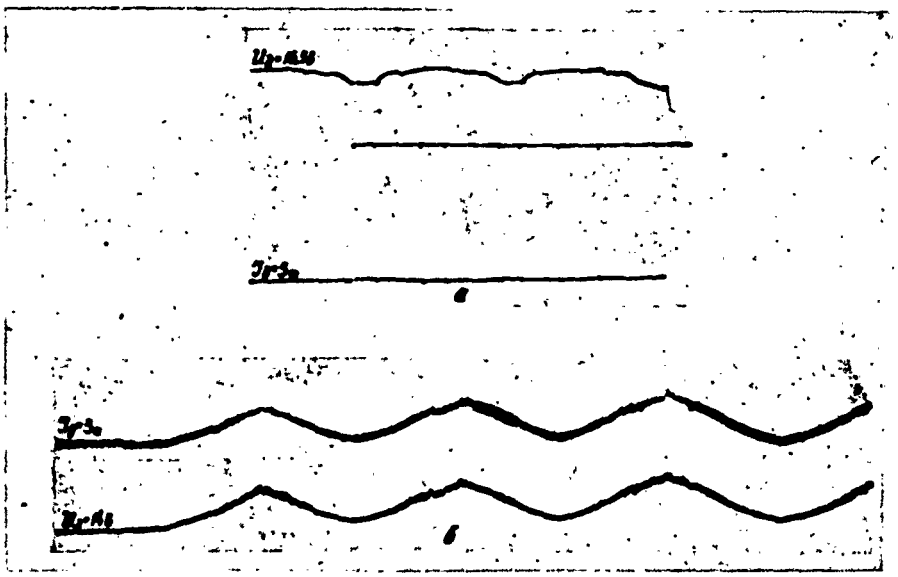

Fig.6.Current and voltage oscillograms at arc length variations a-when powering arc from source according to scheme shown in fig.5,a; b- when powering arc from source according to scheme shown in fig.5,b.

The static characteristic of the system attain a negative slope, i.e. the arc current rises with the rise in length (voltage) of the arc.

In fig.6 are given the resultant voltage and arc current oscillograms at artificial arc length variations.

Having applied such a scheme for welding of metals of low thicknesses in an Argon medium, we derived the possibility of faultlessly welding steel with a thickness of up to 0.1 mm.

Literature

1. K.K.Khrenov; Electric Welding Arc, Mashgiz, Moscow 1949

2. A.G.Ivakhnenko; Technical Cybernetics. Gostekhizdat, Ukr-SSR, 1959

3. O.M.Kostyuk; Equivalence Condition of a Differential Control System and a System of Controlling Troubles, Avtomatika No.1.1961

4. O.M.Milyakh; K.K.Khrenov; Ye.M.Yesibyana, Yu.I.Drabovich, Thesis No 134357 of April 11,1960.

Submitted: July 6,1961

Oleksiy Grigorovich Ivakhnenko

(On the 50-Th Birthday)

On March 30, 1962 have passed 50 years since the day of birth and 25 years of creative, scientific and pedagogical activities of the known Ukrainian scientist in the field of automation, member correspondent of the Academy of Sciences Ukr-SSR O.G.Ivakhnenko.

Oleksiy Grigorovich was born in the village of Kobelyaki, Poltova region in the family of a rural teacher. In 1938 he graduated from the Leningrad,Ulyanov-Lenin Electrical Engineering Institute, having specialized in the field of automation and telemechanics. When still a student, in 1937, he published his first scientific report " On Thermoelements ".

The beginning of O.G.Ivakhnenko's scientific activities dates back in 1938.At that time he worked as a junior scientific coworker at the Automations Laboratory of the Lenin All Union Electrical Engineering Inst. directed by academician S.O. Lebedev. In 1940 O.G.Ivakhnenko publishes the report entitled "Circuits and Calculation of Thyratron Controllers ", which laid the foundation for his highly valuable work on the utilization of series transformers, thyratrons, and later also magnetic amplifiers in AC servomotor control systems. After completing the post-graduateship at the Inst.of Physics of the MDU Oleksiy Grigorovich presents a candidate dissertation, devoted to theoretic investigations of nonlinear follow-up systems.

The entire further scientific activity of the scientist took place at the Electro-Technical Institute of the Academy of Sciences Ukr-SSR and the Kiev Polytechnicum. A number of investigations was devoted to the application of basic conditions of non-linear theory of oscillations when investigating the dynamics of automatic systems. In particular, was proven the advantage of applying the nonlinear quadratic feedback in systems with constant servomotor rate. This idea was then developed under consent in the undertakings of a number of other scientists.

Working in the field of automating measuring capacitors O.G.Ivakhnenko publishes in 1951-1953 a number of reports, in which is shown the physical realizability and practical value of the invariance theory (which was disclaimed at that time) with respect to increasing the accuracy and rapid action of automatic systems. The scientific problems, which originated in connection with the development of the invariance theory, were found to be so numerous and broad, that many outstanding scientists had to take part in the solution of same. In this wide branch O.G.Ivakhnenko selected the field of so-called combination systems, which are used simultaneously as a control principle of deviations and a control principle of troubles as well. The problems of the invariance theory and the theory of combined systems were the subject of Dr. dissertation, which Oleksiy Grigorovich submitted in 1953.

Beginning with 1958 the scientist works in the field of applying the theory of combined systems to extremal control systems. In the monography "Technical Cybernetics" which was published in 1959, the author showed ,that in extremal systems is also possible the realization of invariance conditions in all its forms with the purpose of improving the actions of these systems. It was shown in his recent reports, that all most progressive methods of the control theory are closely connected with the general invariance theory.

Oleksiy Grigorovich combines successfully his scientific activity with pedagogical work. He has schooled many a young scientific worker in the field of automatic control.

O.G.Ivakhnenko published 98 scientific reports and 6 monographies, a sizeable number of his reports was published in foreign editions.

As the head of the Kiev territorial group of National Committee of the Ukr-SSR dealing in automatic control, Oleksiy Grigorovich is devoting much strength and energy to the propaganda of new ideas, organization of regular seminaries, lectures. He is an active contributor to the journal Avtomatika from the day it has been founded.

Greeting O.G.Ivakhnenko on his 50-th birthday, the editorship of the journal wishes him long years of life and new creative successes.

DISTRIBUTION LIST

DEPARTMENT OF DEFENSE	Nr. Copies
HEADQUARTERS USAF	
AFCIN-3D2	1
ARL (ARB)	1
OTHER AGENCIES	
CIA	1
NSA	6
DIA	9
AID	2
OTS	2
AEC	2
PWS	1
NASA	1
ARMY	3
NAVY	3
PGE	12

MAJOR AIR COMMANDS	Nr. Copies
AFSC	
SCFDD	1
ASTIA	25
TDHTL	5
TDBDP	5
AEDC (AEY)	1
SSD (SSF)	2
APGC (PGF)	1
ESD (ESY)	1
RADC (RAY)	1
AFMDC (MDF)	1
AFSWC (SWF)	1
AFMTC (FTY)	1